



# UNIVERSIDAD DE MURCIA

## ESCUELA INTERNACIONAL DE DOCTORADO

Characterization of Caiap and Wdr90 as Novel Inflammasome Components Involved in the Resistance to *Salmonella enterica* serovar Typhimurium.

Caracterización de Caiap y Wdr90 como Nuevos Componentes del Inflamasoma Implicados en la Resistencia a *Salmonella enterica* serovar Typhimurium

**Dña. Ana Valera Pérez**  
**2018**







# TABLE OF CONTENTS

ABBREVIATIONS.....	9
SUMMARY.....	19
INTRODUCTION .....	23
1.    The immune system.....	25
1.1. The innate immune system in fish .....	26
1.2. Adaptive immune system in fish .....	29
2.    Immune system and inflammasomes.....	30
2.1. PRRs.....	31
2.2. Toll like receptors .....	32
2.3. NOD-like receptors.....	32
3.    Inflammasomes.....	35
3.1. Inflammasome receptors .....	36
3.2. Adaptor protein; ASC .....	41
3.3. Effector proteins.....	43
4.    Zebrafish .....	49
4.1. Description, distribution, taxonomy, ecology and reproduction.....	49
5. <i>Salmonella enterica</i> serovar Typhimurium (ST).....	53
6.    Zebrafish-ST infection model in inflammasome research .....	55
7.    New inflammasome components.....	57
7.1. Ankyrin proteins .....	57
7.2. WDR proteins .....	58
AIMS.....	61
MATERIALS & METHODS .....	65
1.    Animals.....	67

2.	DNA constructs .....	67
3.	Cell lines .....	68
4.	sgRNA design.....	68
5.	Morpholinos and RNA/DNA/Protein Injection .....	69
6.	Generation of stable cell lines .....	70
7.	Chemical treatments.....	71
8.	Infection assay .....	71
9.	Tail Fin Wounding .....	71
10.	Whole-Mount <i>In Situ</i> Hybridization (WISH).....	71
11.	Caspase-1 activity assay .....	72
12.	Cell sorting .....	72
13.	Analysis of gene expression .....	73
14.	Transfection .....	74
15.	Dot Blot .....	74
16.	Western Blot .....	74
17.	Immunoprecipitation assays.....	75
18.	Confocal Microscopy.....	75
19.	Recombinant protein purification .....	76
20.	Antibody generation .....	76
21.	Sequence analysis of Caiap in different species .....	77
22.	Statistical analysis .....	77
	RESULTS .....	79
1.	CAIAP.....	81
1.1.	Identification and characterization of Caiap, a Protein Containing a CARD domain and ANK repeats, which is highly conserved from cartilaginous fish to marsupials .....	81

1.2. Zebrafish Caiap is induced upon infection .....	85
1.3. Caiap is required for the inflammasome-dependent resistance to ST in zebrafish .....	88
1.4. Zebrafish Caiap requires Asc to mediate the Inflammasome-dependent resistance to ST .....	92
1.5. Zebrafish Caiap is required for Caspa activation.....	95
2.    WDR90 .....	99
2.1. Identification and characterization of WDR90.....	99
2.2. <i>gbp4</i> induces <i>wdr90</i> expression independently of inflammasome activation.....	100
2.3. Wdr90 is involved in Caspa activation and larval resistance to ST infection.....	102
2.4. Wdr90 acts upstream Asc and caspase-1 to promote ST resistance.....	102
2.5. Human WDR90 interacts with NLRC4 .....	105
3. New tools to study the inflammasome.....	113
3.1. Generation of WDR90 KO mouse macrophages.....	113
2.6. Generation of WDR90 KI human cells.....	115
2.7. Production of antibodies to human WDR90 and zebrafish Asc.....	116
DISCUSSION .....	123
CONCLUSIONS.....	133
REFERENCES.....	137
RESUMEN EN CASTELLANO .....	161



# **ABBREVIATIONS**



°C	Celsius degrees
Ab	Antibody
AGs	Acidophilic granulocytes
AIM2	Absent in melanoma 2
Ala	Alanine
ALRs	AIM2-like receptors
ANOVA	Analysis of variance
AP-1	Activator protein 1
Arg	Arginine
As	Antisense
Asp	Aspartic
ASC	Apoptosis-associated speck-like protein containing a CARD
ATP	Adenosine triphosphate
BCA	Bicinchoninic acid
BSA	Bovine serum albumin
C+	Positive control
C-terminal	Carboxi-terminal
CARD	Caspase Activation and Recruitment Domain
CD	Crohn's Disease
cDNA	Complementary DNA
CHAPS	3-[(3-Cholamidopropyl)dimethylammonio]-1-propanesulfonate
CSFs	Colony stimulating factors
CTL	Cytotoxic T cells

## Abbreviations

Cys	Cysteine
Da	Dalton
DAMP	Damage-associated molecular pattern molecules
DAPI	4',6-diamidino-2-phenylindole
DM	Double mutant
DMEM	Dulbecco's modified Eagle's medium
DMSO	Dimethyl sulfoxide
DN	Dominant negative
DNA	Deoxyribonucleic acid
DNase	Deoxyribonuclease
dpf	Days post-fertilization
dsDNA	Double-stranded DNA
DsRed	Red fluorescent protein from <i>Discosoma</i> sp.
DTT	Dithiothreitol
ECL	Enhanced chemiluminescence
EDTA	Ethylenediaminetetraacetic acid
EGTA	Ethylene glycol tetraacetic acid
ELANE	Neutrophil elastase
ENA	European nucleotide archive
EU	European Union
eGFP	Enhanced GFP
F	Forward primer
FACS	Fluorescence-activated cell sorting

FCS	Fetal Calf Serum
Gbp	Guanylate binding protein
GFP	Green fluorescent protein
Gln	Glutamine
Glu	Glutamic acid
Gly	Glycine
GM-CSF	Granulocyte macrophage colony-stimulating factor
GMP	Guanosine monophosphate
GTP	Guanosine-5'-triphosphate
h	Hours
hu	Human
HEK293	Human Embryonic Kidney 293
HEPES	4-(2-hydroxyethyl)-1-piperazineethanesulfonic acid
HK	Head kidney
hpf	Hours post-fertilization
hpi	Hours post-infection
I $\kappa$ B	Nuclear factor- $\kappa$ B inhibitor
ID	Identification
IFN	Interferon
Ig	Immunoglobulin
IL	Interleukin
IL-1RI	Type I IL-1 receptor
IL-1ra	IL-1 receptor antagonist

## *Abbreviations*

Ile	Isoleucine
IPAF	Ice protease-activating factor
JNK	c-Jun N-terminal kinase
LB	Luria Bertani Broth
Leu	Leucine
LPS	Lypopolisaccharide
LRR	Leucine-rich repeat
Ly	Lymphocytes
Lys	Lysine
Lyz	Lysozyme C
MΦ	Macrophages
mAbs	Monoclonal antibodies
MAPK	Mitogen-activated protein kinase
MDP	Muramyl dipeptide
MHC	Major histocompatibility complex
MO	Morpholino
MOI	Multiplicity of infection
Mpeg1	Macrophage expressed protein 1
Mpx	Myeloperoxidase
mRNA	Messenger RNA
mtDNA	Mitochondrial DNA
myc	Myelocytomatosis
N-terminal	Amino-terminal

NAIP	Neuronal apoptosis inhibitor protein
NACHT	Neuronal apoptosis inhibitor protein NBS Nucleotide binding site
NF- $\kappa$ B	Nuclear factor kappa B
NLRs	NOD-like receptors
NLRA	NLR acidic transactivation domain
NLRC	NLR caspase activation and recruitment domain
NLRCS	NLR-CARD containing family
NLRPs	NLR-PYRIN containing family
NO	Nitric oxide
NOD	Nucleotide – binding oligomerization
ns	Not significant
p	p-value
PAMPs	Pathogen-associated molecular patterns
PBS	Phosphate buffered saline
PCR	Polymerase chain reaction
PGN	Peptidoglycan
PhD	Philosophiae doctor
Phe	Phenylalanine
PI	Propidium iodide
PIs	Principal investigators
PMSF	Phenylmethanesulfonylfluoride
PRRs	Pattern recognition receptors
PTG	Prostaglandin

## Abbreviations

PTGS	Prostaglandin-endoperoxide synthase
PYD	Pyrin domain
R	Reverse primer
RIG-1	Retinoic acid-inducible gene 1
RIP	Receptor interacting protein
RLRs	RIG-1 like receptors
RNA	Ribonucleic acid
RNS	Reactive nitrogen species
ROS	Reactive oxygen species
Rps11	Ribosomal protein S11
RT	Reverse transcription
qPCR	Quantitative PCR
RTS-11	Mononuclear phagocyte cell line of rainbow trout
<i>S. Typhimurium</i>	<i>Salmonella</i> enteric serovar Typhimurium
SCV	<i>Salmonella</i> -containing vacuole
SDS-PAGE	SDS-poliacrylamide gel electrophoresis
SDS	Sodium dodecyl sulfate
S.E.M	Standard error of the mean
SIF	<i>Salmonella</i> induced filaments
SP-1	Specificity protein 1
SPI	<i>Salmonella</i> Pathogenicity Island
Std	Standard control
subsp.	Subspecies

T3SS	Type III Secretion System
Tg	Transgenic
Th	Helper T cell
TIR	Toll-IL-1R homology domain
TLRs	Toll-like receptors
TNF	Tumor necrosis factor
TNFR	Tumor necrosis factor receptor
USA	United States of America
WD40	Tryptophan-aspartic acid (W-D) dipeptide
WDR	WD40 Repeat
wt/vol	Weight/Volume
ZIRC	Zebrafish international resource center
ZFNs	Zinc finger nucleases

## *Abbreviations*

# **SUMMARY**



Inflammasomes are cytosolic molecular platforms that alert the immune system about the presence of the infection. As multiprotein complexes, they consist of NLRs (NOD-like receptors), adaptor proteins ASC and caspase-1. The assembly of the complexes requires the activation signal and depends on the homotypic interactions. Our laboratory has found that zebrafish guanylate-binding protein 4 (Gbp4), an IFN $\gamma$ -inducible GTPase harboring a C-terminal CARD domain, is required for the inflammasome-dependent clearance of *Salmonella* Typhimurium (ST) by neutrophils *in vivo*. Although several key components of the inflammasome have already been characterized, little is known about other potential components. In this Thesis we describe two new inflammasome components and we developed antibodies against inflammasome components in Alpacas as tools to shed light in to inflammasome assembly and function.

On one hand, we report the identification of an evolutionarily conserved protein, that we term Caiap (from CARD- and ANK-containing Inflammasome Adaptor Protein), which has an N-terminal CARD domain and 16 C-terminal ANK domains, and is required for the inflammasome-dependent resistance to *Salmonella* Typhimurium in zebrafish. Intriguingly, Caiap is highly conserved from cartilaginous fish to marsupials but is absent in placental mammals. Mechanistically, Caiap acts downstream flagellin and interacts with catalytic active Caspa, the functional homolog of mammalian caspase-1, through its ANK domain, while its CARD domain promotes its self-oligomerization. Our results therefore point to ANK domain-containing proteins as key inflammasome adaptors required for the stabilization of active caspase-1 in functionally stable, high molecular weight complexes.

On the other hand, we found that zebrafish *wdr90* is highly induced by Gbp4 independently of inflammsome activation. This gene encodes a large protein of unknown functions until date that contains several WD40 domains, which are involved in coordinating multi-protein complex assembly. Its overexpression increased caspase-1 activity and the resistance of the larvae to ST infection, acting upstream of Caspa and Asc. In addition, it was able to alter the distribution of NLRC4, but not of NLRP3 or AIM2, when expressed in HEK293T cells.

## *Summary*

Finally, we have generated WDR90 knockout immortalized bone marrow-derived macrophages and the CRISPR tools to generate KI cell lines to tag endogenous WDR90 with the FLAG epitope to facilitate its detection. In addition, we have produced alpaca antibodies against zebrafish Asc and human WDR90, which will help to shed light into inflammasome assembly, activation and biological functions.

# **INTRODUCTION**



## **1. The immune system**

The immune system is essential for the maintenance of a balanced physiological state, preventing the organism against threats that could alter this balance. The immune system is divided in two blocks; the innate immune system and the adaptive immune system.

The innate immune system detects the presence of microbes and initiates mechanisms to eliminate potentially infectious threats. This system acts as a first barrier against pathogens. It includes physical barriers such as the skin, different cell types like neutrophils, macrophages, dendritic cells, monocytes and epithelial cells, and a wide range of soluble molecules.

On the other hand, the adaptive immune system provides an acquired response which is more specific and long-lasting than the innate immune response. This adaptive immunity is activated after a first contact with infection and it is more effective after each successive contact with the same pathogen. The adaptive immunity includes the complement system, lymphocytes and their secreted antibodies. Lymphocytes appear exclusively in vertebrates and are the key for a stronger immune response as well as immunological memory (Abbas, A. K., Lichtman, A. H., 2015). These cells are derived from hematopoietic stem cells in the bone marrow (Janeway and Medzhitov, 2002) and are capable of specifically recognize individual pathogens. Moreover, lymphocytes are divided into two main categories of cells: T lymphocytes (T cells) and B lymphocytes (B cells) (Figure 1). During the adaptive response, extracellular pathogens are recognized by presenting cells that mediate the response by B cells, which are the cells responsible of antibody (Ab) secretion.

T cells are characterized by the presence of a T-Cell Receptor (TCR) in their surface. They mediate a large number of activities and can be divided in three groups:

- T helper lymphocytes (Th), which have regulatory functions and are involved in the development and production of antibodies by B cells or interacting with phagocytic cells helping them to destroy the pathogens phagocytosed before.

-T Cytotoxic lymphocytes (CTL) that recognize and destroy virus-infected cells (or cells infected with other pathogens), damaged or dysfunctional and tumour cells (Harty *et al.*, 2000).

-Regulatory T cells (Treg) that mediates the tolerance to self-antigens and prevent autoimmune diseases (Bettelli *et al.*, 2006).

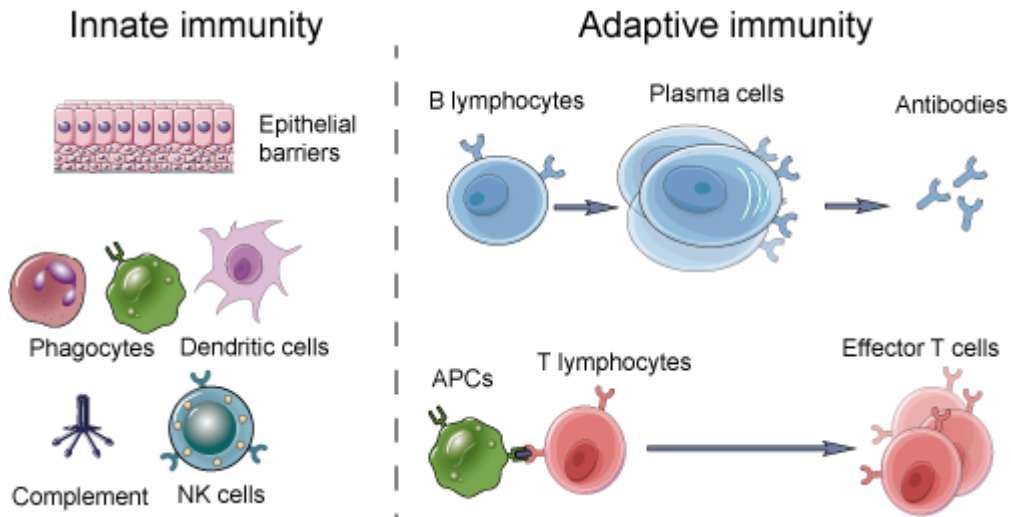


**Figure 1. Scheme of the main components of innate and adaptive immunity.** Innate immunity (left) include natural barriers and phagocytes, dendritic cells, NK cells and the complement system, adaptive immunity (right) include B and T cells, Antigen Presenting Cells (APCs) and Plasma cells.

### 1.1. The innate immune system in fish

In the immune system, the innate system is the most evolutionarily conserved one compared with the adaptive system which is only present in vertebrates. Teleost fish are the first evolutionary group that possesses a well-structured and differentiated immune system, being similar to those in birds and mammals. However, the ecosystem of fish leads to big living differences with higher vertebrates. These differences are also represented in their immune system. For example, in contrast to higher vertebrates, fish are free-living organisms from early embryonic stages of life and depend on their innate immune system to survive. Fish innate response comprises physical barriers (epithelium and mucosa), cellular effectors (phagocytic cells and nonspecific cytotoxic cells) and humoral factors (complement and other acute phase proteins), whereas adaptive response comprises a cellular (Ly) and humoral (Ab) components (Uribe, Folch, Enriquez,

& Moran, 2011). Moreover, specific antibodies can be produced without generating a systemic response (Uribe et al., 2011).

The organs and tissues of the immune system in teleosts have been classified, as in mammals, in primary and secondary organs (See table below) (Neely & Flajnik, 2016). Fish lack bone marrow; its function is taken by the kidney, a primary organ that is the largest site of haematopoiesis until adulthood. Kidney consists of two parts: the anterior or cephalic (head kidney, HK), with mainly hematopoietic function, and posterior, basically with excretory function. Regarding to secondary lymphoid organs, the spleen is the most important but presents few lymphocytes, although may increase in number by administration of an antigen. The spleen in zebrafish remains a small organ that contains large amounts of erythroblasts at 30 days post fertilization. At three months, when lymphoblasts are evident in the spleen, emerging ellipsoids are involved in the capture of antigen. A similar developmental pattern has been described for other teleost spleen, such as that of the Atlantic salmon, grouper and catfish (dos Santos, Romano, de Sousa, Ellis, & Rombout, 2000; Iwama & Nakanishi, 1996).

Function	Mammals	Teleost fish	References
<b>Primary organ</b>	Bone marrow/Thymus	Head kidney/Thymus	(Brinkworth & Thorn, 2013)
<b>Secondary organ</b>	Spleen/Lymph nodes	Spleen	(Boehm, Hess, & Swann, 2012)

Table 1. Comparative primary and secondary organs in mammals and teleost fish

Furthermore, mucus is essential to prevent attachment and inhibit the entry of bacteria, fungi or parasites to the epithelial surfaces and digest microorganisms. Fish mucus possesses a wide battery of lytic enzymes, such as lysozyme and lectins, complement proteins, antibacterial peptides and immunoglobulin M (IgM) and IgT (Boshra, Li, & Sunyer, 2006; Parra, Korytář, Takizawa, & Sunyer, 2016; Saurabh & Sahoo, 2008).

## *Introduction*

Innate cellular response of the fish includes a variety of leukocytes, which phagocytes are very important in innate immunity by its capacity to eliminate viruses, bacteria and parasites because their function is less influenced by the temperature (Rowley *et al.*, 1988; Secombes and Fletcher, 1992; Blazer, 1991; Sepulcre *et al.*, 2002; Lange and Magnadottir, 2003; Magnadottir *et al.*, 2005). Moreover, they can be the initiator of activation and regulation of the specific immune response (Clem *et al.*, 1985; Clem *et al.*, 1991; Vallejo *et al.*, 1992). The process of phagocytosis in fish is almost the same as described for mammalian leukocytes, ending with two mechanisms responsible for the killing of phagocytized microorganisms. The first one is the production of reactive oxygen intermediates (ROS) with a rapid and abrupt increase in the rate of oxygen consumption, known as respiratory burst, being independent on mitochondrial respiration. The second one is the production of nitric oxide (NO) and other nitrogen reactive intermediates (RNS). It is further known that ROS produced by phagocytes of fish have bactericidal activity (Sharp and Secombes, 1993; Skarmeta *et al.*, 1995). In addition, neutrophils possess myeloperoxidase in their cytoplasmic granules, which in the presence of halide and hydrogen peroxide kills bacteria by halogenation of the bacterial cell wall. Moreover, these cells use lysozymes and other hydrolytic enzymes of lysosomes for pathogen elimination (Fischer *et al.*, 2006). On the other hand, the nonspecific cytotoxic cells of fish are morphologically distinct from the large granular lymphocytes of mammals, whereas, they are suggested to be functionally similar (Evans and Jaso-Friedmann, 1992). These cells are able to eliminate a range of spontaneously xenogeneic targets, including parasites in fish and traditional targets of natural killer cells in mammals (Hasegawa *et al.*, 1998). Differently than the natural killer cells of mammals, the nonspecific cytotoxic cells of catfish are not granulated, small lymphocytes that are commonly found in lymphoid tissues, but are rarely found in the blood (Shen *et al.*, 2002).

Beside cellular effectors described above, there are a wide variety of substances (humoral effectors) that act on the innate defence of the fish (Alexander and Ingram, 1992). These molecules may be classified into different groups due to its function. There are bacterial growth inhibitors such as: transferrin, antiproteases and ceruloplasmin; viral replication inhibitors such as interferon; inhibitors of bacterial toxins; lysines such

as lysozyme and chitinase; agglutinins and precipitins such as lectins and C-reactive protein, and finally complement components. In teleosts, as well as in higher vertebrates, the complement system can be activated in three different ways: the classical pathway, which is triggered by Ab binding to the cell surface (Holland and Lambris, 2002), the alternative pathway, which is independent of antibodies and is activated directly by foreign microorganisms, and the lectin pathway, which is activated by the binding of a protein complex consisting of mannose/mannan-binding lectin in bacterial cells (Sakai, 1992). The complement system performs several functions important for the humoral clearance of the pathogens, such as leukocyte chemotactic activity (Lamas and Ellis, 1994), opsonisation (Sakai, 1984a), inactivation of certain toxins (Von Eschen and Rudbach, 1974; Ellis, 1980; Sakai, 1984b), the bactericidal activity (Sakai, 1983), and cytotoxicity and viral inactivation (Sakai, 1992).

## **1.2. Adaptive immune system in fish**

Antibodies are the key mediators of the adaptive immune response, together with its producing cells, lymphocytes. The main, predominant immunoglobulin in teleosts is the IgM class. It is a tetramer and contains eight antigenic combining sites (Acton *et al.*, 1971). *In vitro* studies, using conjugated monoclonal antibodies (mAbs) against specific antigenic determinants on the surface of lymphocytes and functional immunological assays, have shown that fish have two cell populations, which are equivalent to B and T cells of mammals. mAbs against immunoglobulin M (IgM) of teleost serum are able to react with only one of the lymphocyte population (Lobb and Clem, 1982; DeLuca *et al.*, 1983; Secombes *et al.*, 1983; Navarro *et al.*, 1993), which suggest that the surface of Igs may be a marker for B cell-like cells and allow the isolation of the two cell populations of lymphocytes of teleost: Ig<sup>+</sup> e Ig<sup>-</sup>. Further, due to the functional studies, it has been shown that these two populations in fish (Ig<sup>+</sup> and Ig<sup>-</sup> lymphocytes) have the functional characteristics of the B and T lymphocytes of mammals, respectively (DeLuca *et al.*, 1983; Sizemore *et al.*, 1984; Miller *et al.*, 1986; Marsden *et al.*, 1995). Moreover, IgD as a second immunoglobulin isotype (Edholm *et al.*, 2011) and IgT as a third one (Danilova *et al.*, 2005; Hansen *et al.*, 2005; Uribe *et al.*, 2011) have been also identified in fish. Although the functional relevance of IgD remains to be determined, as in mammals, the teleost-specific IgT seems to be specialized in

mucosal immunity. Therefore, those antibodies would play the functional role as the equivalent of mammalian IgA (Zhang et al., 2010; Xu et al., 2013).

The immunological response of the skin and gills is important because they are in direct contact with the environment. Therefore, teleost antibodies are found not only in intestine (Zhang et al., 2010), bile (Jenkins *et al.*, 1994) and systemically in the plasma, but also in the skin (Z. Xu et al., 2016) and gill mucus (Z. Xu et al., 2016).

Like mammals, adaptive immune system of teleost presents memory (Arkoosh and Kaattari, 1991; Whittington *et al.*, 1994; Van Muiswinkel, 1995). After a first contact with the antigen, primary response develops with the production of a specific titer of antibodies in the serum that is increased with the further contact with the same antigen (secondary response). The whole process is dependent on the temperature.

As previously mentioned, the initiation of the adaptive immune response is controlled by macrophages which functions consist of degrading and presenting antigens together with MHC proteins to lymphocytes so that they can recognize the determine antigen (Clem *et al.*, 1985; Vallejo *et al.*, 1992). However, the recent studies in zebrafish shown the existence of a population of dendritic cells with antigen-presenting properties (Lugo-Villarino *et al.*, 2010).

## **2. Immune system and inflammasomes**

As described above, the innate immune system is the first line of defence against pathogens. Microbial detection is achieved through germline-encoded pattern-recognition receptors (PRRs) that survey both the extracellular and intracellular spaces for pathogen-associated molecular patterns (PAMPs), and host-derived danger signals like damage-associated molecular patterns (DAMPs)(Broz & Monack, 2013). PAMPs are exogenous signals, usually essential for microbe survival and therefore commonly preserved. PAMPs molecules include bacterial and viral nucleic acids, structural components such as cell wall components, the bacterial protein flagellin, components of the peptidoglycan bacterial cell wall, and lipopolysaccharide (LPS) from Gram-negative bacteria. Different PAMPs are specifically recognized by two main families of PRRs: the Toll-like receptors (TLRs) and the NOD-like receptors (NLRs).

In contrast, DAMPs are endogenous signals released by damaged or stressed cells that activate different receptors localized in the cytosol (Newton & Dixit, 2012). The main family of DAMPs receptors are NLRs.

Both, PAMPs and DAMPs, achieve an immune and inflammatory response through the activation of PRRs in order to induce pathogen clearance, removal of dead cells and restoration of tissue homeostasis. Maintenance of tissue homeostasis is crucial and insufficient inflammation can cause continuous infection of pathogens, whereas excessive inflammation can lead to chronic or systemic inflammatory diseases (Ahn et al., 2017).

## **2.1. PRRs**

PRRs are classified in five different families depending on their genetic and functional characteristics. The first family discovered about two decades ago is TLR family which are membrane-bound receptors located at the cell surface or on endocytic compartments. Activated TLRs can transduce the signalling to initiate innate and adaptive immune responses. (Cao, 2016; Gao, Xiong, Li, & Yang, 2017a; Qian, Liu, & Cao, 2014). The rest of the family members are unbound intracellular receptors. In this group are included the NLRs, retinoic acid inducible gene-I (RIG-I)-like receptors (RLRs), C-type lectins (CTLs), and absent-in-melanoma (AIM)-like receptors (ALRs). TLRs and CTLs are located in the plasma membrane, while the NLRs, RLRs, and ALRs are intracellular PRRs (Y. K. Kim, Shin, & Nahm, 2016b).

As described above, activation of PRRs leads to an immune and inflammatory response. The main innate response to PAMPs and DAMPs is started by TLRs and NLRs and concludes in the formation of a pro-inflammatory complex called inflammasome. Inflammasome assembly allows auto cleavage of pro-caspase1 to active caspase-1 which leads to an inflammatory response due to the release of inflammatory cytokines. Since inflammasomes are the main subject of this thesis, they will be described in detail further below.

## 2.2. Toll like receptors

Toll-like receptors were first described as transmembrane receptors involved in immune pathways using a *Drosophila melanogaster* model (Hashimoto, Hudson, & Anderson, 1988). Successive findings have described these receptors as a highly conserved family. TLRs are composed by three main structural domains: (1) a N-terminal extracellular leucine-rich repeat (LRR) domain required for ligand binding and microbial sensing through PAMPs; (2) a single transmembrane helix and (3) a C-terminal cytoplasmic Toll-IL-1R homology (TIR) domain involved in intracellular signalling. Agonist binding gets TLRs to dimerize into homodimers or change the conformation of existing dimers. It has been described that TLRs are also able to form different heterodimers depending on the bounding ligand (Bryant, Symmons, & Gay, 2015; Gao, Xiong, Li, & Yang, 2017b). Signalling through TLRs induces the activation of nuclear factor- $\kappa$ B (NF- $\kappa$ B), activator protein-1 (AP-1) and type I IFN. Moreover, the expression of TLRs is cell specific, allowing an adequate response based on the cell type and the microbial challenge (Newton & Dixit, 2012). TLRs are key inducers of the pro-inflammatory cytokines IL-1 and IL-18, but do not directly contribute to the activation of inflammatory caspases (Takeda and Akira, 2005).

The TLR protein family is conserved from insects to mammals, but TLR signalling pathways in fish exhibit different features than those in mammals. TLRs are highly expressed in the skin of zebrafish suggesting a prominent role in the defence against pathogens. To date, it has been described almost a complete set of 20 putative TLR variants in this model organism and the ligands of some of these receptors have been already described (Y. Li, Li, Cao, Jin, & Jin, 2017).

## 2.3. NOD-like receptors

In concordance with TLRs, NLRs play an important role in pathogen recognition. NLRs share three common main domains: (1) a central nucleotide-binding and oligomerization (NACHT) domain; (2) a C-terminal leucine-rich repeats (LRRs) domain which is the sensing motif able to recognize different ligands, as in TLRs; and (3) a N-terminal effector domain (caspase recruitment (CARD) or pyrin (PYD) domains). This N-terminal domain determines the classification of the NLR family into four subfamilies;

the acidic transactivation domain (NLRA), the baculoviral inhibitory repeat-like domain (NLRB), the caspase activation and recruitment domain (CARD; NLRC), and the pyrin domain (NLRP) (Figure 2) (Y. K. Kim, Shin, & Nahm, 2016a).

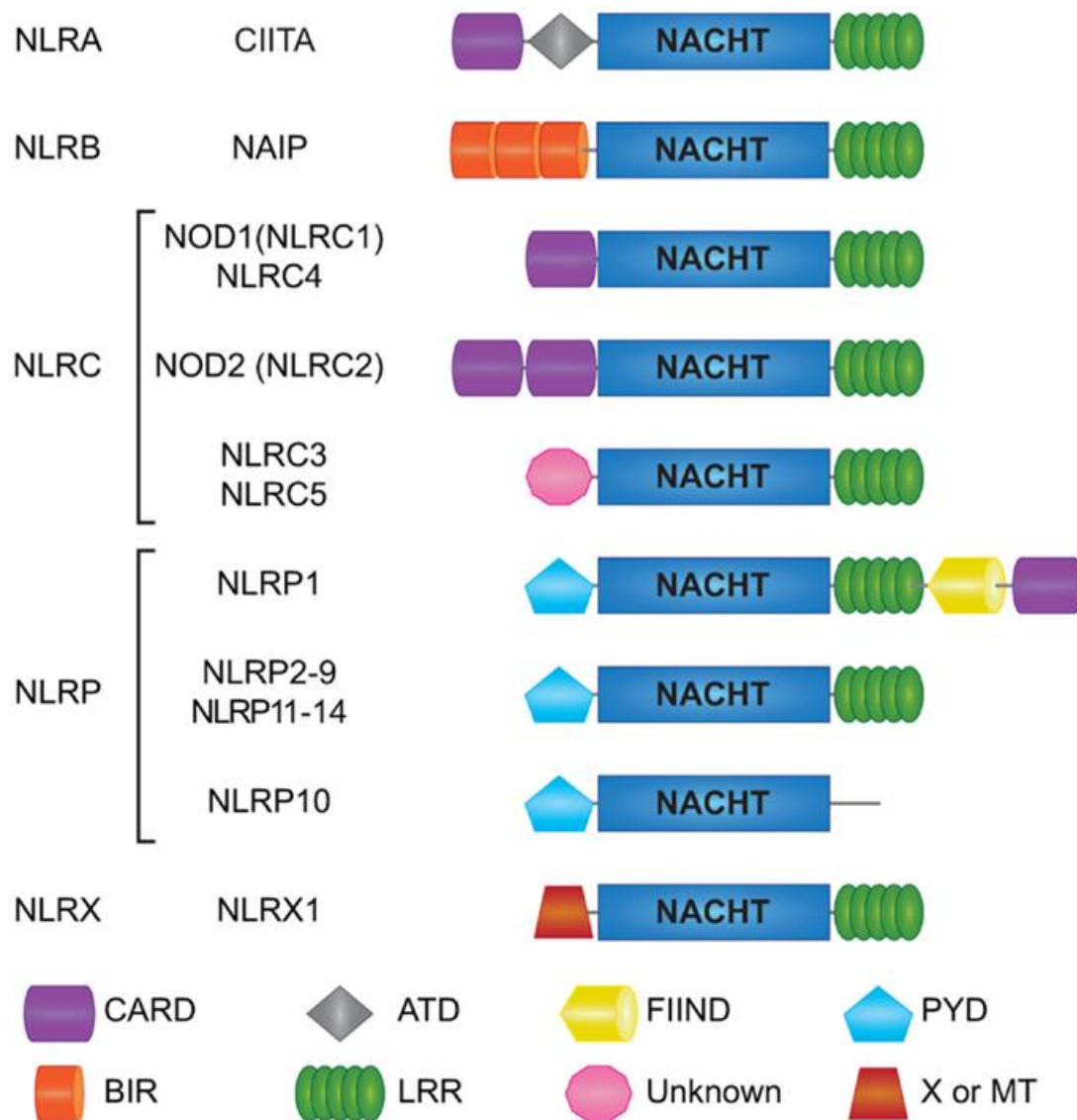


**Figure 2. Schematic representation of individual NLR domains.** CARD; caspase association and recruitment domain, ATD; acidic transactivation domain, FIIND; function to find domain, PYD; pyrin domain, BIR; Baculoviral inhibition of apoptosis protein repeat domain, LRR; leucine-rich repeats, MT; targets NLRX1 to the mitochondria but no sequence homology with traditional mitochondrial targeting sequence has been reported. Adapted from Saxena & Yeretssian, 2014.

NOD-like receptors can also be divided into four broad functional categories: inflammasome assembly, signalling transduction, transcription activation, and autophagy. Acting through the inflammasome, these receptors are the principal PRRs responsible for intracellular defence, which mediate caspase-1 processing and, thereby,

## *Introduction*

the activation of pro-inflammatory cytokines, such as interleukin-1 $\beta$  (IL-1 $\beta$ ) and IL-18, and the induction of a special program of cell death called pyroptosis (Lamkanfi & Dixit, 2014).

The diversity of effector domains allows the NLRs to interact with a wide variety of binding partners, leading to the activation of multiple signalling pathways and to their oligomerization into inflammasomes (Martinon, Mayor, & Tschopp, 2009). The most studied receptors associated to inflammasomes are NOD1, NOD2, NLRP1, NLRP3, NLRC4 (formerly IPAF) and AIM2.

NOD1 and NOD2 both recognize breakdown products of bacterial cell walls ( $\gamma$ -D-glutamyl-meso-diaminopimelic acid [iE-DAP], which is a peptidoglycan component found only in Gram-negative bacteria and MDP from both Gram-positive and Gram-negative bacteria, respectively). Upon ligand sensing, NOD1 and NOD2 oligomerize and recruit RIP2 via CARD-CARD interactions which leads to activation of the NF- $\kappa$ B signalling pathway, which plays an important role in regulating the host immune response (Schroder & Tschopp, 2010). However, a direct relation between these receptors and inflammasome activation has not been reported.

On the contrary, other members of the NLR family such as NLRPs and NLRCs, are involved in caspase-1 activation and the consequent formation of the inflammasome, a multiprotein complex. Eight members of NLRs (NLRP1, NLRP2, NLRP3, NLRP6, NLRP7, NLRP12, NLRC4, and NAIP) and AIM2 have been described to be inflammasome activators (Y. K. Kim et al., 2016a).

The NLR proteins are normally localized in the cytoplasm in an inactive, auto-repressed form. The spontaneous oligomerization and activation of the protein is inhibited by its folded structure. The LRR domain fold intramolecularly back onto the NACHT domain, which is conformationally rearranged when a PAMP binds to the LRR upon a direct or indirect manner. Once it is bound, the NACHT domain is exposed triggering the oligomerization of the receptor and the NLRs effector domain is exposed. Through a homotypic interaction, CARDS and PYDs recruit CARD- and PYD- containing effector molecules, bringing them into close proximity with each other and leading to

their activation (Tschopp, Martinon, & Burns, 2003). These proteins are the ideal molecular platform needed for the activation of inflammatory caspases.

### **3. Inflammasomes**

The concept of inflammasome was described for the first time a decade ago by Tschopp and colleagues. Inflammasome was reported as a large molecular platform required for the oligomerization and activation of the pro-inflammatory protease, caspase-1, consisting of the NLR protein NLRP1, the adaptor protein ASC (also known as PYCARD), and the two members of the inflammatory caspase subfamily, caspases-1 and -5 (Martinon, Burns, & Tschopp, 2002). A few years later other receptors of the inflammasome were described and the implication of this complex in inflammatory diseases, host defence and sepsis protection was showed (Agostini et al., 2004; S. L. Fink & Cookson, 2005; Mariathasan et al., 2004; Saleh et al., 2006).

Inflammasomes are broadly expressed in haematopoietic and non-haematopoietic cells and can trigger numerous downstream responses including production of IL-1 $\beta$ , IL-18, eicosanoids and pyroptotic cell death. Since this first description, research within the inflammasome field has been one of the most studied fields in immunology leading to huge advances. As it was described above, inflammasomes are cytosolic multiprotein complexes usually composed of sensor proteins, mainly from the NLR family, adaptor proteins such as ASC and an effector cysteine-protease enzyme, usually caspase-1. Active caspase-1 cleaves and activates a pore-forming protein called Gasdermin D (GSDMD) (Shi et al., 2015), thereby inducing cytokine release and a lytic highly pyrogenic programmed cell death termed pyroptosis.

Inflammasome activation is an essential component of the innate immune response and is critical for the clearance of pathogens or damaged cells. However, uncontrolled inflammasome activation is also a major driver of autoimmune and metabolic disorders, underlying the importance of understanding this process in physiological and pathological contexts.

### 3.1. Inflammasome receptors

Several types of factors that can activate the inflammasome acting through different receptors (Figure 3). The major studied receptors to date are NLRP1, NLRP3, NLRC4 and AIM2.

In summary, NLRPs proteins recruit the adaptor protein ASC by PYD-PYD interactions, which serves as an adaptor protein recruiting caspase-1 through CARD-CARD interactions, leading to its activation (Dick, Sborgi, Rühl, Hiller, & Broz, 2016). On the other hand, NLRC4 is able to interact directly with caspase-1 through its CARD domain and, therefore, ASC is probably not required in this process (Latz, Xiao, & Stutz, 2013). Exposure of CARD domains of ASC or NLRC4 serves as a platform for CARD domains of caspase-1 to interact, leading to its activation. Active caspase-1 has been shown to cleave several substrates, such as the pro-forms of the cytokines IL-1 $\beta$  and IL-18. It has been demonstrated that there are variable requirements for caspase-1 cleavage depending on the pathogen and the responding NLR (Guey, Bodnar, Manié, Tardivel, & Petrilli, 2014).

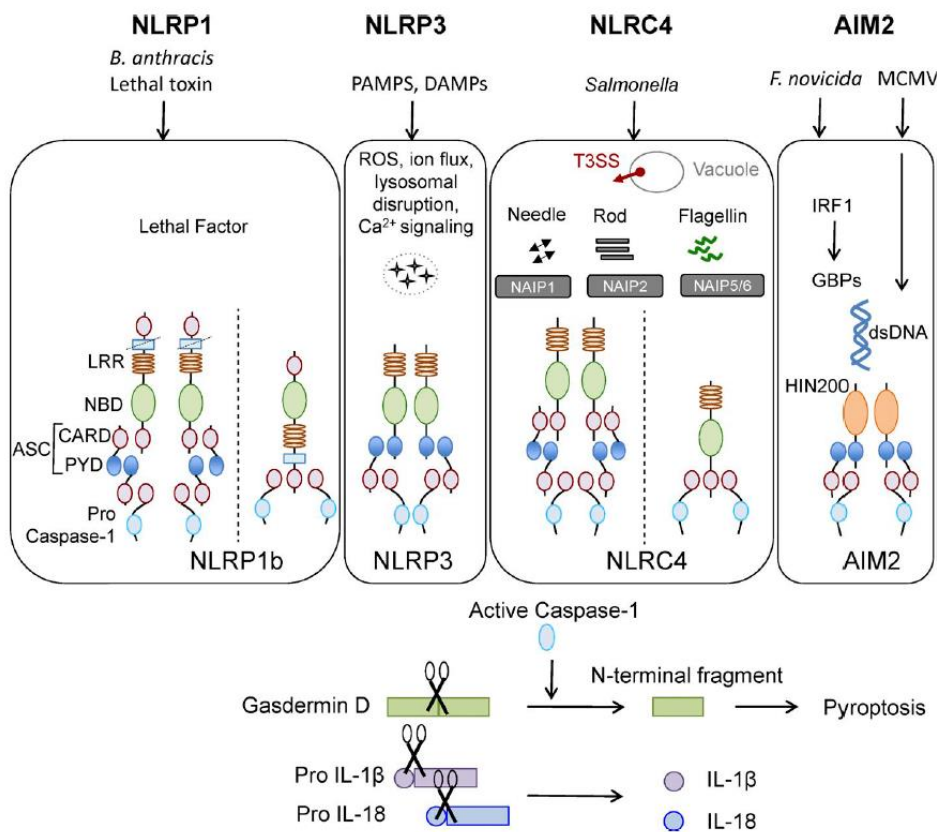


Figure 3. Canonical inflammasomes and their main activators. (Sharma & Kanneganti, 2016)

### 3.1.1. NLRP1

The NLRP1 inflammasome was the first inflammasome described. It is known to be activated by anthrax lethal toxin produced by *Bacillus anthrax*, a bipartite toxin composed of a protective antigen (PA) and a lethal factor (LF). PA generates pores on the host cell membrane, which help LF to enter the cell and cleave NLRP1 at an N-terminal site. This cleavage is required for the induction of inflammasome activation (Frew, Joag, & Mogridge, 2012; Levinsohn et al., 2012). NLRP1 activation also promotes parasite clearance and provides protection against *Toxoplasma gondii* infection in mice (Gorfu et al., 2014). In response to a high dose of LF, the CARD of NLRP1b binds the CARD of pro-caspase-1. This complex is sufficient to drive pro-IL-1 $\beta$  and pro-IL-18 processing and pyroptosis independently of ASC or caspase-1 self-proteolysis. In response to a low dose of LF, the CARD of NLRP1b recruits ASC to form a macromolecular cytoplasmic speck, where caspase-1 undergoes proteolysis and contributes to pro-IL-1 $\beta$  and pro-IL-18 processing (Man & Kanneganti, 2015).

### 3.1.2. NLRP3

NLRP3 inflammasome is the most studied in the inflammasome field. It is expressed mainly by myeloid lineage cells and responds to a wide range of infectious and endogenous ligands and is implicated in the pathogenesis of several autoinflammatory diseases, including arthritis, gout, diabetes, obesity, and Alzheimer's disease (H. Guo, Callaway, & Ting, 2015). The triggers that have been shown to induce NLRP3 activation include pathogen-derived ligands such as microbial cell wall components, nucleic acids, and pore-forming toxins; environmental crystalline pollutants like silica, asbestos, and alum; and endogenous danger signals like ATP, serum amyloid A protein, and uric acid crystals (Sharma & Kanneganti, 2016). In fact, the diversity of its activators is one of the most distinctive features of the NLRP3 inflammasome and makes the possibility of a direct interaction with each activator unlikely. It is therefore assumed that the NLRP3 inflammasome either senses a common secondary activator downstream of these stimuli or responds to cellular stress associated with infection or physiological damage.

Activation of the NLRP3 inflammasome is thought to be regulated at both the transcriptional and post-translational levels. The first signal in inflammasome activation

involves the priming signal activated through TLRs-NF- $\kappa$ B pathway that leads to upregulate the expression of NLRP3. The second signal implies the PAMPs or DAMPs ligands and initiates the assembly of the complex. Several molecular mechanisms have been suggested for NLRP3 activation to induce caspase-1 activation and IL-1 $\beta$  maturation (Jo, Kim, Shin, & Sasakawa, 2016).

### 3.1.3. AIM2

The PYHIN family protein AIM2 is the only inflammasome sensor that does not belong to the NLR family, nevertheless some structural features are shared. AIM2 contains an N-terminal PYD and a C-terminal HIN200 DNA-binding domain. This domain forms an intramolecular complex and are maintained in an autoinhibitory state. Recent work has even suggested that the role of PYD of AIM2 is not to maintain autoinhibition, but to oligomerize and drive filament formation (Morrone et al., 2015). The AIM2 inflammasome is activated by a number of microbial pathogens and dsDNA ligands, including the DNA virus mouse cytomegalovirus (MCMV), the cytosolic bacterium *Francisella novicida* and the dsDNA ligand poly(dA:dT). Cytoplasmic sugar-phosphate backbone of dsDNA binds to AIM2 inducing its activation (Man, Karki, & Kanneganti, 2016). To accomplish sufficient AIM2 inflammasome formation to allow caspase-1 cleavage DNA needs to be double stranded and of more than 80 bp in length (Jin et al., 2012). Since AIM2 lacks a CARD, it essentially requires, similar to NLRPs, the bridging protein ASC to recruit caspase-1. CARD of ASC binds the CARD of pro-caspase-1, forming a macromolecular complex known as the AIM2 inflammasome (Bauernfeind & Hornung, 2013).

### 3.1.4. NLRC4

Specific Gram-negative bacteria encoding type 3 or 4 secretion systems, such as *Salmonella enterica* serovar Typhimurium (ST), *Pseudomonas aeruginosa* and *Legionella pneumophila*, trigger activation of the NLRC4 inflammasome, which is important in innate immunity by its capacity to eliminate viruses, bacteria and parasites because their function. It has been demonstrated that two bacterial proteins, flagellin and PrgJ, activate NLRC4, however, the physical interaction between both PAMPs and NLRC4 has never been shown. NLRC4 activation by these ligands is mediated by NAIP coreceptors, also encoded within the NLR family (Kofoed & Vance, 2011; Zhao et al., 2011). In mice,

NAIP5 and NAIP6 (NLR family, apoptosis inhibitory protein 5 and 6), have been shown to detect flagellin (Lightfield et al., 2011). NAIP5 engagement by flagellin promotes a physical NAIP5–NLRC4 association, rendering full reconstitution of a flagellin-responsive NLRC4 inflammasome in non-macrophage cells.

The related NAIP2 functioned analogously to NAIP5, serving as a specific inflammasome receptor for T3SS rod proteins such as *Salmonella* PrgJ and *Burkholderia* BsaK. PrgJ-NAIP2-NLRC4 inflammasome is assembled into multi subunit disk-like structures through a unidirectional adenosine triphosphatase polymerization, primed with a single PrgJ-activated NAIP2 per disk. Analysis by cryo–electron microscopy (cryo-EM) reconstruction showed that a single PrgJ-activated NAIP2 initiates NLRC4 polymerization in a domino-like reaction to promote the disk assembly (W. Lu et al., 2015).

In addition, the expression of Naip1, Naip2, Naip5, and Naip6 is dependent on IRF8 in murine BMDMs, which is required for the optimal activation of NLRC4 inflammasome but dispensable for the activation of NLRP3 and AIM2 inflammasomes (Karki et al., 2018).

On the other hand, only one NAIP orthologue has been found in humans (known as hNAIP) and this is necessary to sense a type III secretion needle protein (Figure 4). Unfortunately, it remains to be determined whether and how human NLRC4 senses flagellin without another NAIP homologues (Latz et al., 2013).

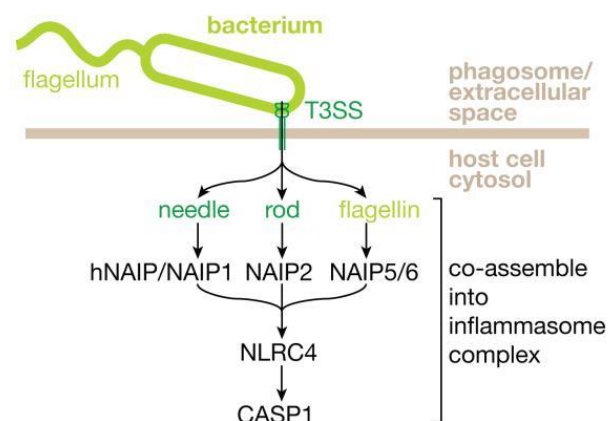


**Figure 4. Recognition of bacterial flagellin and T3SS components by NAIPs** (Vance, 2015)

## Introduction

The ligand-bound NAIPs appear to drive conformational changes in NLRC4 that expose the NACHT domain for the recruitment and activation of further NLRC4 molecules (Diebolder, Halff, Koster, Huizinga, & Koning, 2015; Z. Hu et al., 2013; Zehan Hu et al., 2015).

In addition to these NAIP sensors, recent studies showed the importance phosphorylation of NLRC4 at serine 533 for activation of the NLRC4 inflammasome following infection with *S. Typhimurium* or transfection of flagellin purified from *S. Typhimurium* which occurs previous to the NLRC4 activation by NAIPs (Matusiak et al., 2015; Qu et al., 2012). However, this post-translational modification is required for optimal caspase-1 activation, but it is not essential. NLRC4 mutant S533A, like wild-type NLRC4, can bind to NLRP3 protein that is induced after infection and then NLRP3 engages ASC to activate caspase-1 (Qu et al., 2016a).

The NLRC4 oligomers nucleate the filament formation of the adapter protein ASC and protease caspase-1 providing an efficient response against infections through the removal of infected cells by pyroptosis and the propagation of inflammation through IL-1 $\beta$  and IL-18. Furthermore, NLRC4 can interact directly with caspase-1 to induce cell death and an eicosanoids storm that includes prostaglandins and leukotrienes release and rapidly initiate inflammation and vascular fluid loss (von Moltke et al., 2012). This pathway also leads to actin reorganization which helps to arrest bacteria inside dying macrophages for further elimination by neutrophils (Man, Ekpenyong, et al., 2014), and this process occurs independently of IL-1 $\beta$  or IL-18 production (Figure 5) (Sellin et al., 2014). Accordingly, NLRC4 activation in epithelial cells is specifically required to control pathogen load during *S. Typhimurium* infection. At the same time, neutrophils activate the NLRC4 inflammasome themselves during acute *S. Typhimurium* infection and are a major cell compartment for IL-1 $\beta$  production during acute peritoneal challenge *in vivo*. Importantly, unlike macrophages, neutrophils do not undergo pyroptosis upon NLRC4 inflammasome activation (K. W. Chen et al., 2014).

Other studies indicate that NLRC4 activates an alternative cell death program morphologically similar to apoptosis in caspase-1 or GSDMD deficient BMDMs. In this case, caspase-8 is recruited to the Naip5/NLRC4/ASC (Lee et al., 2018; Mascarenhas et al., 2017).

Overall, all these studies highlight the importance of NLRC4 inflammasome in cellular responses beyond the conventional roles of cytokine release and pyroptosis. Moreover, human genetic studies expose that gain-of-function mutations in NLRC4 are associated with autoinflammation and enterocolitis and that NLRC4 has a role in inflammasome independent mechanisms such as cancer protection (Duncan & Canna, 2018; Hafner-Bratkovič, 2017).

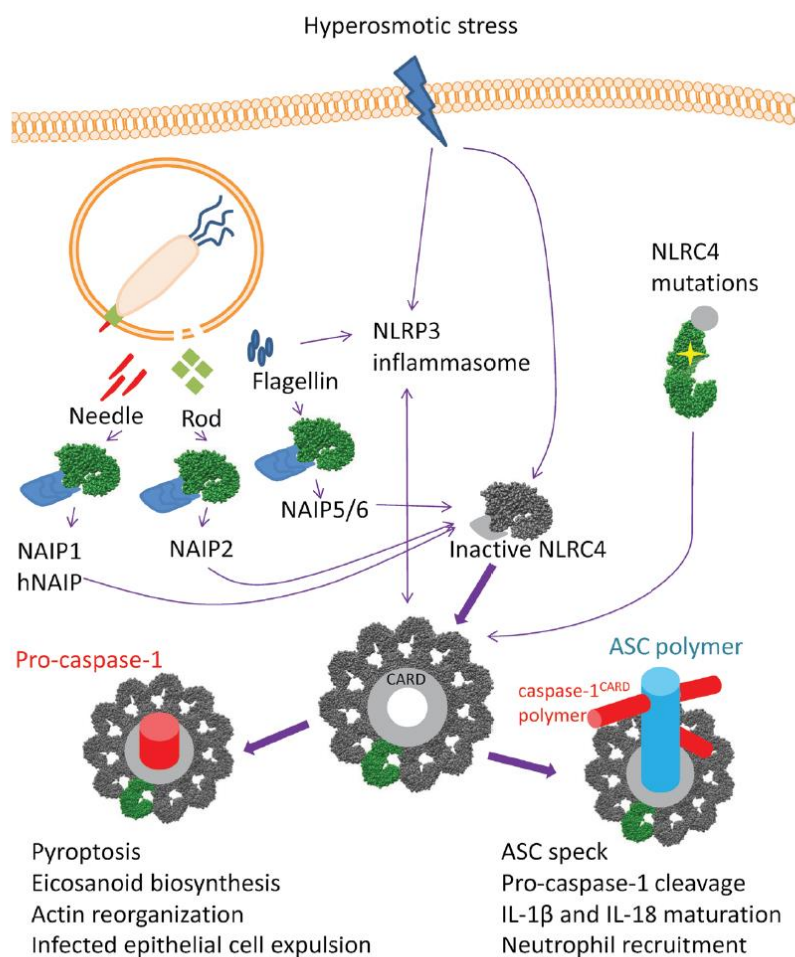


**Figure 5 Crosstalk between NLRC4 and NLRP3** (Hafner-Bratkovič, 2017)

### 3.2. Adaptor protein; ASC

Another molecule essential in assembly of the inflammasome complex is ASC, also called PYCARD. In this multiprotein assembly complex ASC protein plays an important role. This adaptor molecule was originally identified in the insoluble cytosolic fraction, called speck, of the cells undergoing apoptosis (J Masumoto et al., 1999). It is

composed of an N-terminal PYD domain and a CARD domain, which allows the interaction with other inflammasome components.

The interaction between major inflammasome components occurs through homotypic PYD–PYD or CARD–CARD interactions. The PYD and CARD domains possess nucleating ability that allows them to induce oligomerization, forming the structural basis for assembly of inflammasomes (Dick et al., 2016; A. Lu et al., 2014). Recent studies show that assembly of the ASC speck involves oligomerization of ASC-PYD into filaments and cross-linking of these filaments by ASC-CARD. The CARD domain is essential to form the ASC speck, as ASC mutants with a non-functional CARD only assemble filaments and moreover disrupt endogenous specks in primary macrophages.

Systematic site-directed mutagenesis of ASC-PYD is used to identify oligomerization-deficient ASC mutants (ASCE80R or ASCY59A) and demonstrate that ASC speck formation is required for efficient processing of IL-1 $\beta$ , but dispensable for GSDMD cleavage and pyroptosis induction (Figure 6) (Dick et al., 2016).

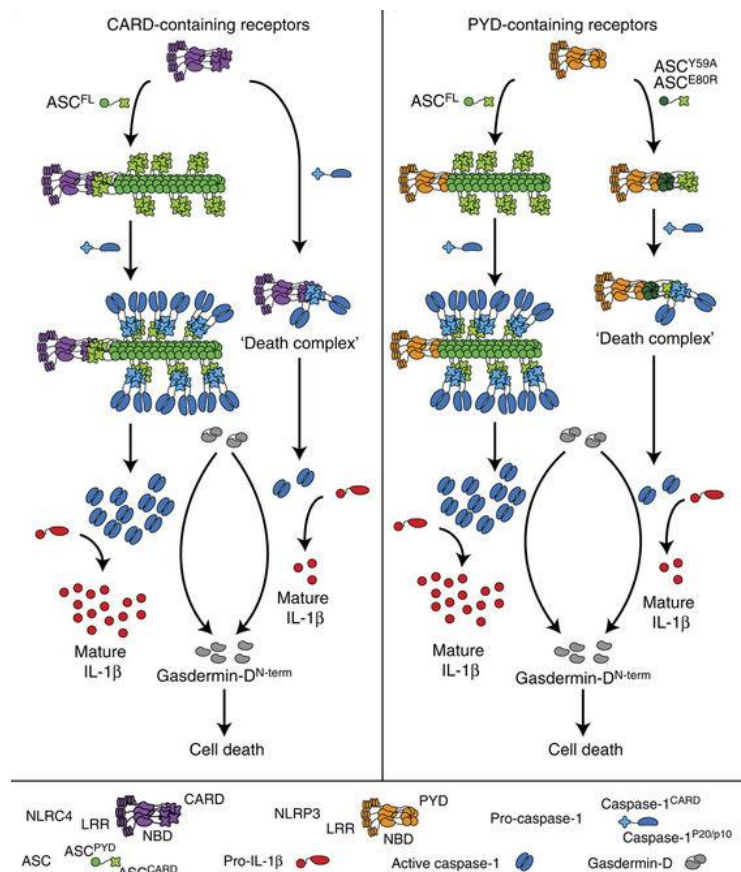


Figure 6. ASC oligomerization model. Adapted from Dick et. al, 2016.

### 3.3. Effector proteins

#### 3.3.1. Caspase-1

Caspases are a family of cysteine proteases that cleave after aspartate residues (Asp) (E. A. Miao et al., 2010). Although caspase-mediated processing can result in substrate inactivation it may also generate active signalling that participates in ordered processes (McIlwain *et al.*, 2013) and develop key roles in the apoptosis and proteolytic activation of cytokines (Nicholson, 1999; Boatright and Salvesen, 2003; Nadiri *et al.*, 2006). In humans, the caspase family includes 13 members, whose functions seem to correlate with their phylogenetic relationship (Lamkanfi *et al.*, 2002). Cell death caspases are initiators (caspase-2, -8, -9, and -10) and executioners (caspase-3, -6, and -7) of apoptosis (Nadiri *et al.*, 2006). Initiator caspases sense death signals, and activate more downstream effectors caspases, which cleave cellular substrates, mediating the changes associated with apoptosis. Human inflammatory caspases include caspase-1, -4, -5 and -12. In mice, caspase-5 is absent but they have an additional inflammatory caspase, caspase-11, which has probably arisen by tandem gene duplication of caspase-4 (Nadiri *et al.*, 2006). The arrangement of the exon-intron structure of the inflammatory caspases, suggest that they originated from the same ancestral gene. Both inflammatory and apoptotic caspases are synthesized as inactive zymogens, situated in the cytosol and share a common conserved structure composed of a prodomain and a catalytic region (Lamkanfi *et al.*, 2002; Nadiri *et al.*, 2006; Miao *et al.*, 2011).

Caspase-1 is one of the best characterized inflammatory caspases. Originally, caspase-1 was found in an attempt to purify the enzyme responsible for IL-1 processing (Thornberry *et al.*, 1992), although later it was also shown to be able to activate IL-18 (Gracie *et al.*, 2003; Martinon and Tschopp, 2004; Dinarello, 2005). While Caspase-1 was once thought to also process IL-33, this is no longer believed to be the case (Cayrol *et al.*, 2009; Luthi *et al.*, 2009; Talabot-Ayer *et al.*, 2009; Ali *et al.*, 2010). Caspase-1, like other pro-inflammatory caspases, contains an N-terminal caspase-recruitment domain (CARD), and a catalytic region composed of both a large (p20) and a small (p10) subunits with a conserved Gln-Ala-Cys-X-Gly active site sequence (where X is Arg, Gln or Gly) found in the large subunit. There are other structural proteins that have this CARD

## Introduction

domain, like the adaptor protein ASC that binds to caspase-1, producing the oligomerization of pro-caspase-1 within the inflammasome, facilitating the caspase auto-cleavage into the p20 and p10 subunits (Stehlik *et al.*, 2003; Mariathasan *et al.*, 2004). These p10 and p20 subunits, once released, form an active heterotetramer that acts as a very efficient IL-1-converting enzyme (Guey *et al.*, 2014). However, this dogma has recently been challenged by an elegant study (Boucher *et al.*, 2018). Thus, in the cell, the dominant species of active caspase-1 dimers elicited by inflammasomes are in fact full-length p46 and a transient species, p33/p10. In addition, p33/p10 autoprocessing occurs with kinetics specified by inflammasome size and cell type, and this releases p20/p10 from the inflammasome, which becomes unstable and protease activity is terminated.

Although pro-caspase-1 is constitutively expressed in resting cells, it remains inactive in the cytoplasm until inflammatory cells, like monocytes or macrophages, receive the appropriate stimulus (Martinon *et al.*, 2002). In addition, caspase-11 (also known as caspase-4) is critical for caspase-1 activation and IL-1 production in macrophages infected with *Escherichia coli*, *Citrobacter rodentium* or *Vibrio cholerae* (Kayagaki *et al.*, 2011). In macrophages, K<sup>+</sup> release induces a rapid and strong activation of caspase-1, triggering the processing and release of the mature IL-1 (Gudipaty *et al.*, 2003). Although the channel involved in this mechanism has remain elusive for decades, a recent study has identified the two-pore domain K<sup>+</sup> channel (K2P) TWIK2 as the K<sup>+</sup> efflux channel triggering NLRP3 inflammasome activation in mouse macrophages (Di *et al.*, 2018).

Interestingly, functions for caspase-1 different for those known to date have recently been identified. Thus, it has been shown that caspase-1 can stimulate the biogenesis of the membrane to repair the damage produced by the pore-forming toxins, promoting cell survival as a mean of resisting infection by pathogenic bacteria (Gurcel *et al.*, 2006). It has also been shown that caspase-1 takes part in the NF- $\kappa$ B activation via TLR2 and TLR4 (Miggin and O'Neill, 2006). These results highlight the importance of this enzyme to regulate different aspects of the immune response.

Despite the importance of caspase-1 in inflammation, the information on the presence and activity of this enzyme in fish is scant. Inflammatory caspases have so far

only been found in vertebrates (Martinon and Tschopp, 2004). In zebrafish and pufferfish, two subgroups of inflammatory caspases with a highly conserved caspase domain were discovered. The first subgroup is formed by Caspa and Caspb with highly conserved catalytic domain, and with an N-terminal pyrin domain (PYD) rather than the typical CARD of inflammatory caspases (Lamkanfi *et al.*, 2002; Huising *et al.*, 2004). Nevertheless, recent studies have demonstrated that Caspa is the functional homologue of mammalian CASP1 in zebrafish and mediates inflammasome effector functions in both neutrophils and macrophages (Kuri *et al.*, 2017; Tyrkalska *et al.*, 2016; Vincent, Freisinger, Lam, Huttenlocher, & Sauer, 2016). Curiously, the first caspase-1 homologue of fish showing the N-terminal CARD domains has been identified in gilthead seabream (López-Castejón *et al.*, 2008) but this caspase-1 is unable to process IL-1 (Angosto *et al.*, 2012).

### 3.3.2. IL1

IL-1 is the common name for a diverse family of proteins (11 cytokines), of which IL-1 $\alpha$ , IL-1 $\beta$ , IL-1 receptor antagonist (IL-1ra) and IL-18 are the most representative and studied, although several newly discovered molecules show a clear homology to this group (Dinarello, 1997; Dinarello, 1999; Busfield *et al.*, 2000; Smith *et al.*, 2000; Debets *et al.*, 2001; Lin *et al.*, 2001; Pan *et al.*, 2001). Members of that family induce a complex network of pro-inflammatory cytokines and via expression of integrins on the surface of leukocytes and endothelial cells, regulate and initiate inflammatory responses (Dinarello, 2011).

Both IL-1 $\alpha$  and IL-1 $\beta$  are produced by many different cell types (Oppenheim *et al.*, 1986), including neutrophils, natural killer cells, B-lymphocytes, T-lymphocytes and cells of the central nervous system. However, the main producing cells are blood monocytes and tissue macrophages (Lepe-Zuniga and Gery, 1984; Dinarello *et al.*, 1986; Dinarello, 1988; Arend *et al.*, 1989), which are an important source because of their strategic locations, ability to synthesize large amounts of IL-1 and to process the IL-1 precursor more effectively than other cells.

The alignment of vertebrates IL-1 amino acid sequences shows higher homology in regions containing the secondary structure of the IL-1 $\beta$  molecule. The IL-1 family

signature is conserved in the IL-1 $\beta$  sequences of mammals, birds and amphibians, but is only partially conserved in fish.

IL-1 $\alpha$  and IL-1 $\beta$  bind to the same receptor molecule, which is called IL-1RI. There is a third ligand of this receptor – the Interleukin 1 receptor antagonist (IL-1Ra), which does not activate downstream signalling, so it acts as an inhibitor of IL-1 $\alpha$  and IL-1 $\beta$  signalling by competing with them for binding sites of the receptor (Weber *et al.*, 2010; Dinarello, 2011). Activation of the signalling pathways lead to activation of many transcription factors, such as NF- $\kappa$ B, AP-1, c-Jun N-terminal kinase (JNK) and p38 MAPK (Simi *et al.*, 2007; Weber *et al.*, 2010).

The role of IL-1 in the immune response has been partly elucidated by expression studies. In mammals, IL-1 $\beta$  is produced in response to many stimuli, including bacterial LPS, numerous microbial products, cytokines (TNF, IFN- $\gamma$ , GM-CSF and IL-2), T-cell/antigen-presenting cell interactions and immune complexes (Stylianou and Saklatvala, 1998). Similar studies have revealed that bird, amphibian and fish IL-1 show a similar expression pattern to its mammalian counterpart. In chicken, IL-1 $\beta$  is quickly induced in blood monocyte-derived macrophages, reaching optimal levels within 1 h after LPS treatment (Weining *et al.*, 1998). The *Xenopus* IL-1 $\beta$  transcript was inducible *in vivo* following injection with LPS (Zou *et al.*, 2000a). In fish, IL-1 expression studies have usually been performed by RT-PCR or Northern blot and it has been shown that *in vivo* and *in vitro* treatment with LPS is able to induce IL-1 mRNA in all the species tested, including carp, trout, seabass and catshark (Zou *et al.*, 1999a; Zou *et al.*, 1999b; Zou *et al.*, 2000b; Scapigliati *et al.*, 2001; Engelsma *et al.*, 2001; Bird *et al.*, 2002a). In trout many expression studies have been developed. Thus, it is known that stimulation with 5 g/ml LPS induces the expression of IL-1 1 h after stimulation, reaching maximum levels after 4 h. In addition, culture temperature has a marked effect on IL-1 expression, because a temperature increase acts as a positive regulator in IL-1 synthesis (Zou *et al.*, 2000b). Moreover, IL-1 expression levels of the trout mononuclear phagocyte cell line RTS-11 are up-regulated after LPS treatment (Brubacher *et al.*, 2000). In seabream, IL-1 mRNA accumulation is induced in leukocytes after bacterial challenge (Chaves-Pozo *et al.*, 2004) or *in vitro* stimulation with different PAMPs (Sepulcre *et al.*, 2007). The protein is also accumulated in leukocytes activated with LPS or bacterial DNA, as detected by

western blot using a polyclonal Ab to seabream (Pelegrín *et al.*, 2004). Furthermore, seabream is not processed by Casp1 and the stimuli known to activate the NLRP3 and NLRC4 inflammasomes fail to promote IL-1 $\beta$  processing and release by seabream macrophages (Angosto *et al.*, 2012). In European seabass and zebrafish, however, *in vitro* studies reported that Casp1 and Caspa, respectively, processed IL-1 $\beta$  (Reis, do Vale, Pereira, Azevedo, & Dos Santos, 2012; Vojtech, Scharping, Woodson, & Hansen, 2012).

### 3.3.3. Pyroptosis and GDSMD

Many forms of the programmed cell death pathways are critical for organogenesis, development, immunity or even the maintenance of homeostasis in multicellular organisms. Inflammasome activation leads to a distinct form of programmed cell death termed pyroptosis. Pyroptosis consists on a highly pro-inflammatory form of cell death, essential in the innate immune response to prevent the spread of the intracellular infection. It is characterized by cellular lysis, release of intracellular components, and an inflammatory response. Pyroptosis is induced by the activation of pro-inflammatory caspases within inflammasomes (Bergsbaken, Fink, & Cookson, 2009; Boucher, Chen, & Schroder, 2016).

Pyroptosis was described for the first time in 1992, when the Sansonetti's laboratory observed that murine macrophages infected with the Gram-negative bacterium, *Shigella flexneri*, were undergoing a form of cell death which was similar to apoptosis (Zychlinsky, Prevost, & Sansonetti, 1992). A few years later similar observations were seen in cells infected with a closely related pathogen, *S. Typhimurium*, reporting the presence of DNA degradation, changes in nuclear morphology and finally vacuole formation (Monack, Raupach, Hromockyj, & Falkow, 1996). In addition to these apoptosis-like features, Cookson and co-workers reported that cell death by such infected cells also presented features similar to other death type: necrosis (Brennan & Cookson, 2000). Pyroptosis involves the formation of 1- to 2-nm pores on the cell membrane (de Vasconcelos, Van Opdenbosch, Van Gorp, Parthoens, & Lamkanfi, 2018; S. L. Fink & Cookson, 2005). It further proceeds through cytoplasmic swelling, osmotic lysis, and release of intracellular contents. Similar to apoptosis are the features of nuclear condensation and DNA damage (S. L. Fink & Cookson, 2006), but differing from apoptosis the nucleus remains intact and karyorrhexis does not occur.

Furthermore, cells dying by necrosis or pyroptosis secrete pro-inflammatory cytokines and release their cytoplasmic content, into the extracellular space (Z. S. Guo, Liu, & Bartlett, 2014), whereas in classic apoptosis, the retention of plasma membrane integrity and the formation of apoptotic bodies render it an immunologically silent death mode (Figure 7).

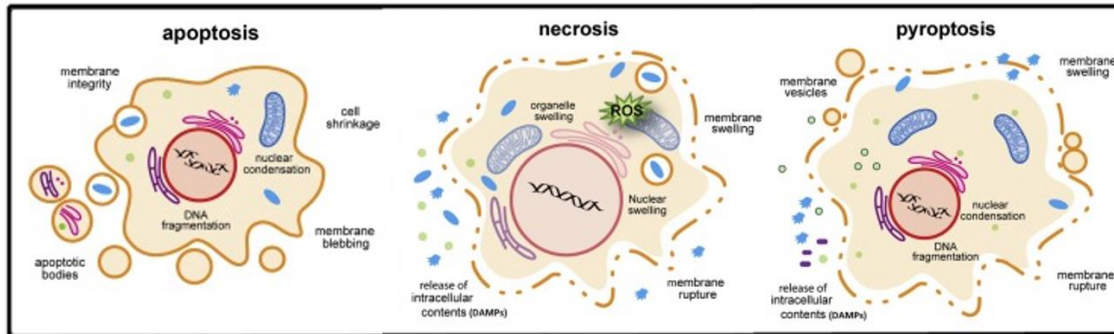


**Figure 7. Three key modes of cell death.** In classic apoptosis, the retention of plasma membrane integrity and the formation of apoptotic bodies render it an immunologically silent death mode. Whereas, cells dying by necrosis or pyroptosis secrete pro-inflammatory cytokines and release their cytoplasmic content, into the extracellular space (Guo et al., 2014).

Beside the formation of pores in the plasma membrane was directly linked to pyroptotic cell death, the exact mechanism underlying the formation of these pores remained unknown. In 2015, GSDMD was simultaneously identified by different researcher as the main pore formation mediator during pyroptosis (Kayagaki et al., 2015; Shi et al., 2015). GSDMD acted downstream caspase-1 and caspase-11 and it was shown that GSDMD is a substrate of caspase-1 and its cleavage at the predicted site during inflammasome activation was required for pyroptosis and IL-1 $\beta$  secretion (W. He et al., 2015). Once is cleaved GSDMD N-terminal domain assembles membrane pores to induce cytolysis, whereas its C-terminal domain inhibits cell death through intramolecular association with the N domain (Z. Liu et al., 2018).

Pyroptosis occurs mainly in innate immune cells, such as monocytes and macrophages (Edgeworth, Spencer, Phalipon, Griffin, & Sansonetti, 2002; S. L. Fink, Bergsbaken, & Cookson, 2008). Pyroptosis of infected cells is appearing as an important mechanism of microbial clearance (E. A. Miao et al., 2010), in addition to host defence mechanisms coordinated by inflammasome dependent IL-1 $\beta$  (K. W. Chen et al., 2014) and IL-18 (Franchi et al., 2012). Macrophage pyroptosis releases S.

*S. Typhimurium* from its intracellular replicative niche, and therefore increases its susceptibility to neutrophil mediated extracellular destruction. Recent studies show that, in contrast to its activation in macrophages, GSDMD cleavage and activation in neutrophils was caspase independent and mediated by a neutrophil-specific serine protease, neutrophil elastase (ELANE), released from cytoplasmic granules into the cytosol in aging neutrophils. ELANE-mediated GSDMD cleavage was upstream of the caspase cleavage site and produced a fully active ELANE-derived NT fragment (GSDMD-ENT) that induced lytic cell death (Kambara et al., 2018).

The ability to undergo pyroptotic death is not unique to immune cells. For example, pyroptosis of the gut epithelium promotes the extrusion of infected cells into the gut lumen, preventing *S. Typhimurium*, and probably other pathogens, from traversing the epithelial barrier to invade the host (Knodler et al., 2014).

## 4. Zebrafish

### 4.1. Description, distribution, taxonomy, ecology and reproduction

Taxonomically, the zebrafish (*Danio rerio*) is a derived member of the genus *Danio*, of the family Cyprinidae, order Cypriniformes. Zebrafish (zf) is a small shoaling cyprinid fish, which size reaches maximum 60 mm (Figure 8). Their natural range is close to the Ganges and Brahmaputra river basins in north-eastern India, Bangladesh, and Nepal. They are most commonly encountered in shallow ponds and standing water bodies with visibility to a depth of approximately 30 cm, often connected to rice cultivation (Spence *et al.*, 2008).



**Figure 8. Adult zebrafish. Adapted from [www.zebrafishfilm.org](http://www.zebrafishfilm.org)**

Zebrafish are promiscuous and breed seasonally during monsoon season, which occur from April to August (spawning has also been recorded outside wet season, suggesting that breeding may be seasonal as a result of food availability). Mating behaviour is also heavily influenced by photoperiod, as spawning begins immediately at first light during breeding season and continues for about an hour. In order to initiate courtship about 3 to 7 males chase females and try to lead female towards a spawning site by nudging her and/or swimming around her in a tight circle. The female releases 5 to 20 eggs at a time. This cycle repeats for about an hour. While the presence of female pheromones is required for initiation of courtship behaviour in the male, male gonadal pheromones are required by the female for ovulation to occur. There is limited evidence for male-male competition and female mate preference (Spence *et al.*, 2006). When a breeding pair reaches the spawning site, the male aligns his genital pore with the female's and begins to quiver, which causes the female to release her eggs and the male to release his sperm. Although time to hatch depends on water temperature, most eggs hatch between 48 and 72 hours after fertilization. Chorion thickness and embryo activity also impact incubation time. Zebrafish are approximately 3 mm upon hatching and are immediately independent. They are able to swim, feed, and exhibit active avoidance behaviors within 72 hours of fertilization (Engeszer *et al.*, 2004; Engeszer *et al.*, 2007a; Engeszer *et al.*, 2007b).

Zebrafish are omnivorous, feeding primarily on zooplankton and insects, although phytoplankton, filamentous algae and vascular plant material, spores and invertebrate eggs, fish scales, arachnids, detritus, sand, and mud have also been reported from gut content analyses (Spence *et al.*, 2008).

### 4.1.1. Zebrafish as a vertebrate research model

During many years zebrafish was used in aquarium field but nowadays and taking in account all advantages in research of this models is every day more popular between researchers. Main features of the model are:

- Small size. Low maintenance cost and small space needed.
- Robust fish. High resistance to pathogens.
- High fecundity and large production of embryos (around 200 eggs/female/week).

- Short generation time (for a vertebrate). Typically 3 to 4 months, making it suitable for selection experiments.
- Zebrafish eggs are large relative to other fish (0.7 mm in diameter at fertilization time), optically transparent and externally developed following fertilization, making them easily accessible to embryonic manipulation and imaging.
- Transparency of zebrafish embryos, together with the large availability of transgenic lines, let *in vivo* tracking of cells.
- Rapid development, which is very similar to the embryogenesis in higher vertebrates including humans, the precursors develop to all major organs within 36 hours, and larvae display food seeking and active avoidance behaviour within five days after fertilization (2 to 3 days after hatching).
- Type-based forward genetics doable.
- Easy to transfer among different labs by transporting their eggs.
- The zebrafish genome has now been completely sequenced, making it an even more valuable research organism.
- As a vertebrate, zebrafish shares considerable genetic sequence similarity with humans.
- It is relatively easy to knockdown specific genes by using morpholinos and overexpressing proteins by mRNA or plasmids.
- Existence of a centralized online resource for the zebrafish research community (<http://zfin.org>), making easier the work with this model.

As a vertebrate, zebrafish has special value as a model of human disease and for the screening of therapeutic drugs (Chakraborty *et al.*, 2009) and is often more tractable for genetic and embryological manipulation and cost effective than other vertebrate models such as mice (Trede *et al.*, 2004).

Use of reverse genetics approaches using zinc finger nucleases (ZFNs) (Meng *et al.*, 2008) and a transposon strategy (Kawakami, 2004) for generating transgenic zebrafish, which help in analysing new roles of additional genes in larval and adult zebrafish. Furthermore, recent advances demonstrate that the CRISPR-Cas system functions *in vivo* to induce targeted genetic modifications in zebrafish embryos with

## *Introduction*

efficiencies similar to those obtained using zinc finger nucleases and transcription activator–like effector nucleases (Hwang et al., 2013) which have radically reduced the efforts to introduce targeted genome engineering (J. Liu et al., 2017).

All these advantages have led to the increased interest of scientists using zebrafish as an animal model research in the last years, therefore, research in inflammasome using zebrafish has also increased. Although several key components of the inflammasome have already been characterized in mammals, little is known about the proteins that form part of the inflammasome in other vertebrate groups (Angosto & Mulero, 2014). At present, the function of NLRs in lower vertebrates and invertebrates is less well understood than that in mammals. Three distinct NLR subfamilies were found when mining genome databases of various non-mammalian vertebrates; the first subfamily (NLR-A) resembles mammalian NODs, the second (NLR-B) resembles mammalian NLRPs, and the third (NLR-C) appears to be unique to ray-finned fish (class Actinopterygii) (Laing, Purcell, Winton, & Hansen, 2008), containing 405 NLR genes that are unique to teleost fish (Howe et al., 2016). Recent reports have indicated that several members of the mammalian NLR family, namely NOD1, NOD2 and NLRC3, are conserved in zebrafish, and probes the importance of NOD-like receptors for innate antibacterial immunity in teleost fish (Y. Li et al., 2017).

In addition, the zebrafish has a ASC orthologue (accession number NM\_131495), which encodes for the ASC adaptor protein and it has been already used to facilitate the study of endogenous ASC dynamics (Kuri et al., 2017). However, orthologs of caspase-1 seem to be restricted to the superorders Protacanthopterygii (trout and salmon) and Acanthopterygii (seabream, seabass, and medaka) of ray-finned fish (Angosto et al., 2012; López-Castejón et al., 2008), while most primitive Ostariophysi (catfishes and zebrafish) do not have caspase-1 orthologs. Fortunately, a functional homolog of mammalian caspase-1 has been reported in the zebrafish, caspase a (Caspa), which harbors N-terminal PYD and C-terminal CARD domains (Junya Masumoto et al., 2003; Vincent et al., 2016). It has recently been shown that the activation of different inflammasomes is fine-tuned by several proteins, including the interferon-induced guanylate-binding proteins (B.-H. Kim et al., 2016; Tyrkalska et al., 2016). Therefore,

many pieces are still necessary to solve this puzzle and to elucidate which proteins are involved in inflammasome activation.

## **5. *Salmonella enterica* serovar Typhimurium (ST)**

Infectious diseases, such as salmonellosis, are responsible for one-third of all mortality worldwide and have become a significant public health threat in both developed and developing countries. *Salmonella* is a global food-borne pathogen that infects and replicates within macrophages of both humans and animals and cause an estimated 93.8 million salmonellosis infections and 155,000 deaths globally each year (Sotomayor et al., 2018). A critical step in disease pathogenesis for many clinically important bacteria is their ability to infect and survive within host cells. Control of its infection is difficult due to the bacterium high tolerance to environmental stress, widespread distribution, multiple drug resistance, and adaptability. Moreover, continuous genetic re-assortment in *Salmonella*, leads to increased virulence and the emergence of resistance to multiple drugs, is of significant public health concern (Branchu, Bawn, & Kingsley, 2018; H.-M. Chen, Wang, Su, & Chiu, 2013).

*Salmonella* is a gram-negative, non-spore-forming, rod-shaped bacteria, which belong to the *Enterobacteriaceae* family. These microorganisms can range from around 0.7 to 1.5  $\mu\text{m}$  in diameter and 2 to 5  $\mu\text{m}$  in length. They are facultative anaerobes and show predominantly peritrichous motility.

Virulence of *Salmonella* species is mainly due to type III secretion systems (T3SSs) are multiprotein structures which transport proteins across the two membranes of the bacterial cell and a third membrane of the target host cell (Cornelis & Van Gijsegem, 2000). Once inside the cell, these proteins can alter cellular functions such as cytoskeleton structure, membrane transport, signal transduction, and cytokine expression (Sotomayor et al., 2018). These changes allow for the invasion and permanence of the bacterium in the infected cell.

ST encodes two different T3SSs, which are responsible for the performance of a range of virulence functions during the infection. The *Salmonella* Pathogenicity Island 1 (SPI-1) T3SS is still activated in extracellular bacteria and translocate effectors through

## Introduction

the host cell plasma membrane. Those actions lead to localized actin polymerization, membrane ruffling and entry of bacteria into the host cell (Galán, 2001), where they remain in a membrane-bound compartment known as the *Salmonella*-containing vacuole (SCV). The second T3SS, also encoded by a pathogenicity island (SPI-2), is activated already in intracellular bacteria, probably in response to low  $[Ca^{2+}]$  and  $[Fe^{2+}]$ , acidic pH and low osmolarity (Lee *et al.*, 2000; Zaharik *et al.*, 2002; Garmendia *et al.*, 2003) in the SCV. SPI-2 gene expression begins at 1 h after uptake of bacteria by host cells, and increases with the time, over the next few hours (Cirillo *et al.*, 1998; Uchiya *et al.*, 1999; Beuzón *et al.*, 2000; Knodler *et al.*, 2002; Kuhle and Hensel, 2002; Garmendia *et al.*, 2003). The expression of SPI-2 genes and associated effectors is controlled by the SsrA-SsrB, two component of regulatory system, which are encoded within SPI-2 (Cirillo *et al.*, 1998).

The SPI-2 T3SS secretes three proteins – SseB, SseC and SseD – that are required for translocation of the effector proteins into and across the vacuolar membrane (Nikolaus *et al.*, 2001), and therefore they are considered to be components of a translocon. The translocated effectors are encoded both within and outside SPI-2, and enable intracellular replication of bacteria in macrophages, epithelial cells and fibroblasts (Hensel *et al.*, 1995; Ochman *et al.*, 1996; Cirillo *et al.*, 1998; Hensel *et al.*, 1998; Beuzón *et al.*, 2000; Beuzón *et al.*, 2002). Usually, SCVs form *Salmonella* induced filaments (SIF). This process can control the integrity of the SCV membrane and its expansion, which is necessary for bacterial cell division. It is also possible that by controlling vesicular fusion on the SCV, these bacterial proteins ensure delivery of nutrients to the SCV, thereby facilitating bacterial replication. However, in some cases the bacteria do not have the time or the capability to modify the vacuole leading to the fusion of the SCV with phagolysosome triggering intra-vacuole destruction or autophagy. In other cases, *Salmonella* damages the SCV membrane triggering vacuole destruction, allowing bacteria to escape into the cytosol, where they can be destroyed, particularly in activated macrophages, or multiply extensively especially in epithelial cells (Wiedemann *et al.*, 2014).

## 6. Zebrafish-ST infection model in inflammasome research

Activation of the innate immune response in zebrafish embryos occurs after ST infection. This infection model was well-established previously by Stockhammer and co-workers (2009). There are different routes of the infection depending on what is the purpose of the study. The most common are: duct of cuvier, yolk sac circulation valley, caudal vein and blood islands for used to study phagocytosis (Benard *et al.*, 2012). The hindbrain ventricle (Phennicie *et al.*, 2010) and tail muscle injection (Lin *et al.*, 2009) are used for macrophage migration. The otic vesicle (Le Guyader *et al.*, 2008) is usually used for neutrophil migration and notochord is used for *Mycobacterium marinum* mutants injection being permissive compartment for its growth that are strongly attenuated when injected in other tissues (Benard *et al.*, 2012). Finally, yolk sac injection is used for systemic infection (van der Sar *et al.*, 2003; Benard *et al.*, 2012) (Figure 9).

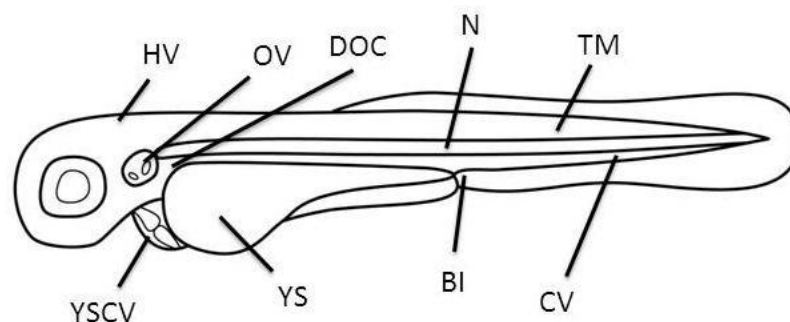


**Figure 9. Locations in zebrafish explored as sites for infections** (HV- Hindbrain, OV- Otic Vesicle, DOC -Duct of Cuvier, N - Notochord, TM - Tail Muscle, YSCV - Yolk Sac Circulation Valley, YS -Yolk Sac, BI - Blood Islands, CV - Caudal Vein).

Nowadays, several studies support the usefulness of this infection model in multiple inflammation and infection research (Howlader *et al.*, 2016; Torraca & Mostowy, 2018), including inflammasome research (Sofia de Oliveira *et al.*, 2015; Kuri *et al.*, 2017; Tyrkalska *et al.*, 2016). Our group has recently reported using this model that the IFN $\gamma$ -inducible GTPase Gbp4 is involved in inflammasome activation and ST clearance (Tyrkalska *et al.*, 2016), which occurs in two steps: first neutrophils are recruited to the infection site through the inflammasome independent production of CXCL8 and LTB4 and then ST is cleared through the Gbp4 inflammasome-dependent biosynthesis of prostaglandin D2. Notably, the CARD domain of Gbp4 is required, but

dispensable, for the assembly into the inflammasome, while its GTPase activity is indispensable for inflammasome assembly, caspase-1 activation and ST clearance (Figure 10).

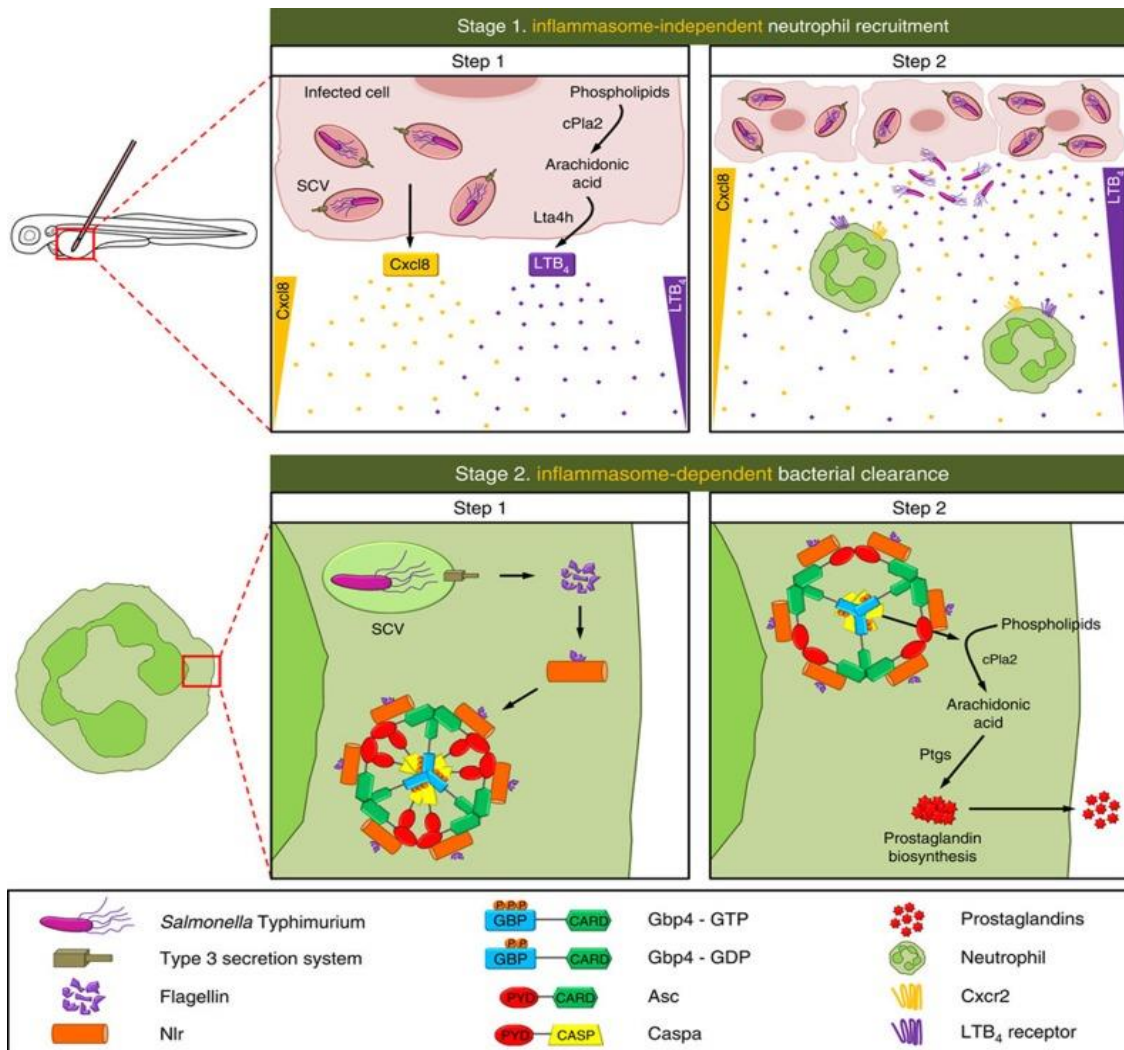


**Figure 10. Proposed model for ST infection resolution in zebrafish.** Stage 1, step1: infected cells release Cxcl8 and LTB4 in an inflammasome-independent manner. Stage 1, step 2: neutrophils are recruited to the infection sites via Cxcl8 and LTB4 gradients and phagocytose ST. Stage 2, step1: ST taken up by neutrophils localized to the Salmonella-containing vacuole (SCV) where it uses its T3SS to translocate bacterial proteins to the cytosol. Flagellin, being one of those bacterial proteins, can be recognized by cytosolic NLRs, probably NLRP3 and NLRC4, which consequently induce the assembly of a Gbp4 and Asc through CARD domains allowing the subsequent recruitment of pro-Caspa. Stage 2, step2: the hydrolysis of GTP to GDP or GMP by Gbp4 results in a conformational change in the inflammasome complex that allows the activation of Caspa via autocleavage, resulting in the induction of PG biosynthesis through the activation of cPla2 and via Ptgs (also known as cyclooxygenases)(Tyrkalska et al., 2016).

## 7. New inflammasome components

As it has been described above, not only NLRs, ASC and CASP1 are part of the inflammasome. Inflammasome complex includes a wide number of molecules which intervene in its function, some of them remaining unknown. Due to its implication in host defence, inflammation and a wide number of diseases, a complete knowledge of the function of this complex is needed. In order to define it, researchers keep looking for new insights in the inflammasome field. For example, the reported Gbp4, GSDMD or LRRK2. (W. Liu et al., 2017; Ramos-Junior & Morandini, 2017; Tyrkalska et al., 2016)

Moreover, most NLRs have the ability to recruit the adaptor protein ASC. Many proteins contain repeating amino acid sequences, which act as the building blocks that form the underlying architecture of specific protein-binding interface. Amino acid sequence repeats containing proteins are therefore potential putative inflammasome components. Within these domains ankyrin repeats (ANK) domains and tryptophan-aspartic acid (WD) domains in WD-repeats (WDR) proteins are important in large protein complexes interaction.

### 7.1. Ankyrin proteins

Ankyrin repeats (ANK), consisting of 33 amino acid residues that are highly conserved among many representatives of the plant, animal, and protozoa kingdoms (Mosavi, Cammett, Desrosiers, & Peng, 2004), are one of the most frequently observed. ANK was first discovered in the yeast cell cycle regulator Swi6/Cdc10 and the *Drosophila* signalling protein Notch (Breedon & Nasmyth, 1987), and owes its name to the cytoskeletal protein ankyrin, which contains 24 copies of this repeat (Lux, John, & Bennett, 1990). Although most proteins with ANK present 6 of these repeats, that number can vary from 2 to 34. Domains containing ANK span a wide range of functions including protein–protein interactions, such as the recruitment of a substrate to the catalytic domain of an enzyme or the assembly of stable multiprotein complexes (Dueber, Yeh, Chak, & Lim, 2003; Prehoda, Scott, Mullins, & Lim, 2000).

Researching CARD/ANK containing proteins, in this Thesis we report the identification of an evolutionarily conserved N-terminal CARD and C-terminal ANK

domains, termed Caiap from CARD- and ANK-containing Inflammasome Adaptor Protein, which is characterized in this Thesis.

## **7.2. WDR proteins**

WD-repeat proteins belong to a large and fast-expanding conservative protein family. WDR proteins are defined by the presence of WD40 domains. These domains are called WD40 domains due to the conserved WD dipeptide and the length of approximately 40 amino acid residues in a single repeat. More precisely the WD40 domain is defined as a 44–60 residue sequence unit that typically contains the GH dipeptide 11–24 residues from its N-terminus and the WD40 dipeptide at the C-terminus (Neer, Schmidt, Nambudripad, & Smith, 1994). They are found in all eukaryotes, but rarely in prokaryotes, and are one of the most abundant protein interaction domains in the human proteome (C. Xu & Min, 2011), existing more than 340 WD40 domain containing proteins according to a SMART database (Letunic, Doerks, & Bork, 2009). The WD40 repeats in a protein fold into a  $\beta$ -propeller architecture that can contain 4 to 8 WD40 repeats but are typically seven-bladed with an overall doughnut shape (**Figure 11**). Importantly, the central pore of the WDR domain frequently mediates interactions with peptide regions of key interaction partners.

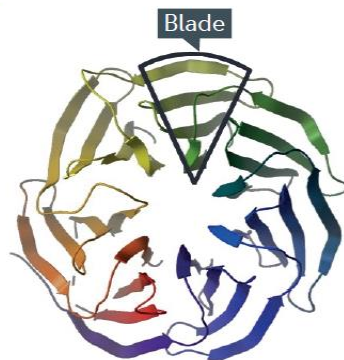


**Figure 11. WD40 structure.** WDR proteins usually form a circular 7-  $\beta$ -propeller blades. Adapted from Schapira et al., 2017

The common function of these WD40 domain proteins is to serve as a rigid scaffold for protein-protein interaction, and to coordinate downstream events, such as ubiquitination and histone methylation. WDR domains are often essential subunits of multiprotein complexes involved in a wide range of cellular processes, including G

protein-coupled receptor signalling, DNA damage sensing and repair, the ubiquitin–proteasome system, cell growth and division, epigenetic regulation of gene expression and chromatin organization, and the immune system. Consequently, they have critical roles in many essential biological functions ranging from signal transduction, transcription regulation, to apoptosis, and are also associated with several human diseases (Schapira, Tyers, Torrent, & Arrowsmith, 2017a). Moreover, WD40 proteins function as an interchangeable substrate receptor to target different substrates selectively.

All of these features make WDR proteins as potential participators of multiprotein complexes, and some of them has been already described such as Apaf-1 in apoptosomes (Chai & Shi, 2014) and the recently described LRRK2 in the NLRC4 inflammasome (W. Liu et al., 2017). In this Thesis, using the zebrafish-ST infection model we have discovered another WDR protein, WDR90, whose expression depends on Gbp4 and that participates in the NLRC4 inflammasome in response to ST infection, as it will be discussed in the results section.



**AIMS**



**The specific objectives of the present work are:**

1. Molecular, functional and phylogenetic characterization of Caiap. Role in the regulation of inflammasome assembly and activation.
2. Molecular and functional characterization of Wdr90. Role in the regulation of inflammasome assembly and activation.
3. Generation of new tools for inflammasome research.



**MATERIALS &  
METHODS**



## 1. Animals

Wild-type zebrafish (*Danio rerio* H. Cypriniformes, Cyprinidae) were obtained from the Zebrafish International Resource Center (ZIRC, Oregon, USA) and mated, staged, raised and processed as described in the zebrafish handbook (Westerfield, 2000). The transgenic lines *Tg(mpx:eGFP)i114*, with green fluorescent neutrophils (Renshaw *et al.*, 2006), were provided by Prof. Stephen A. Renshaw. The transgenic line *Tg(mpeg1:eGFP)gl22*, with green fluorescent macrophages (Ellett *et al.*, 2011), was provided by Prof. Graham J. Lieschke., and the *Tg(lyz:DsRED2)nz50* (Hall *et al.*, 2007) with red fluorescent neutrophils by Prof. Phil Crosier.

The experiments performed comply with the Guidelines of the European Union Council (Directive 2010/63/EU) and the Spanish RD 53/2013. Experiments and procedures were performed as approved by the Bioethical Committees of the University of Murcia (approval numbers #75/2014, #216/2014 and 395/2017) and the Bioethical Committee of the Universidad Austral de Chile number #293/2017).

Alpacas (*Vicugna pacos* H. Artiodactyla, Camelidae) were provided by Criadero Machalí and by Llamas del Sur (Temuco, Chile) and handled and maintained as described in the llama and alpaca care handbook (Cebra, Anderson, Tibary, Van Saun, & Johnson, 2014).

## 2. DNA constructs

The genes encoding zebrafish Wdr90, wild type Gbp4, the GTPase-dead mutant Gbp4KS→AA, Gbp4CARD, the double mutant Gbp4KS→AA/CARD, Caiap, CaiapΔCARD (deletion from I12 to Y97), wild-type (WT) Flag-Caspa, catalytic inactive Flag-Caspa mutant (C230A) and WT Asc-eGFP were synthesized by GenScript Corporation. The *cmv/sp6:caiap-mCherry*, *cmv/sp6:caiapΔCARD-mCherry*, and *uas:caiap-mCherry*; *cmc2:eGFP* constructs were generated by MultiSite Gateway assemblies using LR Clonase II Plus (Life Technologies) according to standard protocols and using Tol2kit vectors described previously (Kwan *et al.*, 2007). The zebrafish Caspa and Asc-Myc construct in the pcDNA3 backbone was previously described (Masumoto *et al.*, 2003). The MYC-tagged hNLR4 construct was a gift from Barbara Kazmierczak.

The inducible lentiviral construct FgH1tUTG was a gift from Marco Herold (Addgene plasmid #70183) and lentiCas9-Blast was a gift from Feng Zhang (Addgene plasmid #52962). Packaging plasmids psPAX2 and pMD2.G were a gift from Didier Trono (Addgene plasmid #12260 and #12259).

### **3. Cell lines**

HEK293T cells and HeLa-Cas9 cells (CRL-11268; American Type Culture Collection; gift from Prof. A. Saurin, University of Dundee, Scotland, respectively) were grown in Dulbecco's modified Eagle's medium (DMEM) supplemented with 10% fetal bovine serum (FBS), 2 mM Glutamax and 1% penicillin-streptomycin (Life Technologies). HEK293T cells were split before to reach 80% confluence twice per week. Immortalized BMDM cells (a gift from Prof. P. Broz, University of Lausanne, Switzerland) were cultured in DMEM supplemented with 10% FBS and 10% L929 supernatant.

### **4. sgRNA design**

To design the *Knock-out* sgRNAs the WTSI Genome Editing CRISPR design software (Hodgkins et al., 2015) was used (<http://www.sanger.ac.uk/htgt/wge/>). To clone individual sgRNAs, 24-bp oligonucleotides containing the sgRNA sequences were synthesized (Sigma). They included a 4-bp overhang for the forward (TCCC) and complementary reverse (AAAC) oligos to enable cloning into the BsmB-I site of the lentiviral construct.

To design the *Knock-in* sgRNAs we used the Zhang Lab CRISPR design software (<http://crispr.mit.edu/>). Guides were synthesized (Invitrogen) with an overhang forward (GGAAAGG) and reverse (GTCCGCCGTTTT) to allow cloning into the pU6 vector using Dpn1 (Thermo Fisher Scientific). sgRNA sequences are shown in Table 2.

Guide	Sequence	Exon	Use
mWDR90-g1	TCCCGTACCTTGTCCGGTATGGCCA	10	KO
mWDR90-g2	TCCCACGTCCTTCAGTTCGCGATG	8	KO
mWDR90-g3	TCCCGAACCACGACCTCACCGCCG	13	KO
mWDR90-g4	TCCCTAACAGACAACTTTGCACGC	5	KO
hWDR90-1	ACGAAACACCGCAGGTTTACACC	42	KI
hWDR90-2	GCAGGTTTACACCGTCCGCCAGG	42	KI

Table 2. sgRNA guides used in this study.

## 5. Morpholinos and RNA/DNA/Protein Injection

Specific morpholinos were resuspended in nuclease-free water to 1 mM, 2 mM or 3 mM (Table 3). *In vitro*-transcribed RNA was obtained following manufacturer's instructions (mMESSAGE mMACHINE kit, Ambion). Morpholinos and RNA were mixed in microinjection buffer (0.5x Tango buffer and 0.05 % phenol red solution) and microinjected into the yolk sac of one-cell-stage embryos using a microinjector (Narishige) (1 nl per embryo). The same amount of MOs and/or RNA were used in all experimental groups. The efficiency of the MOs was checked by RT-PCR and Western blot.

In some experiments, *Tg(mpeg1:GAL4)<sup>g/25</sup>* one-cell stage embryos were injected with a solution containing 100pg *uas:caiap-mCherry; cmlc2:eGFP* construct and 50pg Tol2 RNA in microinjection buffer (0.5x Tango buffer and 0.05% phenol red solution). Embryos were sorted at 2 dpf according to the presence or absence of green fluorescence in their heart before being infected (see below).

For crispr experiments, sgRNAs obtained by *in vitro* transcription using the MAXIscript T7 Kit (Ambion) were first checked *in vitro* using 100 ng of an amplicon containing the target sequence, 30 nM sgRNA and 30 nM EnGen Cas9 NLS from *Streptococcus pyogenes* (New England Biolabs). Injection mixes were then prepared with 500 ng/ $\mu$ l Cas9 and 100 ng/ $\mu$ l control (5'-CGTTAATCGCGTATAATACG-3') or *caiap* (5'-GGGCCACACCGCTGTTGCTG-3') sgRNA in 300 mM KCl buffer, incubated for 5 min at 37°C and used directly without further storage.

Gene	ENA or Ensembl ID	Target	Sequence (5'→3')	Concentration (mM)	Reference
<i>gfp4</i>	ENSDARG00000068857	e1/i1	GCTGTTTGTGTGTCTCT AACCTGTT	0.1	Tyrkalska et al., 2016
<i>caiap</i>	ENSDARG00000092758	atg/5'UT R	CTGGTTGAGCCCATGT CCAGTGCTT	0.16	Tyrkalska et al., 2017
<i>asc</i> ( <i>pycard</i> )	ENSDARG00000040076	atg/5'UT R	GCTGCTCCTTGAAAGA TTCCGCCAT	0.6	Tyrkalska et al., 2016

Table 3. Morpholinos used in this study. The gene symbols followed the Zebrafish Nomenclature Guidelines ([http://zfin.org/zf\\_info/nomen.html](http://zfin.org/zf_info/nomen.html)). ENA, European Nucleotide Archive (<http://www.ebi.ac.uk/ena/>).

## 6. Generation of stable cell lines

For *Knock-out* generation, HEK293T were transfected with lipofectamine 2000 following the manufacturer's instructions. Briefly, 8  $\mu$ L lipofectamine; 1.2  $\mu$ g pMD2.G, 0.4  $\mu$ g psPAX2 and 1.5  $\mu$ g of our vector of interest (either lenti-Cas9 or vector containing sgRNA). After 24h, the media was replaced and cells were further incubated for 2 days. Viral particles were obtained from filtered supernatants with a 0.45  $\mu$ m filter and used to transduce  $5.0 \times 10^4$  iBMDMs cells, with 8  $\mu$ g/ml polybrene. The transduction mix was centrifuged at 1,000 xg for 1h at 30°C. Pelleted cells were then resuspended in fresh complete media and plated in a 12 well plate for 2 weeks. Stable cell lines were selected with Blasticidin (10 $\mu$ g/ml) for 10 days or sorting of the top 5% eGFP expressing population for cells transduced with lentiCas9 and FgH1tUTG vectors, respectively. Treatment with doxycycline hyclate (Sigma-Aldrich; D9891) at 1  $\mu$ g/ml for 3 days was used to induce the expression of gRNAs. Cells were then maintained as per usual after the treatment.

For *Knock-in* generation, HeLa cells were transfected with lipofectamine 2000 following the manufacturer's instructions with 1 $\mu$ g of each plasmid. Stable cell lines were selected with Puromycin (4 $\mu$ g/ml) for 2 days then induced with doxycycline (1 $\mu$ g/ml for 2 days) and sorted by GFP positive.

## 7. Chemical treatments

In some experiments, 2 dpf embryos were manually dechorionated and treated by bath immersion with caspase-1 inhibitor Ac-YVAD-CMK (100  $\mu$ M, Peptanova) or the diluted in egg water supplemented with 1% DMSO.

## 8. Infection assay

Infection experiments were performed using *S. Typhimurium* 12023 (wild type) or *S. Typhimurium* 12023 expressing DsRedT3 (de Oliveira *et al.*, 2015). Overnight cultures in Luria-Bertani medium (LB) were diluted 1/5 in LB with 0.3 M NaCl, incubated at 37 °C until 1.5 optical density at 600 nm was reached, and finally diluted in sterile PBS.

Zebrafish one-cell embryos were injected with MOs and/or mRNAs. Larvae of 2 dpf were dechorionated manually, anesthetized in embryo medium with 0.16 mg/ml tricaine and 10-50 bacteria (Yolk sac) or 100 bacteria (Otic vesicle) per larvae were microinjected. Larvae were allowed to recover in egg water at 28-29 °C, and monitored for clinical signs of disease or mortality over 5 days. All the survival assays have been performed three times, using 40-100 larvae per treatment in each independent experiment. Each graph shows the mean result of the three experiments, having an accumulated sample size of 120-300 larvae per treatment.

Cells were stimulated with 1 $\mu$ g/ $\mu$ L of LPS for 4h before the infection and then infected using a MOI of 10. The plates were centrifuged for 15 min at 1500 g and placed at 37°C for 90 min.

## 9. Tail Fin Wounding

Tail fin amputation was performed at 3 dpf as previously described (S. de Oliveira *et al.*, 2013) in casper larvae.

## 10. Whole-Mount *In Situ* Hybridization (WISH)

Transparent Casper embryos were used for WISH (Thisse, Thisse, Schilling, & Postlethwait, 1993). *caiap* sense and antisense RNA probes were generated using the DIG RNA Labeling Kit (Roche Applied Science) from linearized plasmids. Embryos were

imaged using a Scope.A1 stereomicroscope equipped with a digital camera (AxioCam ICC 3, Zeiss).

## **11. Caspase-1 activity assay**

Zebrafish one-cell embryos were injected with MOs and/or mRNAs. 2 dpf larvae were dechorionated and infected with different strains of *S. Typhimurium* into the yolk sac (MOI=50). 3 dpf larvae were collected and used to measure the caspase-1 activity as described before (Tyrkalska et al., 2017). The caspase-1 activity was determined with the fluorometric substrate Z-YVAD-AFC (caspase-1 substrate VI, Calbiochem) as described previously (López-Castejón *et al.*, 2008). In brief, larvae were lysed in hypotonic cell lysis buffer [25 mM 4-(2-hydroxyethyl) piperazine-1-ethanesulfonic acid (HEPES), 5 mM ethylene glycol-bis(2-aminoethylether)-N,N,N',N'-tetraacetic acid (EGTA), 5 mM dithiothreitol (DTT), 1:20 protease inhibitor cocktail (Sigma-Aldrich), pH 7.5] on ice for 10 min. For each reaction, 80 µg of proteins were incubated for 90 min at 25°C with 50 µM Z-YVAD-AFC and 50 µl of reaction buffer [0.2% 3-[(3-cholamidopropyl)dimethylammonio]-1-propanesulfonate (CHAPS), 0.2 M HEPES, 20% sucrose, 29 mM DTT, pH 7.5]. After the incubation, the fluorescence of the AFC released from the Z-YVAD-AFC substrate was measured with a FLUOstar spectofluorometer (BGM, LabTechnologies) at an excitation wavelength of 405 nm and an emission wavelength of 492 nm. All the caspase-1 activity assays have been performed three times, using 25-40 larvae per treatment in each independent experiment. Three independent experiments were performed and one is shown as a representative result.

## **12. Cell sorting**

Approximately 300–500 non-infected and infected larvae from the lines *Tg(mpx:eGFP)i114* and *Tg(mpeg1:eGFP)gl22* were anesthetized in tricaine at 24 hpi, minced with a razor blade, incubated at 28°C for 30 min with 0.077 mg/ml Liberase (Roche). The resulting cell suspension was passed through a 40-µm cell strainer. Cell sorting was performed on a SH800Z (Sony).

### 13. Analysis of gene expression

Total RNA was extracted from whole embryos/larvae, larvae heads or sorted cell suspensions with TRIzol reagent (Invitrogen) following the manufacturer's instructions and treated with DNase I, amplification grade (1 U/ $\mu$ g RNA; Invitrogen). SuperScript III RNase H Reverse Transcriptase (Invitrogen) was used to synthesize first-strand cDNA with oligo(dT) primer from 1  $\mu$ g of total RNA at 50°C for 50 min. Real-time PCR was performed with an ABI PRISM 7500 instrument (Applied Biosystems) using SYBR Green PCR Core Reagents (Applied Biosystems). Reaction mixtures were incubated for 10 min at 95°C, followed by 40 cycles of 15 s at 95°C, 1 min at 60°C, and finally 15 s at 95°C, 1 min 60°C and 15 s at 95°C. For each mRNA, gene expression was normalized to the ribosomal protein S11 (*rps11*) content in each sample by Pfaffl method (Pfaffl, 2001). The primers used are shown in Table 4. In all cases, each PCR was performed with triplicate samples and repeated at least with two independent samples.

Gene	ENA ID	Name	Sequence (5'→3')	Use
<i>rps11</i>	NM_213377	F1	GCGTCAACGTGTCAGAGTA	RT-qPCR
		R1	GCCTCTCTCAAACGGTTG	
<i>asc</i>	NM_131495	F	ATTTTGAGGGCGATCAAGTG	
		R	GCATCCTCAAGGTCATCCAT	
<i>gbp4</i>	NM_001082945		ACTGGGAGATGTGGAAAAGGGCG	
			CCATAGCCTTGTTGTCGATCACCCC	
<i>il1b</i>	NM_212844	F5	GGCTGTGTGTTGGGAATCT	
		R5	TGATAAACCAACCGGGACA	
<i>wdr90</i>	XM_003201346	F4	CTGCATGATGCTGTTCTC	
		R4	ATGTCACTTCTGCCTGTCCG	
<i>caiap</i>	NM_001025492	F2	AGCGCAGATATTGTTGCATAAGGGC	
		R2	GCCCCACACGCAGTAGCAG	
<i>caiap</i>	NM_001025492	F	AGGCCATTGTGTATTTTCTGCT	Validation of gRNA
		R	AAGCTCATTGCAGCTATTGACA	

Table 4. Primers used in this study. The gene symbols followed the Zebrafish Nomenclature Guidelines ([http://zfin.org/zf\\_info/nomen.html](http://zfin.org/zf_info/nomen.html)). ENA, European Nucleotide Archive (<http://www.ebi.ac.uk/ena/>).

## 14. Transfection

HEK293T were transfected with Lipofectamine 2000 following the manufacturer's instructions. Cells were usually plated on a 6 or 24 well plate or in a 10 cm diameter plate and transfected when 80% of confluence was reached. DNA mix and Lipofectamine mix were prepared separately using serum free DMEM and were incubated for 10 min. Both components were mixed, incubated for another 20 min and added to the cells. Final quantities are shown in Table 5. After 6h media was replaced with a complete DMEM. Samples were usually taken 24h after transfection. For experiments involving the WDR90 plasmid time was extended to 48h.

Plate size	DNA	Lipofectamine 2000	DMEM (vol. final)
10 cm	5 µg	9 µl	4.8 ml
6 wells	1 µg	1.5 µl	800 µl
12 wells	0.5 µg	0.75 µl	400 µl
24 wells	0.25 µg	0.45 µl	200 µl

Table 5. Amount DNA and Lipofectamine used in this study

## 15. Dot Blot

For Dot Blot assays recombinant proteins and BSA were incubated for 20 min from 150 ng/µl to 0,59 ng/µl in a nitrocellulose membrane. Membranes were blocked with 1% casein in PBST for 1h RT and incubated for 30 min with the alpacas' pre and post-immune serum at different concentrations (1:500, 1:1000 and 1:5000), then washed with PBST 3 times and incubated with secondary antibody  $\alpha$ -llama conjugated with HRP (1:5000) 30 min RT. After repeated washes, the signal was detected with the enhanced chemiluminescence reagent and ChemiDoc XRS Biorad.

## 16. Western Blot

Transfected cells were washed twice with PBS and solubilized in 200 µl of lysis buffer (50 mM Tris-HCl, pH 7,5, 1% IGEPAL, 150 mM NaCl and a 1:20 dilution of the protease inhibitor cocktail P8340 from SigmaAldrich). Samples were centrifuged (13.000  $\times g$ , 10 min) and resolved on 10-8% SDS-PAGE and transferred to nitrocellulose membranes. Membranes were block 1h at RT and incubated overnight at 4°C as indicated in Table 6. For detection, corresponding horseradish peroxidase conjugated secondary antibodies (1:5000

dilution; Amersham) were used. After repeated washes, the signal was detected with the enhanced chemiluminescence reagent and ChemiDoc XRS Biorad.

Epitope	Primary antibody/ concentration	Secondary antibody (HRP)	Blocking and incubation buffer
FLAG	$\alpha$ -FLAG-HRP (Sigma-Aldrich)/ 1:5000	-----	5% nonfat milk in TBST
MYC	$\alpha$ -MYC (Invitrogen)/ 1:5000	$\alpha$ -mouse (1:10000)	5% nonfat milk in TBST
GFP	$\alpha$ -GFP-HRP (1:10000)	-----	5% nonfat milk PBST
WDR90	$\alpha$ -WDR90 (Sigma)/ (1:1000)	$\alpha$ -rabbit (1:10000)	2% BSA
	$\alpha$ -WDR90 (This work)/ (1:1000)	$\alpha$ -llama (1:5000)	in PBST
Asc	$\alpha$ -Asc (This work)/ (1:1000)	$\alpha$ -llama (1:5000)	2% BSA in PBST

Table 6. Antibodies used in this study

## 17. Immunoprecipitation assays

Cell lysate (1 mg) was incubated for 2 h at 4°C under gentle agitation with 40  $\mu$ l of slurry of ANTI-FLAG® M2 or Myc Affinity Gels (Sigma-Aldrich). The immunoprecipitates were washed four times with lysis buffer containing 0.15 M NaCl and then twice with PBS. Finally, the resin was boiled in SDS sample buffer and the bound proteins were resolved on 10 or 15% SDS-PAGE and transferred to nitrocellulose membranes (BioRad) for 50 min at 300 mA. Blots were probed with specific antibodies to FLAG (Sigma-Aldrich), Myc (ThermoFisher), and mCherry (ThermoFisher), and then developed with enhanced chemiluminescence reagents (GE Healthcare) according to the manufacturer's protocol.

## 18. Confocal Microscopy

Cells grown on coverslips were fixed with 4% paraformaldehyde in PBS, incubated 20 min at room temperature with 20 mM glycine, permeabilized with 0.5% NP40 and blocked for 1 h with 2% BSA. Cells were then labelled with anti-FLAG

monoclonal (1:5000) or anti-Myc polyclonal (1:2000) (Sigma-Aldrich), followed by Alexa 488-conjugated secondary antibody (Thermofisher) and DAPI (Life Technologies). Samples were mounted using a mounting medium from Dako and examined with a Leica laser scanning confocal microscope AOBs and software (Leica Microsystems). The images were acquired in a 1,024 × 1,024 pixel format in sequential scan mode between frames to avoid cross-talk. The objective used was HCX PL APO CS × 63 and the pinhole value was 1, corresponding to 114.73 μm.

## **19. Recombinant protein purification**

The synthesized sequence for hWDR90 recombinant protein was cloned into vector pET30a with His tag for protein expression in *E. coli*. *E. coli* strain BL21 was transformed with recombinant plasmid and a single colony was inoculated into LB medium with antibiotic and incubated in 37°C at 150 rpm O/N. The culture was diluted 1/10 into LB medium and incubated in 30°C at 150rpm until the OD<sub>600</sub> =0.6 was reached. Culture medium was changed to Y2T medium prewarmed at 42°C and bacteria were incubated for 30 minutes. Culture was cooled down to 16°C, OD<sub>600</sub> was adjusted to 0.6 and protein expression was induced with 0.001 mM IPTG at 16°C for 40h. Cells were harvested by centrifugation and the pellets were resuspended with lysis buffer followed by 3 pulses of 20 seconds of sonication. The cell lysate was sterilized by 0.22 μm filters and the protein was purified using AminoLink Plus Coupling Resin (Thermo Fisher Scientific). Purified protein was stored in aliquots of 250μg until immunization.

## **20. Antibody generation**

Alpacas were immunized every 15 days 4 times with 250ug of the protein of interest with adjuvant (Gerbu Fama). From each individual 150ml of blood was extracted 40 days forward to the first immunization. Peripheral Blood Lymphocytes (PBL) were separated using a Ficoll gradient and the total RNA was isolated with QIAamp RNA Blood Mini kit (Qiagen Inc, Valencia, CA) following the manufacturer's instructions.

To purify the antibodies contained in the alpacas' serum, the antigen was covalently linked to NHS-activated agarose beads (Thermo Scientific) following the manufacturer's instructions. Briefly, NHS beads were prewashed with HCl 1mM and incubated with the antigen in a carbonate buffer pH 8.3 RT for 3h. Beads were washed

and inactivated with 0.5 M NaCl and 0.5 M Ethanolamine. Columns were stored at 4°C with PBS, 0.5 M NaCl and 0.1% sodium azide.

Alpacas' serum was diluted in PBS and sterilized with a 0.2µm filter and added to the column prewashed with coupling buffer. Column was washed with a 10 mM Tris/HCl, 0.5 M NaCl buffer (pH 7.5), and the antibodies were eluted with acid glycine (0.1M; pH 2.25), then the eluent was neutralized with Tris/HCl (1M, pH 8). The eluted antibodies were stored at 4°C with 10% glycerol and 0.1% sodium azide.

## **21. Sequence analysis of Caiap in different species**

Zebrafish Caiap was identified by searching the CARD protein family (PF00619) in the PFAM database. Zebrafish full-length Caiap sequence was then compared with other known Caiap sequences, obtained from The Universal Protein Resource (UniProt) database and with the newly identified variants by multiple sequence alignment carried out with the ClustalX version 2.1 program. The molecular weights were estimated using the Protein Molecular Weight tool from The Sequence Manipulation Suite. The domains of the proteins deduced from the nucleotide sequences were determined using the Simple Modular Architecture Research Tool (SMART), from the European Molecular Biology Laboratory (EMBL) website (Letunic et al., 2009). Finally, three-dimensional structure predictions were performed using The IntFOLD Integrated Protein Structure and Function Prediction Server (McGuffin, Atkins, Salehe, Shuid, & Roche, 2015) and visualized with The PyMOL Molecular Graphics System, Version 1.8 Schrödinger, LLC. The ModFOLD Quality Assessment Server (Version 4.0) was used to check the accuracy of the models (McGuffin, Buenavista, & Roche, 2013).

## **22. Statistical analysis**

Data are shown as mean ± SEM and they were analysed by analysis of variance (ANOVA) and a Tukey multiple range test to determine differences between groups. The differences between two samples were analyzed by the Student's *t*-test. A log rank test with the Bonferroni correction for multiple comparisons was used to calculate the statistical differences in the survival of the different experimental groups. A chi-square test was used to determine differences in the number of specks formed by Caiap in HEK293T cells. All the experiments were performed at least three times, unless

## *Material & Methods*

otherwise indicated. The sample size for each treatment is indicated in the graph or in the figure legend or in corresponding section of the Materials and Methods. Statistical significance was defined as  $p < 0.05$ .

# RESULTS



# 1. CAIAP

## 1.1. Identification and characterization of Caiap, a Protein Containing a CARD domain and ANK repeats, which is highly conserved from cartilaginous fish to marsupials

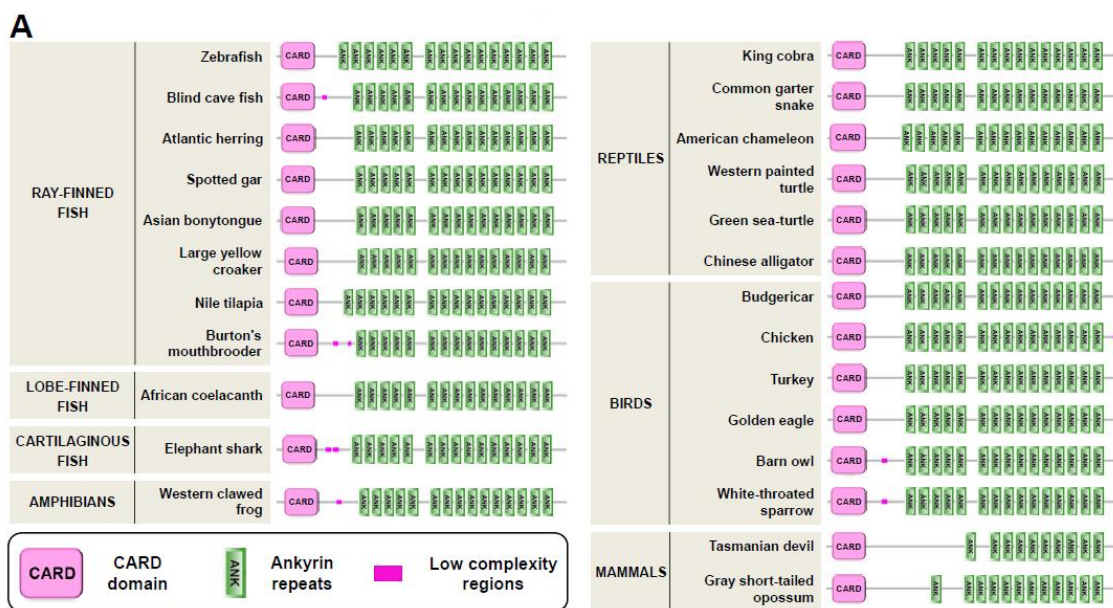
A PFAM search to identify proteins harbouring CARD domains revealed the presence of Caiap (CARD-ANK Inflammatory Adaptor Protein) in the zebrafish. The *caiap* gene contains two exons and a single open reading frame encoding a putative polypeptide of 744 amino acids (predicted molecular mass of 80.9 kDa) (Figure 12) with an N-terminal CARD domain and 16 C-terminal ANK repeats (Figure 13A).



**Figure 12. Sequence alignment of Caiap gene in different species.** (A) Diagram showing the exons/introns organization of zebrafish *caiap* gene, indicating the position where the Caiap MO and gRNA binds to the 5'- untranslated region in pre-mRNA. (B) Multiple alignment of zebrafish Caiap sequence with other identified Caiap sequences. The predicted CARD sequences are black boxed and yellow boxed indicate the ANK domains. (\*) Identity in one position; (: ) conservative substitutions in one position; (.) semiconservative substitutions in one position. The accession numbers for Caiap sequences are XP\_685576 for zebrafish (*Danio rerio*), XP\_007259539 for blind cave fish (*Astyanax fasciatus mexicanus*), XP\_012694853 for atlantic herring (*Clupea 900 harengus*), XP\_006635081 for spotted gar (*Lepisosteus oculatus*), KPP59498 for Asian bonytongue (*Scleropages formosus*), KKF28470 for large yellow croaker (*Pseudosciaena crocea*), XP\_006002757 for African coelacanth (*Latimeria chalumnae*), XP\_005479286 for Nile tilapia (*Oreochromis niloticus*), XP\_007901907 for elephant shark (*Callorhynchus milii*), XP\_014189326

for Burton's mouthbrooder (*Haplochromis 905 burtoni*), XP\_008107583 for American chameleon (*Anolis carolinensis*), XP\_013917140 for common garter snake (*Thamnophis sirtalis*), XP\_006025802 for Chinese alligator (*Alligator sinensis*), XP\_005284853 for western painted turtle (*Chrysemys picta bellii*), ETE70266 for king cobra (*Ophiophagus hannah*), XP\_007059125 for green sea-turtle (*Chelonia mydas*), XP\_010714589 for turkey (*Meleagris gallopavo*), XP\_004936902 for chicken (*Gallus gallus*), XP\_005151355 for budgerigar (*Melopsittacus undulatus*), XP\_011570978 for golden eagle (*Aquila chrysaetos canadensis*), XP\_009961493 for barn owl (*Tyto alba*), XP\_005482422 for white-throated sparrow (*Zonotrichia albicollis*), XP\_002931656 for western clawed frog (*Xenopus tropicalis*), XP\_003767351 for Tasmanian devil (*Sarcophilus harrisii*), and XP\_007480566 for gray short-tailed opossum (*Monodelphis domestica*).

Strikingly, uncharacterized orthologs of zebrafish Caiap were found in many organisms, including phylogenetically distant ray-finned fish species, cartilaginous fish (elephant shark), lobe-finned fish (coelacanth), amphibian, reptiles, birds, and marsupials. However, we failed to find a Caiap ortholog in placental mammals, invertebrates, protochordates (amphioxus and sea squirts), jawless fish (lamprey), and lung fish by using homology and synteny searches. Phylogenetic analysis confirmed that the origin of Caiap predated the split of fish and tetrapods more than 450 million years ago, suggesting, therefore, that Caiap was lost in lung fish and placental mammals during evolution (Figure 13B).





Species	Identity/similarity (%)
<b>Ray-finned fish</b>	
Blind cave fish	66.0/79.4
Atlantic herring	60.2/74.3
Spotted gar	55.3/73.5
Asian bonytongue	52.9/70.4
Large yellow croaker	50.0/66.4
Nile tilapia	48.4/64.8
Burton's mouthbrooder	47.7/64.1
<b>Lobe-finned fish</b>	
African coelacanth	49.9/69.1
<b>Cartilaginous fish</b>	
Elephant shark	48.2/65.2
<b>Reptiles</b>	
American chameleon	50.1/70.4
Common garter snake	50.0/69.2
Chinese alligator	49.8/70.5
Western painted turtle	49.7/70.1
King cobra	49.6/68.5
Green sea-turtle	48.2/68.9
<b>Birds</b>	
Turkey	49.6/67.4
Chicken	49.5/67.8
Budgerigar	49.3/67.8
Golden eagle	48.9/67.3
Barn owl	48.2/67.0
White-throated sparrow	48.0/65.0
<b>Amphibians</b>	
Western clawed frog	47.5/68.5
<b>Mammals</b>	
Tasmanian devil	35.7/57.2
Gray short-tailed opossum	35.3/55.4

**Table 7.** Amino acid identity and similarity between zebrafish Caiap and other vertebrate Caiap sequences.

Multiple alignment of all Caiap identified revealed that the CARD domain and ANK repeats were the best conserved regions of the protein. More interestingly, three-dimensional structural prediction revealed an identical tertiary structure of Caiap in all vertebrate groups (Figure 14A, B). In fact, all the structures perfectly fitted when superimposed (Figure 14C).

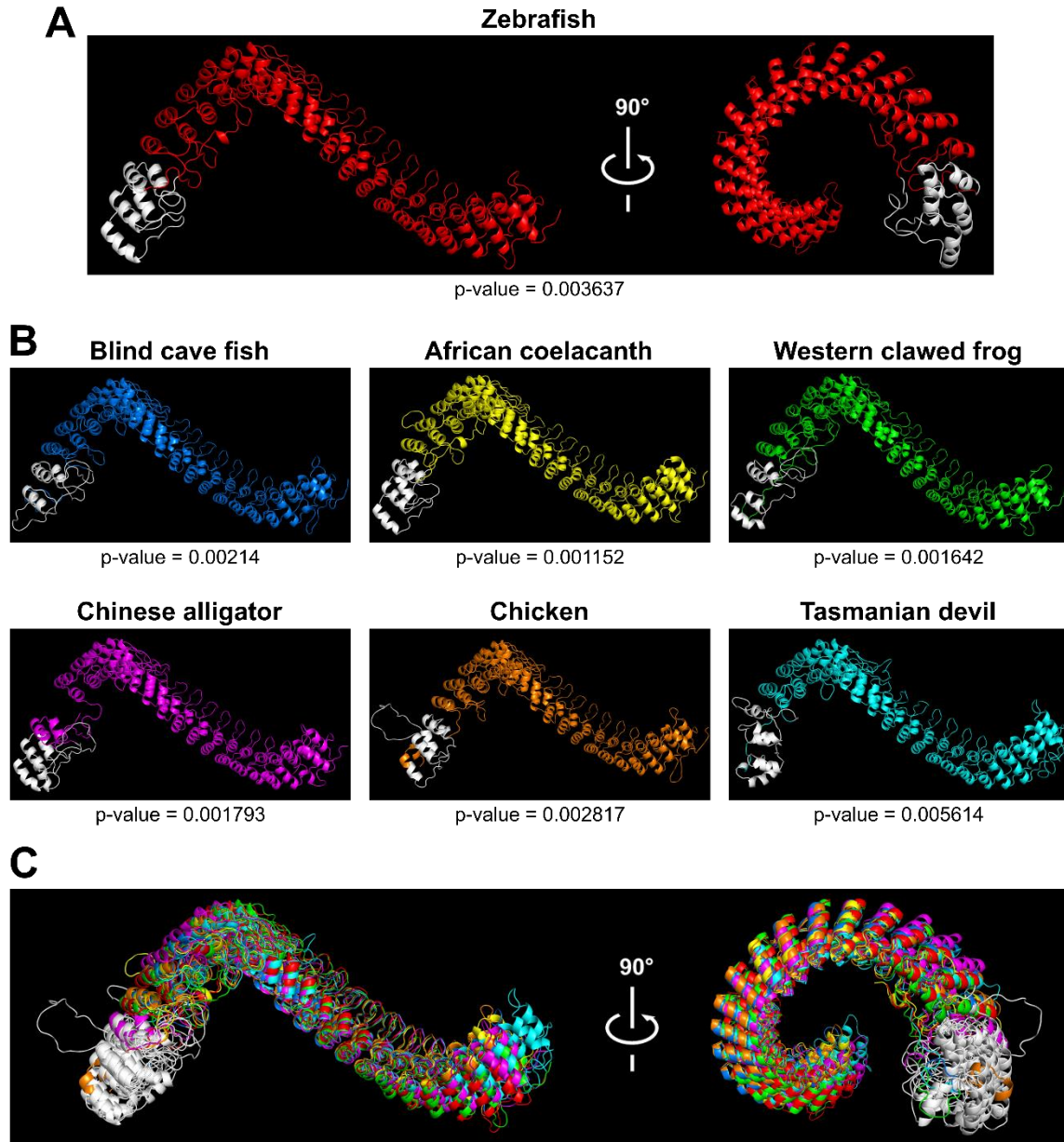


**Figure 14. Tridimensional models of Caiap structures in different species.** (A, B) 3D models showing Caiap proteins from zebrafish (*Danio rerio*) (A), and blind cave fish (*Astyanax fasciatus mexicanus*), western clawed frog (*Xenopus tropicalis*), African coelacanth (*Latimeria chalumnae*), Chinese alligator (*Alligator sinensis*), chicken (*Gallus gallus*), and Tasmanian devil (*Sarcophilus harrisii*) (B) with corresponding accuracies. (C) The 3D Caiap models from all species shown in (A, B) were superimposed. The CARD domains are shown in white.

## 1.2. Zebrafish Caiap is induced upon infection

The expression profile of zebrafish Caiap was examined using RT-qPCR and WISH. It was found that the mRNA levels of *caiap* transcripts were maternally transferred, since they peaked at fertilization time and then rapidly declined (Figure 15A). In adult fish,

*caiap* transcripts were detected in kidney, the hematopoietic organ of adult fish, heart, and skin, but not in muscle, ovary, gills, eye, or brain (Figure 15B). In addition, the mRNA levels of *caiap* were seen to be weakly higher 24 h post-infection (hpi) in the infection site of zebrafish larvae infected with ST (Figure 15C). As expected, the gene encoding pro-inflammatory IL-1 $\beta$  robustly increased in infected larvae (Figure 15C).

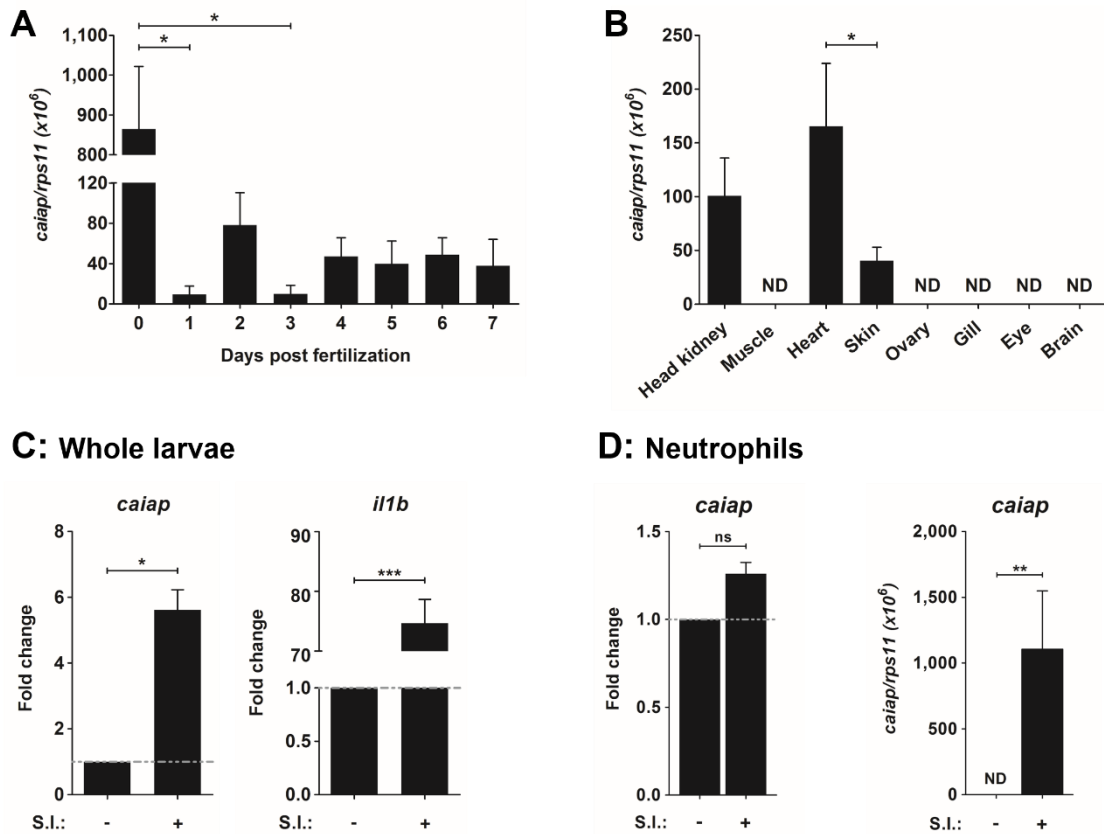


**Figure 15. Zebrafish *caiap* is induced in macrophages upon ST infection.** The *caiap* (A–E) and *il1b* (C) mRNA levels were measured by RT-qPCR in wild-type 0–7 dpf whole larvae (A), in head kidney, muscle, heart, skin, ovary, gills, eye, and brain of 12-month-old wild-type adult fish (B), and whole larvae (C), neutrophils (D), and macrophages (E) from 3 dpf larvae which were previously infected with ST or not at 2 dpf ( $n = 3$ ). ns, not significant; \* $p < 0.05$ ; \*\* $p < 0.01$ ; \*\*\* $p < 0.001$ . ND, not detected.

To further confirm the RT-qPCR results, WISH was performed in infected and wounded larvae. Although no positive cells were observed in non-infected larvae, a few small round *caiap* positive cells were found at the infection site (the otic vesicle), the number of positive *caiap* cells increasing from 4 to 24 hpi (Figure 16A). Similarly, a few *caiap* cells were also observed in the wound 24 h after transection of the tail fin tip (Figure 16B).

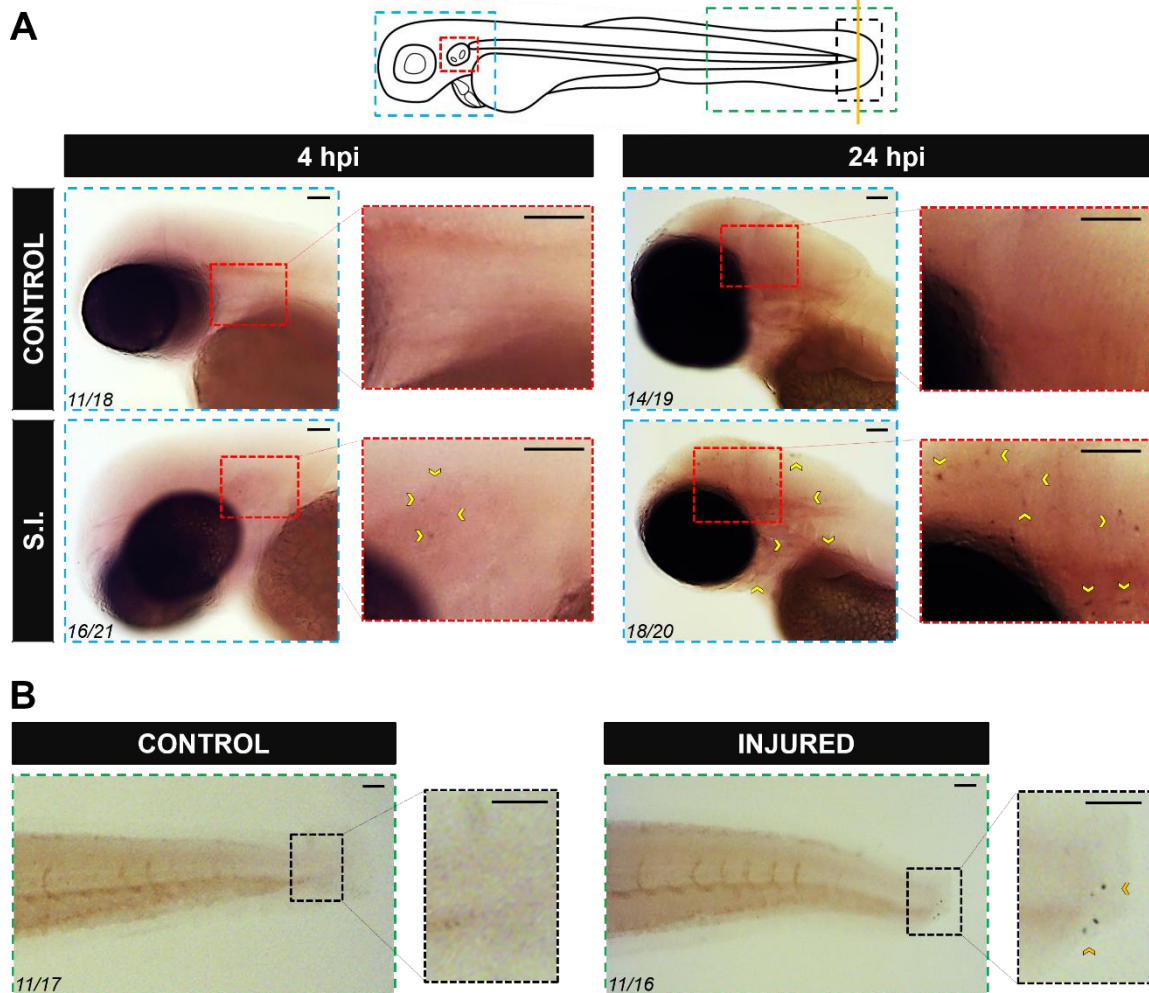


**Figure 16. Zebrafish *caiap* is induced in discrete cells at the infection site.** Zebrafish 2 dpf larvae were infected with ST in the otic vesicle (A) or tail wounded (B). At the indicated times, WISH was performed using antisense probes to the *caiap* gene. Note the presence of *caiap*+ cells at both the infection and injured sites (arrowheads). The areas shown are indicated in the larval scheme with boxes of different colors. Numbers in pictures represent the animals with the shown phenotype per total analyzed animals. S.I., ST infection. Scale bar: 0.5 mm.

As expected, no positive cells were observed when using the *caiap* sense probe (Figure 17). This result suggested that both infection and wounding are able to induce the expression of *caiap* in immune cells recruited to the infection and wounding sites, namely, macrophages (Gray et al., 2011; Zakrzewska et al., 2010) and neutrophils ((S. de Oliveira et al., 2013; Sofia de Oliveira et al., 2015; Tyrkalska et al., 2016). Therefore, macrophages and neutrophils were sorted from *mpeg1:eGFP* (Renshaw et al., 2006) and *mpx:eGFP* (Ellett, Pase, Hayman, Andrianopoulos, & Lieschke, 2011) transgenic larvae,

respectively, upon infection with ST and the transcript levels of *caiap* were analyzed by RT-qPCR in both cells types. The results showed that while *caiap* transcripts drastically increased in macrophages upon ST infection (Figure 15D), they remain unaltered in neutrophils upon infection (Figure 15E).

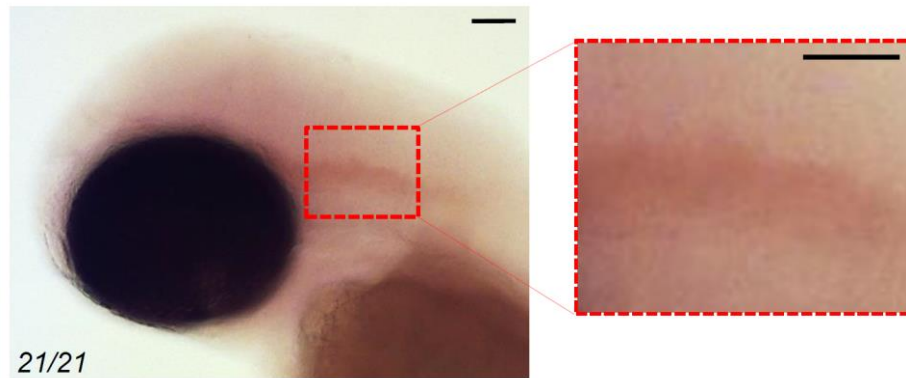


**Figure 17. Control of WISH results shown in Figure 16.** Zebrafish 2 dpf larvae were infected with ST in the otic vesicle. WISH was performed at 4 hpi using sense probes to the *caiap* gene. Note that no positive cells were observed at the infection site. The area shown is indicated in the larval scheme with boxes of different colors in Figure 16. Numbers in pictures represent the animals with the shown phenotype per total analyzed animals. Scale bar: 0.5 mm.

### **1.3. Caiap is required for the inflammasome-dependent resistance to ST in zebrafish**

To further characterize zebrafish Caiap we used a morpholino (MO)-mediated gene knockdown strategy whereby the MO was able to bind the translation start of the *caiap* mRNA and, therefore, to inhibit its translation (Figure 12). The efficiency of the MO was validated by using a caspase-1 activity assay with a fluorogenic substrate, Z-YVAD-AFC (Figure 18A,C), which has previously been shown to be processed by gilthead seabream caspase-1 (Compan et al., 2012; López-Castejón et al., 2008; Tyrkalska et al., 2016) and zebrafish Caspa (Junya Masumoto et al., 2003). Caiap morphant animals injected with 1 pg/egg MOs showed reduced caspase-1 activity but they developed normally and were viable (Figure 18C and D). However, Caiap-deficient larvae showed increased susceptibility to WT ST compared with their control siblings (Figure 5D) and impaired caspase-1 activity in response to the infection (Figure 18C). Additionally,

infection susceptibility and decreased caspase-1 activity were both fully reversed by injection of non-targetable *caiap* mRNA, confirming the specificity of the MO (Figure 18C and D). In contrast, forced expression of *Caiap* $\Delta$ CARD failed to rescue the high susceptibility and impaired caspase-1 activation of *Caiap*-deficient larvae (Figure 18E and F), suggesting that the CARD domain is indispensable for *Caiap* function. Furthermore, *Caiap* crisprant larvae also showed higher susceptibility to ST infection and reduced caspase-1 activity upon infection than their WT siblings (Figure 19). Although forced ubiquitous expression of *caiap* mRNA alone barely increased the resistance to ST infection (Figure 18D, Figure 20A and 7A) and caspase-1 activity (Figure 18C, Figure 20B and 7B), forced expression of *caiap* in macrophages, using the macrophage-specific promoter *mpeg1* (Ellett et al., 2011), resulted in increased resistance to ST infection (Figure 18G).

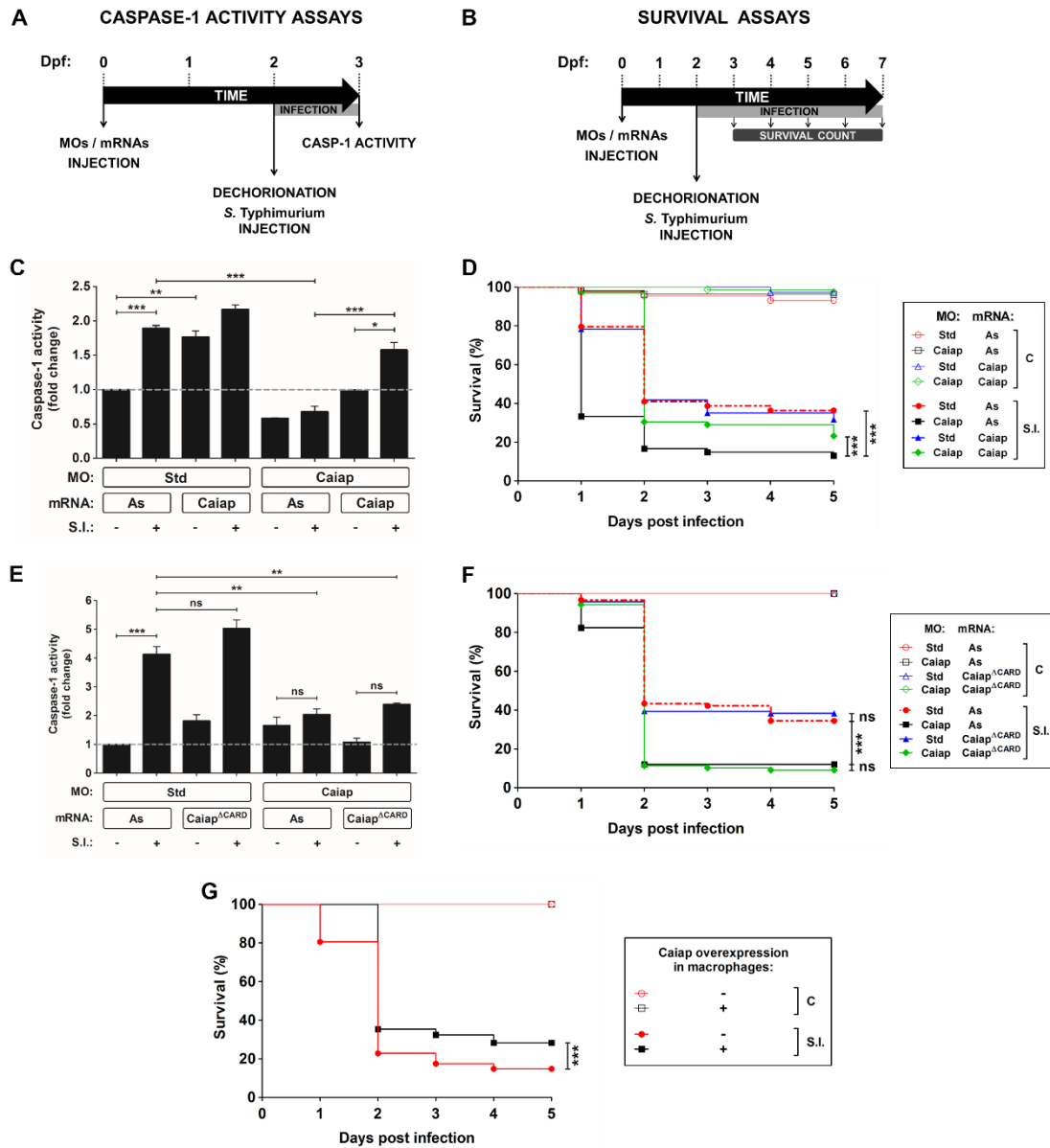


**Figure 18. Zebrafish Caiap is required for the inflammasome-dependent resistance to *S. Typhimurium*.** (A) Scheme showing the experimental procedure used for the caspase-1 activity assays. Zebrafish one-cell embryos were injected with MOs and/or mRNAs, dechorionated and infected at 2 dpf via the yolk sac with ST with a MOI of 50, and collected and pooled (25–35 larvae) at 24 hpi to measure caspase-1 activity. (B) Scheme showing the experimental procedure used for the survival assays. Zebrafish one-cell embryos were injected with MOs and/or mRNAs, dechorionated and infected at 2 dpf via the yolk sac with ST at a MOI of 10, and the number of surviving larvae counted daily during the next 5 days. At least three independent experiments were performed with a total number of 300 specimens/ treatment. (C–F) Zebrafish one-cell embryos were injected with standard control (Std) (C–F) or Caiap MOs (C–F), or with antisense (As) (C–F), Caiap (C,D) or Caiap<sup>ΔCARD</sup> (E,F) mRNAs, infected at 2 dpf with wild-type ST and the caspase-1 activity (C,E) and survival (D,E,G) were determined as described in Figures 5a,c, respectively. The sample size for each treatment is 30 for (c,e), and 300 for (D,F,G). S.I., ST infection. \*\*p < 0.01; \*\*\*p < 0.001.

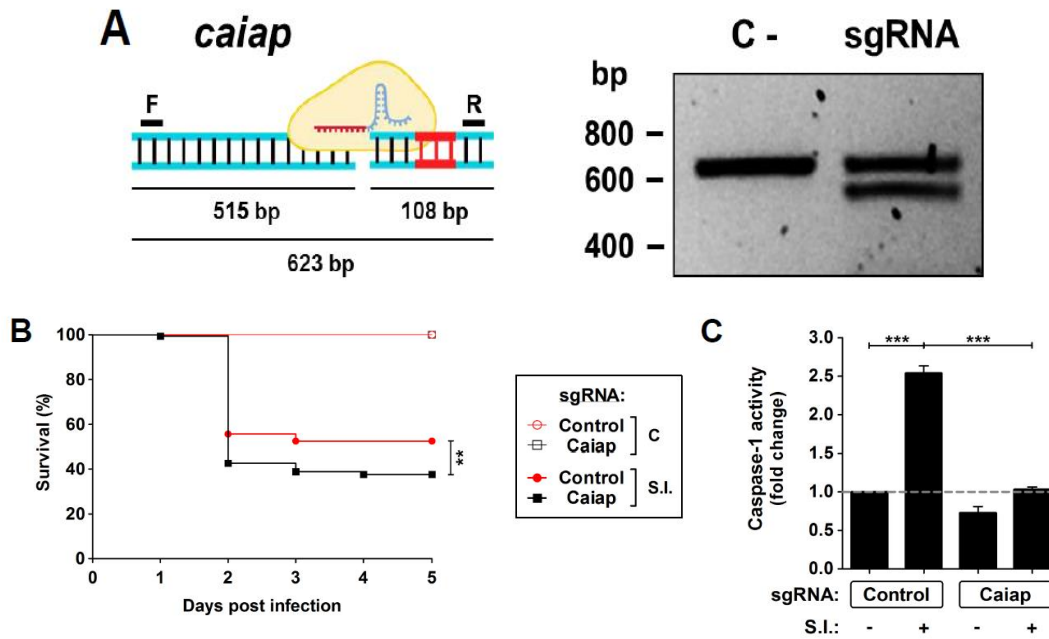


**Figure 19. *Caiap* crisper larvae show high ST susceptibility and impaired caspase-1 activation.** (A) Diagram showing the *Caiap* gRNA target at the 623 bp amplicon obtained with primers F and R, and the resulting digestion fragments. (B) Electrophoresis agarose gel stained with RedSafe showing the original amplicon in the sample incubated with Cas9 alone (C-) and the original amplicon and the expected 515 bp digestion fragment in the sample incubated with *Caiap* gRNA and recombinant Cas9. (C, D) Zebrafish one-cell embryos were injected with control or *Caiap* gRNA and recombinant Cas9. At 2 dpf, embryos were infected with ST and survival (C) and caspase-1 activity (D) were determined as described in Figures 5B and 5A, respectively. S.I., ST infection; \*\* $p < 0.01$ ; \*\*\* $p < 0.001$ .

Notably, *Caiap* levels did not affect fish susceptibility (Figure 20A,C) or caspase-1 activity (Figure 20B,D) in response to a syngenic double ST mutant for SPI-1 and SPI-2, which contains a large number of genes encoding a type 3 secretion system that is required for virulence in mouse (Shea, Beuzon, Gleeson, Mundy, & Holden, 1999) and zebrafish (Tyrkalska et al., 2016), comparing with the controls. Moreover, the impact of *Caiap* on ST infection seemed to depend on flagellin, since the virulence of the flagellin mutant strain (FlIC/FljB) of ST (Edward A Miao et al., 2006) was not affected by *Caiap* (Figure 20E,F), while the increased larval resistance and caspase-1 activity to ST which overexpresses flagellin (FlICON) (E. A. Miao et al., 2010) were found to be *Caiap*-dependent (Figure 20E,F). These results suggest that *Caiap* functions downstream of flagellin, although other PAMPs may also regulate *Caiap* activation.

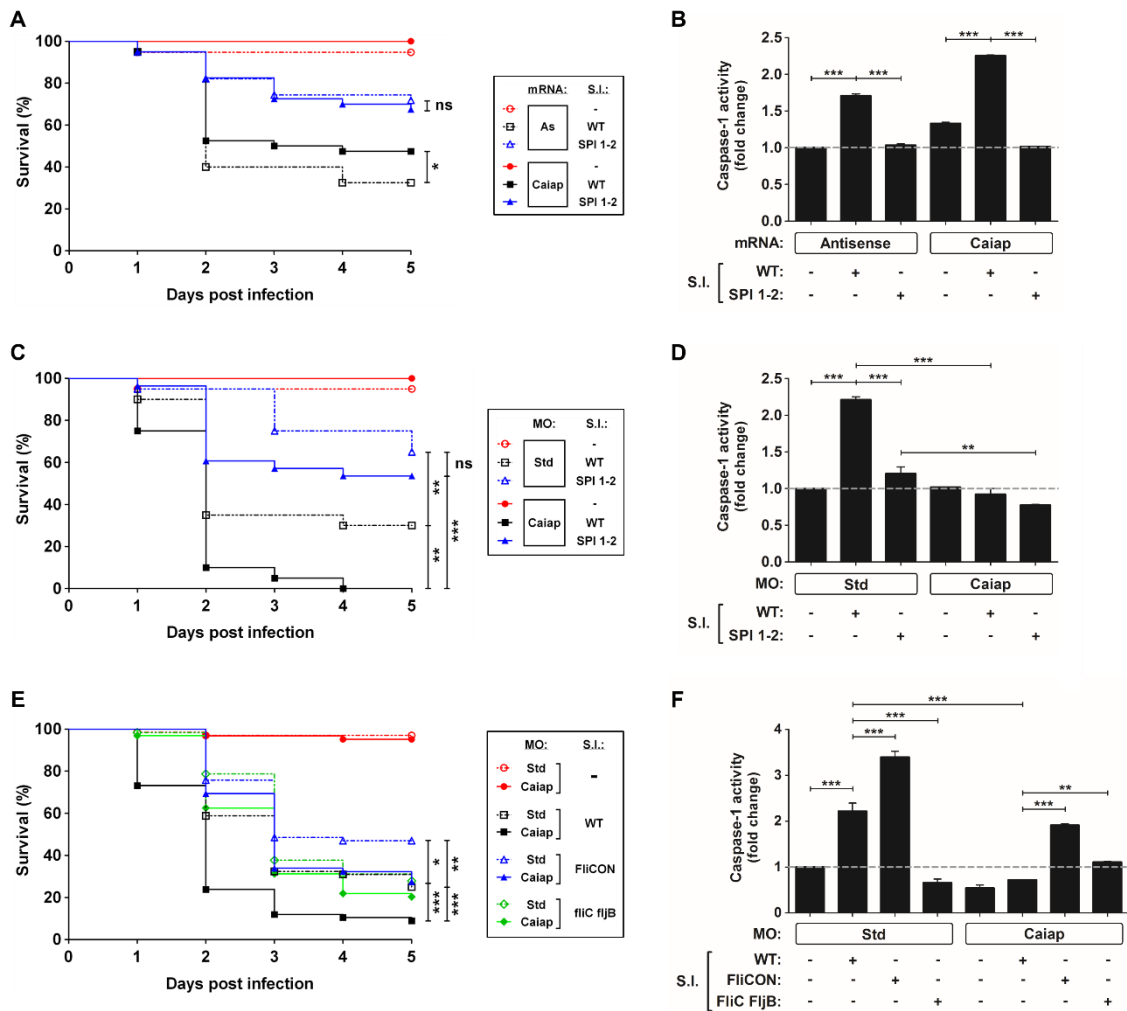
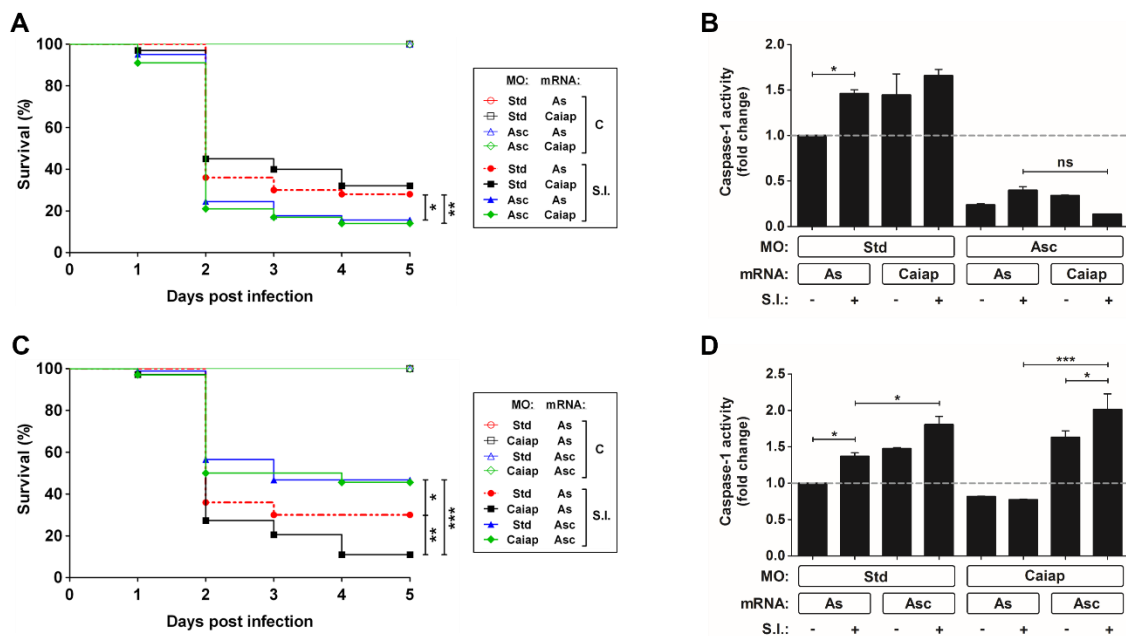


**Figure 20. The type 3 secretion system and flagellin of *S. Typhimurium* act upstream Caiap.** (A–F) Zebrafish one-cell embryos were injected with standard control (Std) or Caiap MOs, or with antisense (As) or Caiap mRNAs, infected at 2 dpf with wild-type (WT) (A–F), the double mutant SPI 1–2 (A–D), FliCON or FliC F1jB ST (A,F) and the survival (A,C,E) and caspase-1 activity (B,D,F) were determined as described in Figures 18 A,B, respectively. The sample size for each treatment is 300 for (A,C,E), and 30 for (B,D,F). S.I., ST infection; ns, not significant; \* $p < 0.05$ ; \*\* $p < 0.01$ ; \*\*\* $p < 0.001$ .

### 1.4. Zebrafish Caiap requires Asc to mediate the Inflammasome-dependent resistance to ST

Most inflammasomes require the adaptor protein ASC for their assembly, activation, and function. However, some NLRs that contain a CARD domain can bind directly to caspase-1. To this group belongs NLRC4, which has been shown to take part in host defences against bacterial infection (Case, 2011; Case & Roy, 2011). However, it has recently been found that ASC can strengthen the signal of the NLRC4 inflammasome

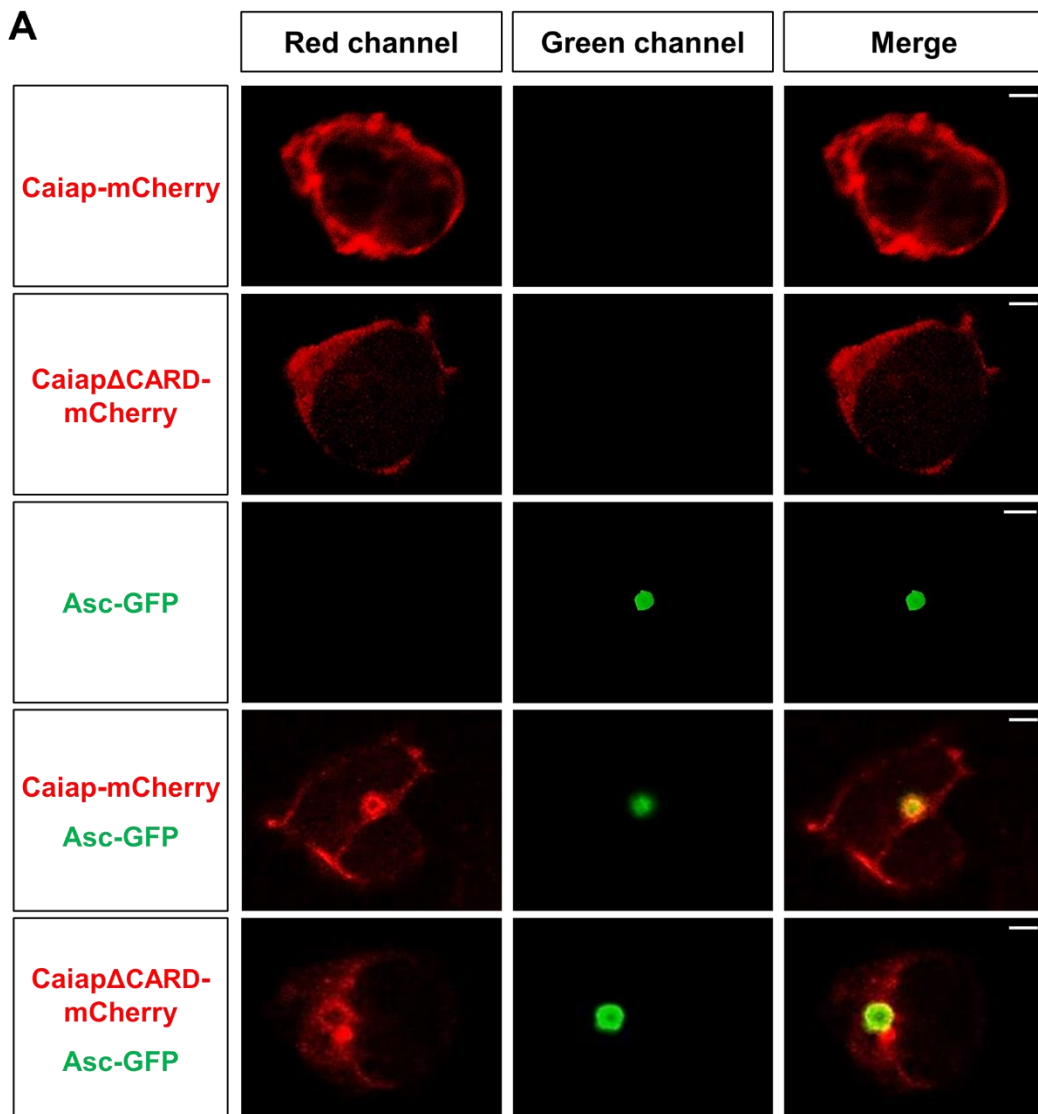
(Latz et al., 2013) or being required for some specific responses (Broz, von Moltke, Jones, Vance, & Monack, 2010). The presence of a CARD domain in Caiap suggests that it may directly recruit and activate Caspase-1 without the need for ASC, at least in most evolutionarily advanced species where true orthologs of mammalian caspase-1 with CARD domain exist. To check this, we ablated Asc using a previously validated translation-blocking MO (Tyrkalska et al., 2016). Genetic depletion of Asc in zebrafish drastically increased the susceptibility to ST of both WT and Caiap-deficient larvae (Figure 21A). In addition, Asc deficiency inhibited basal and Caiap-induced caspase-1 activity in non-infected and infected larvae (Figure 21B). Conversely, forced expression of Asc strongly increased larval resistance to the infection and caspase-1 activity, both effects being largely independent of Caiap (Figure 21C andD).

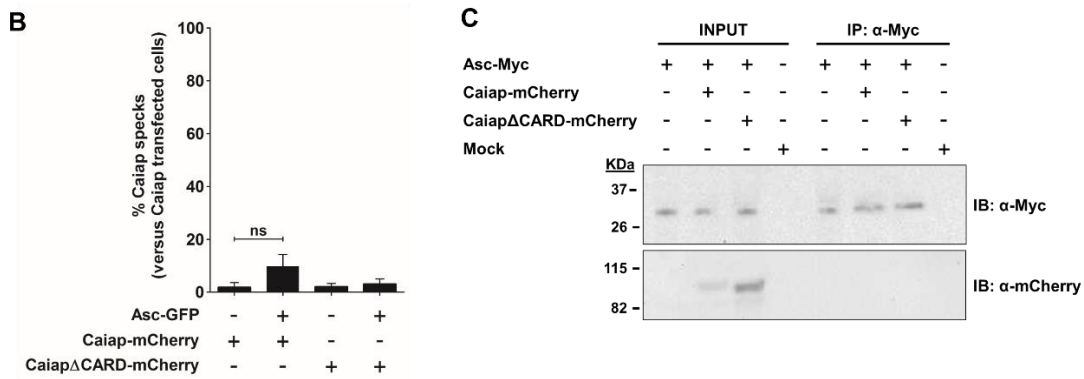


**Figure 21. Asc is required for the Caiap-mediated resistance to *S. Typhimurium*.** Zebrafish one-cell embryos were injected with standard control (Std), Asc (A,B) or Caiap (C,D) MOs or in combination with antisense (As), Caiap (A,B) or Asc (C,D) mRNAs, infected at 2 dpf and survival (A,C) and caspase-1 activity (B,D) determined as described in Figure 18A,B, respectively. S.I., ST infection. The sample size for each treatment is 300 for (A,C), 30 for (B,D), ns, not significant; \* $p < 0.05$ ; \*\* $p < 0.01$ ; \*\*\* $p < 0.001$ .

*Results: CAIAP*

Unexpectedly, however, reconstitution of Caiap and Asc complexes in HEK293T cells, which lack each of these components, showed that Caiap and Caiap $\Delta$ CARD fused to mCherry were both diffusely distributed in the cytosol in the absence of Asc but formed a ring around the speck in the presence of Asc (Figure 22A, B). In addition, co-immunoprecipitation assays confirmed that Caiap was unable to physically interact with Asc (Figure 22C).

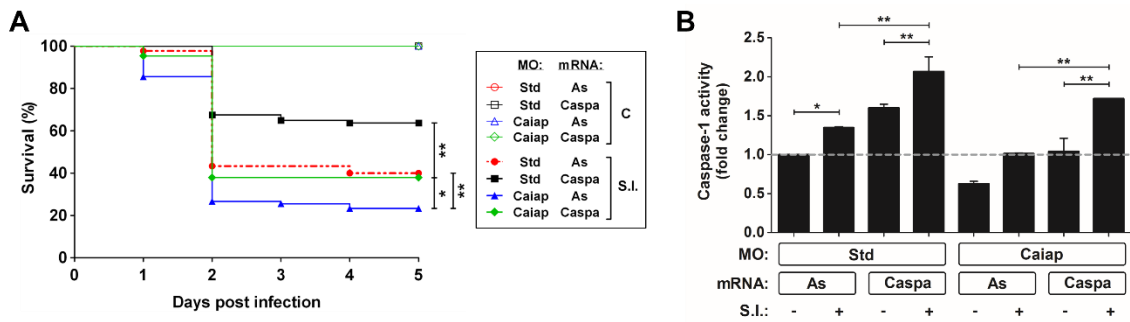




**Figure 22. Asc does not interact directly with Caiap.** HEK293T cells were transfected with zebrafish *Caiap*-mCherry or *Caiap*ΔCARD-mCherry in the presence or absence of zebrafish *Asc*-Myc, fixed at 48 h post-transfection, immunostained and imaged using a laser confocal microscope (A,B) or lysed, immunoprecipitated with anti-Myc Affinity Gel, and probed with antibodies to Myc and mCherry (C). Representative views of maximum-intensity projection images of HEK293T cells are shown in (A), quantitation of the percentage of *Caiap* specks in relation to the total number of *Caiap* transfected cells is shown in (B) and representative blots are shown in (C). The sample size is 50 (B). Scale bar, 5 μm; ns, not significant; \* $p < 0.05$ ; \*\* $p < 0.01$ ; \*\*\* $p < 0.001$ .

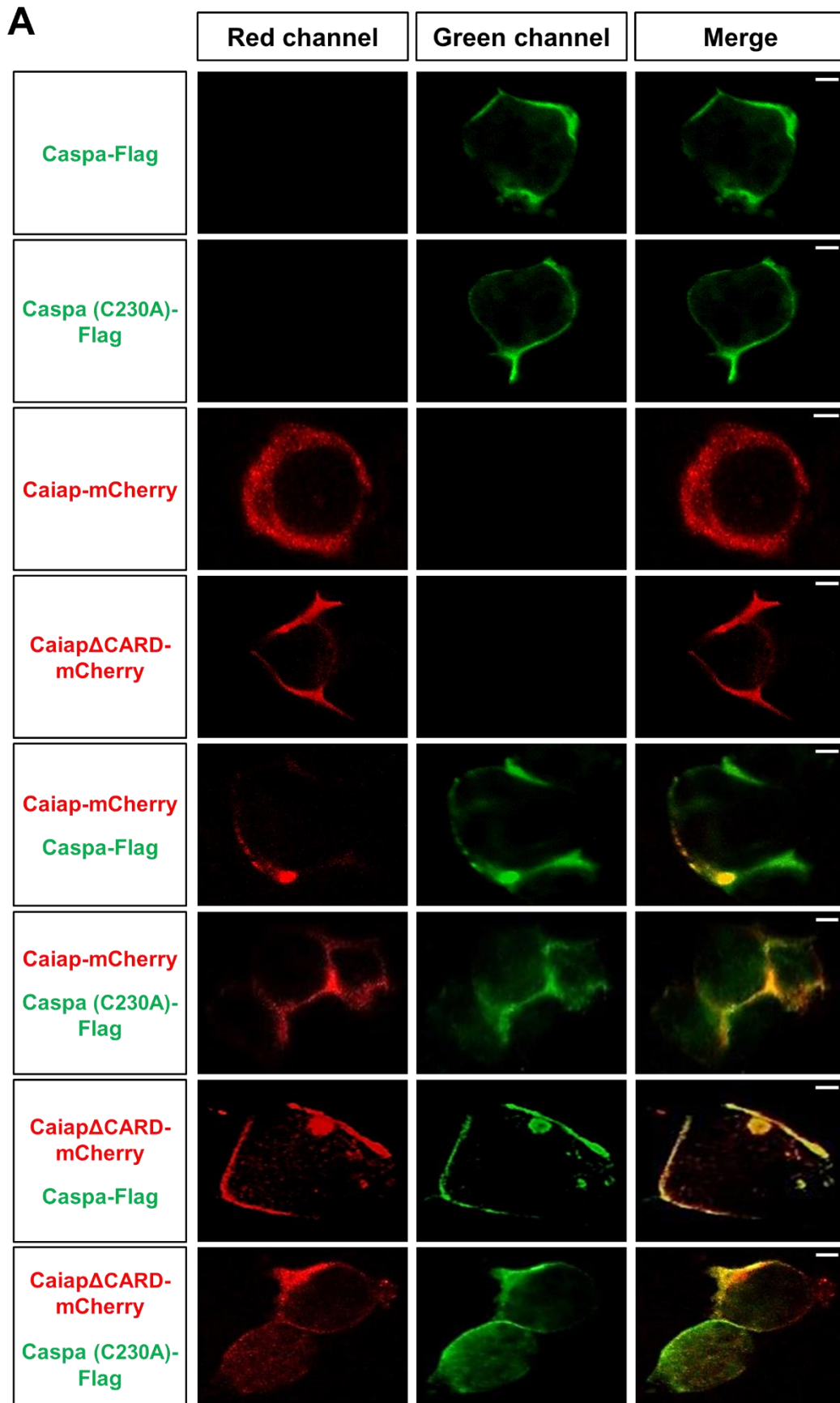
### 1.5. Zebrafish *Caiap* is required for Caspa activation

Caspase a (Caspa, also known as Caspy) is considered the functional homolog of mammalian caspase-1, since it preferentially cleaves AcYVAD-AMC, a caspase-1 substrate, and interacts and co-localizes at the speck with zebrafish *Asc* in HEK293T cells (Junya Masumoto et al., 2003). In addition, recent studies have demonstrated *in vivo* that Caspa is the effector enzyme of the zebrafish inflammasome in both macrophages (Vincent et al., 2016) and neutrophils (Tyrkalska et al., 2016). Therefore, we next analyzed whether the forced expression of Caspa was able to rescue the high ST susceptibility of *Caiap*-deficient larvae. The results showed that Caspa was indeed able to rescue the infection susceptibility (Figure 23A) but only partially caspase-1 activity (Figure 23B) of *Caiap*-deficient larvae. In addition, forced expression of Caspa alone increased the resistance of larvae to ST infection (Figure 23A), confirming previous results (Tyrkalska et al., 2016).



**Figure 23. Caspa is required for the Caiap-mediated resistance to *S. Typhimurium*.** (A,B) Zebrafish one-cell embryos were injected with standard control (Std) or Caspa mRNAs. At 2 dpf, embryos were infected with ST and survival (A) and caspase-1 activity (B) were determined as described in Figures 7A,B, respectively. S.I., ST infection. The sample size for each treatment is 300 for (A), 30 for (B), ns; not significant; \* $p < 0.05$ ; \*\* $p < 0.01$ ; \*\*\* $p < 0.001$ .

The above results show that Caiap acts through Asc and Caspa to promote ST resistance, although this does not clarify the mechanism by which Caiap plays this function. We therefore reconstituted Caiap and Caspa complexes in HEK293T cells and, surprisingly, WT Caiap and Caiap $\Delta$ CARD were both able to form specks in the presence of wild type but not of catalytic inactive mutant Caspa (Figure 24C and D). These results were further confirmed by pull down assays, in which WT Caiap and Caiap $\Delta$ CARD were able to physically interact with WT Caspa but not with catalytic inactive Caspa (Figure 24E). In addition, while WT Caiap overexpressed in HEK293T cells self-oligomerized, assayed under nonreducing conditions, Caiap $\Delta$ CARD required active Caspa to fully oligomerize (Figure 24F). Taken together, these results show that Caiap interacts with catalytic active Caspa (P20/P10) through its ANK domain and self-oligomerizes *via* its CARD domain.



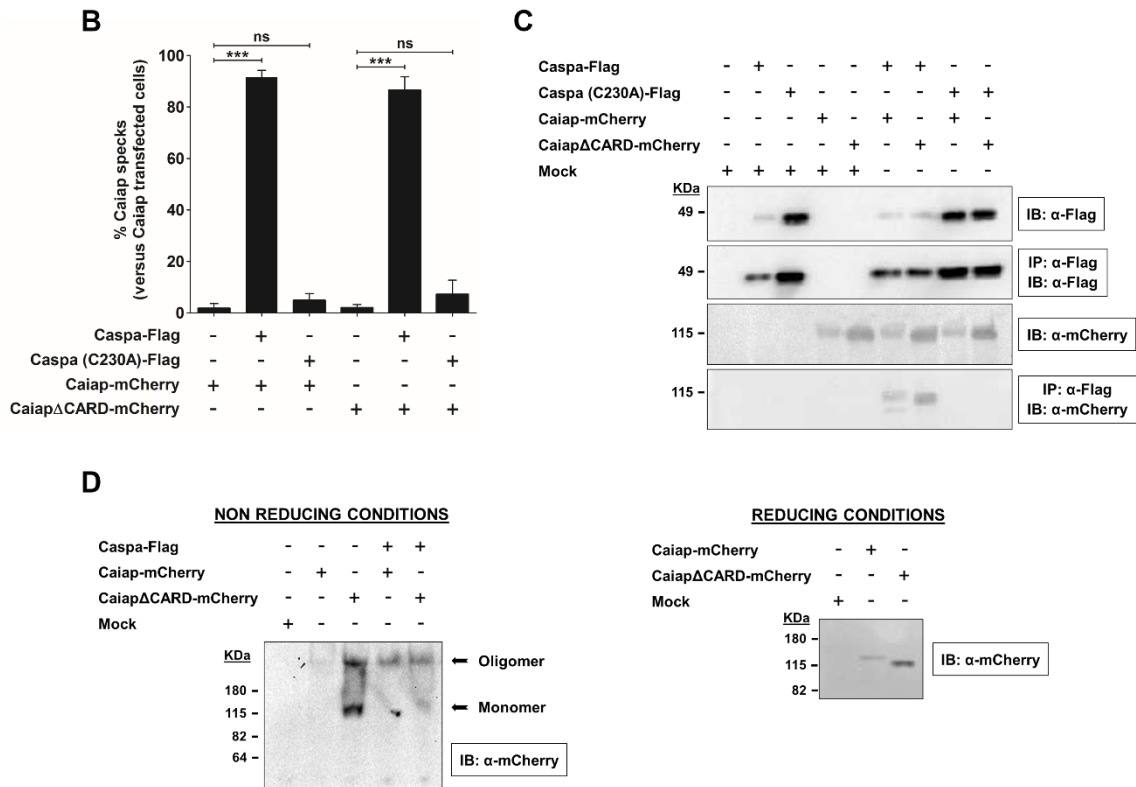


**Figure 24. Asc is required for the Caiap-mediated resistance to *S. Typhimurium*.** (A-D) HEK293T cells were transfected with zebrafish Caiap-mCherry or CaiapΔCARD-mCherry in the presence or absence of zebrafish wild-type FLAG-Caspa or catalytic inactive FLAG-Caspa (C230A), fixed at 48 h post-transfection and imaged using a laser confocal microscope (A,B), or lysed and immunoprecipitated with ANTI-FLAG M2 Affinity Gel and probed with antibodies to FLAG and mCherry (C) or lysed and resolved under non-reducing and reducing conditions (D). Representative views of maximum-intensity projection images of HEK293T cells are shown in (A), quantitation of the percentage of Caiap specks in relation to the total number of Caiap transfected cells is shown in (B) and representative blots are shown in (C,D). The sample size for is 50 for (B). Scale bar, 5 μm; not significant; \* $p < 0.05$ ; \*\* $p < 0.01$ ; \*\*\* $p < 0.001$ .

## 2. WDR90

### 2.1. Identification and characterization of WDR90

A previous RNA-Seq analysis performed in our laboratory from zebrafish larvae infected and uninfected with ST showed a direct correlation between the expression of *gbp4*, which encodes a new component of inflammasome described by our group in 2016 (Tyrkala et al., 2016), and *wdr90*, which encodes an uncharacterized protein. The zebrafish sequence for Wdr90 (F1RA29\_DANRE) had a 49% identity with the human WDR90 (Q96KV7\_HUMAN), which was 72% identical to the mouse sequence (Q6ZPG2\_MOUSE). Alignment of the 3 species sequence is shown in Figure 25.



**Figure 25. WDR90 sequence alignment for human, mouse and zebrafish species. The accession numbers are Q96KV7\_HUMAN (human), Q6ZPG2\_MOUSE (mouse) and F1RA29\_DANRE (zebrafish). (|) Identity in one position; (|) conservative substitutions in one position; (-) semiconservative substitutions in one position.**

While the zebrafish annotation of Wdr90 is still unreviewed, their mammalian counterparts are already established. The human WDR90 had 5 isoforms produced by

alternative splicing. The canonical isoform had a molecular weight of 188kDa and is composed mainly by WD40 domains (Figure 26).

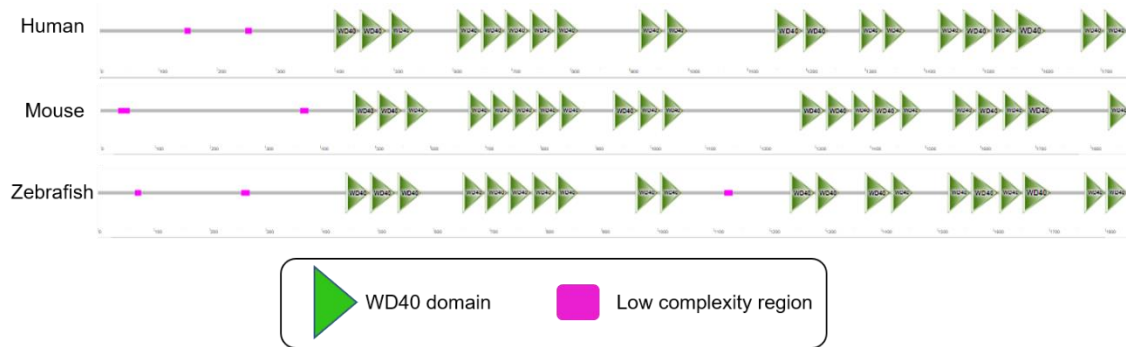


**Figure 26. Molecular characteristics of WDR90.** Diagrams showing the domain organization generated of human (Q96KV7\_HUMAN), mouse (Q6ZPG2\_MOUSE) and zebrafish (F1RA29\_DANRE) WDR90. The WD40 domains (SMART accession number SMS000320) are shown as green boxes and low complexity regions are shown as pink boxes. The amino acid sequence for the 3 species were analysed using the SMART database (<http://smart.embl-heidelberg.de>).

## 2.2. *gpb4* induces *wdr90* expression independently of inflammasome activation

In order to confirm the transcriptomic data previously mentioned, the expression of *wdr90* in zebrafish was checked by RT-qPCR analysis after the forced expression of Gbp4 mRNA in zebrafish embryos. As Gbp4 is a protein with a GTPase activity needed for regulating inflammasome activation, larvae were also injected with a mutant form of Gbp4, Gbp4 KS/AA, which lacks GTPase activity. *wdr90* mRNA levels increased in larvae forced to express wild type Gbp4, whereas GTPase-deficient Gbp4 failed to do so (Figure 27), pointing the importance of the GTPase domain in the regulation of *wdr90* expression.

We examined whether pharmacological inhibition of caspase-1 with the irreversible caspase-1 inhibitor Ac-YVAD-CMK, which was shown to inhibit Caspa (Tyrkalska et al., 2016). The results showed that the increased mRNA levels of *wdr90* mediated by Gbp4 were unaffected by Caspa inhibition, indicating that Gbp4 regulates *wdr90* gene expression independently of the inflammasome (Figure 28A). This result was further confirmed by the inability of forced expression of Asc to induce *wdr90* mRNA levels (Figure 28B). However, ST infection induced *wdr90* expression, as well as those of *il1b*, which was used as a positive control (Figure 28C and 28D). Collectively, these

results suggest that Gbp4 regulates *wdr90* mRNA levels independently of the inflammasome and that Wdr90 may be involved in infection since their transcript levels were induced by ST.

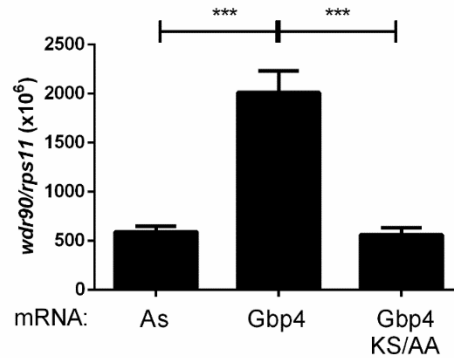


**Figure 27. Gbp4 regulates *wdr90* expression in zebrafish.** *Wdr90* mRNA levels were measured by RT-qPCR in 72 hpf larvae forced to express antisense (As, control), Gbp4 or the mutant Gbp4 KS/AA. \*\*\* $p < 0.001$ .

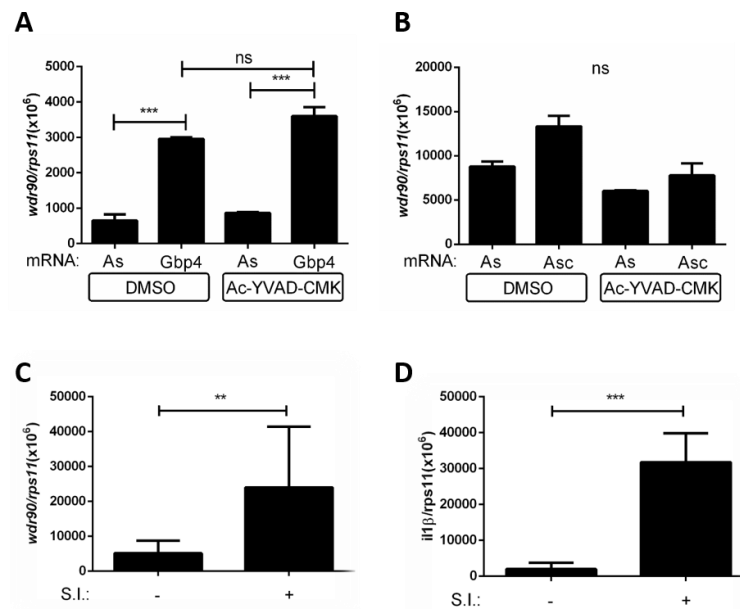


**Figure 28. The induction of *wdr90* expression by Gbp4 is independent of the inflammasome.** (A, B) *wdr90* expression in 72 hpf larvae forced to express antisense (As, control), *gbp4* (A), *asc* (B) mRNAs after being treated by immersion with the vehicle alone (DMSO) or 100  $\mu$ M of the caspase-1 inhibitor Ac-YVAD-CMK for 24 h. (C, D) *wdr90* (C) and *il1b* (D) expression in 72 hpf larvae left uninfected (-) or 24 h after ST infection (+). \* $p < 0.05$ ; \*\*\* $p < 0.001$ . ns, not significant.

### 2.3. Wdr90 is involved in Caspa activation and larval resistance to ST infection

The above results prompted us to examine whether Wdr90 is involved in inflammasome activation and ST clearance in zebrafish. Forced expression of *wdr90* mRNA led to higher resistance to ST infection (Figure 29A) and increased caspase-1 activity (Figure 29B). These results pointed out Wdr90 as a novel inflammasome component involved in ST clearance in zebrafish.

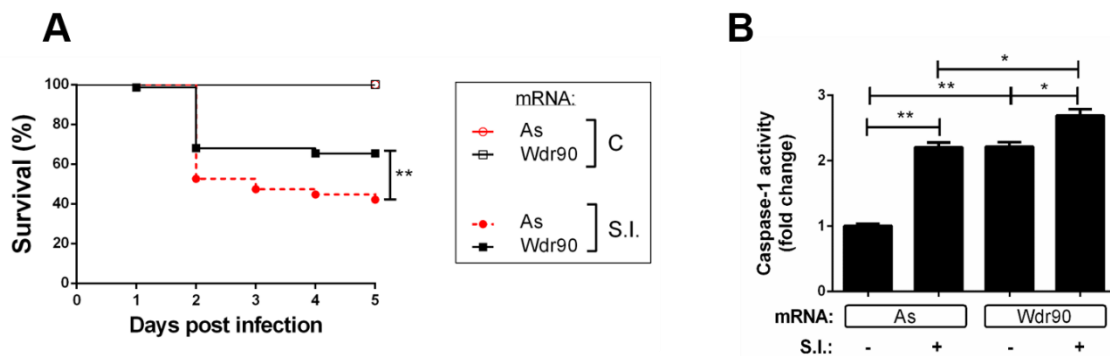


**Figure 29. Forced expression of *wdr90* increases larval resistance to ST infection (S.I.) and caspase-1 activity.** Survival (A) and caspase-1 activity (B) determined as indicated in Figures 18A and 18B, respectively, of zebrafish larvae forced to express antisense (As) or *wdr90* mRNAs and left uninfected (-) or infected at 2 dpf with ST (+). \*  $p < 0.05$ ; \*\*  $p < 0.01$ ; \*\*\*  $p < 0.001$ .

To further characterize the role of Wdr90, we depleted Wdr90 expression by using a specific morpholino at different concentrations but, unfortunately, the doses needed to block its expression were lethal for the larvae, probably suggesting other essential functions of Wdr90 in larval development. This is not unexpected, since a very recent publication showed a role of Wdr90 in ciliogenesis in *Chlamydomonas* (Hamel et al., 2017).

### 2.4. Wdr90 acts upstream Asc and caspase-1 to promote ST resistance

As we were not able to deplete Wdr90 expression in zebrafish larvae, we further characterize the role played by Wdr90 in inflammasome by using forced expression conditions in combination with specific MO to Asc and Gbp4, which had been shown to reduce larvae resistance and caspase-1 activity after ST infection (Tyrkalska et al., 2016).

While ASC is not always required in mammals for inflammasome activation, zebrafish Asc is essential for its function (Bezbradica & Schroder, 2017). To determine if high expression levels of Wdr90 were able reverse the effects caused by the lack of Asc, we used an Asc morpholino. Our results showed that genetic depletion of Asc increased larval susceptibility to ST infection independently of Wdr90 expression levels (Figure 30A). Moreover, the ablation of Asc also fully reduced basal and Wdr90-induced caspase-1 activity under both infection and non-infection conditions (Figure 30B). Similarly, Gbp4 depletion reduced larvae resistance to the infection and caspase-1 activity, and forced expression of Wdr90 failed to reverse the higher susceptibility to ST of Gbp4-deficient larvae (Figure 30C), whereas caspase-1 activity was slightly recovered (Figure 30D).

To confirm that Wdr90 was promoting increased larval resistance to ST by activating the inflammasome, larvae were exposed to the specific caspase-1 inhibitor Ac-YVAD-CMK in combination with Wdr90 overexpression. The result confirmed a role of Wdr90 in inflammasome-dependent resistance to ST infection of zebrafish larvae, since increased levels of Wdr90 failed to reverse the high larval susceptibility to ST (Figure 30E) and reduced caspase-1 activity (Figure 30F) promoted by inhibition of Caspa. Collectively, these results indicate that Wdr90 is acting upstream Asc and Caspa, and probably Gbp4, to promote ST resistance in zebrafish larvae.

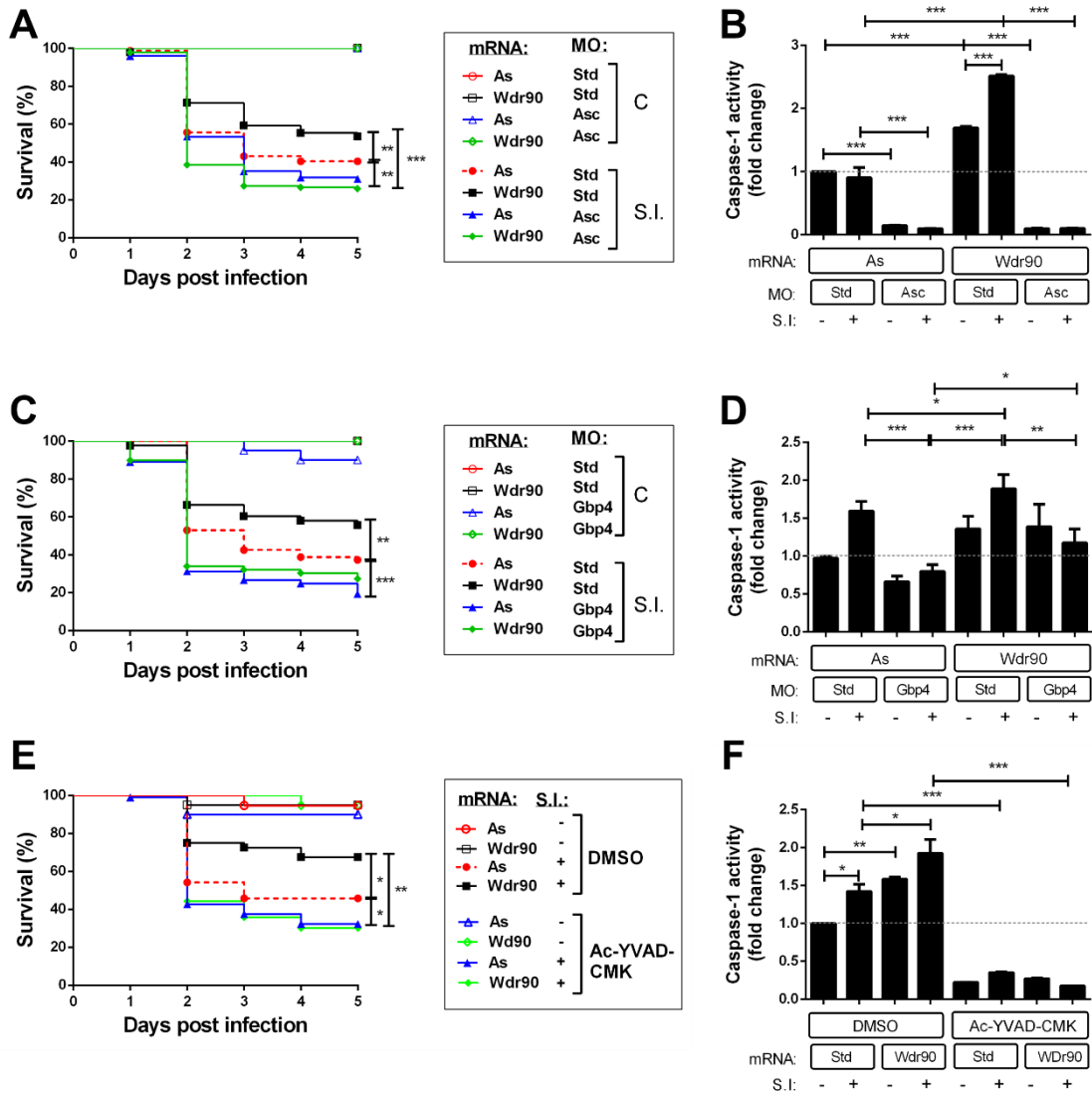


**Figure 30. Zebrafish *Wdr90* acts upstream Caspa, Asc and Gbp4 in ST resistance.** Zebrafish one-cell embryos were injected with standard control (Std) (A–D), Asc (A–B) or Gbp4 MOs (C–D) alone or combined with antisense (As) or *Wdr90* mRNAs (A–F). Larvae were treated at 1 dpf with DMSO or 100  $\mu$ M of Ac-YVAD-CMK (E, F), then infected at 2 dpf with wild-type ST and the caspase-1 activity (B,D,F) and survival (A,C,E) were determined as described in Figures 18A,B, respectively. The sample size for each treatment is 20 for (E,F), 30 for (B,D), and 300 for (A,C). S.I., ST infection. \*\* $p < 0.01$ ; \*\*\* $p < 0.001$ .

## **2.5. Human WDR90 interacts with NLRC4**

Inflammasome complex has an enormous importance in human health (Lamkanfi, Walle, & Kanneganti, 2011). Thus, one of the main aims of research in the inflammasome field is to reach a deeper understanding of the function of the complex and its different components, as well as to identify other proteins that participate in its functions. The data obtained in the zebrafish model led us to check if human WDR90 is able to interact with other inflammasome components upstream of ASC and CASP1. In order to do, we ectopically expressed human WDR90 tagged with a FLAG epitope on its C-terminal (huWDR90-FLAG) with different inflammasome receptors in HEK293T cells, which lack all these components. We found that the expression of WDR90 was very low, so we decided to optimize the transfection conditions in order to get an optimal expression of WDR90 in this cell type. HEK293T were transfected with WDR90-FLAG and its expression was checked by immunofluorescence (IF) at 24, 48 and 72 hours post-transfection. Our results showed a low expression of WDR90 24h post-transfection, which increased at 48h and it was maintained at 72h (Figure 31A). Notably, WDR90 was found in the cytosol but not in the nucleus. We next decided to carry out the western blot (WB) of WDR90 FLAG at 48h post-transfection, including a pcdna3-FLAG as a negative control and huCASP1-FLAG as a positive control of expression. However, although the expression of WDR90 was well detected in by IF, it was hardly detected by WB (Figure 31B).

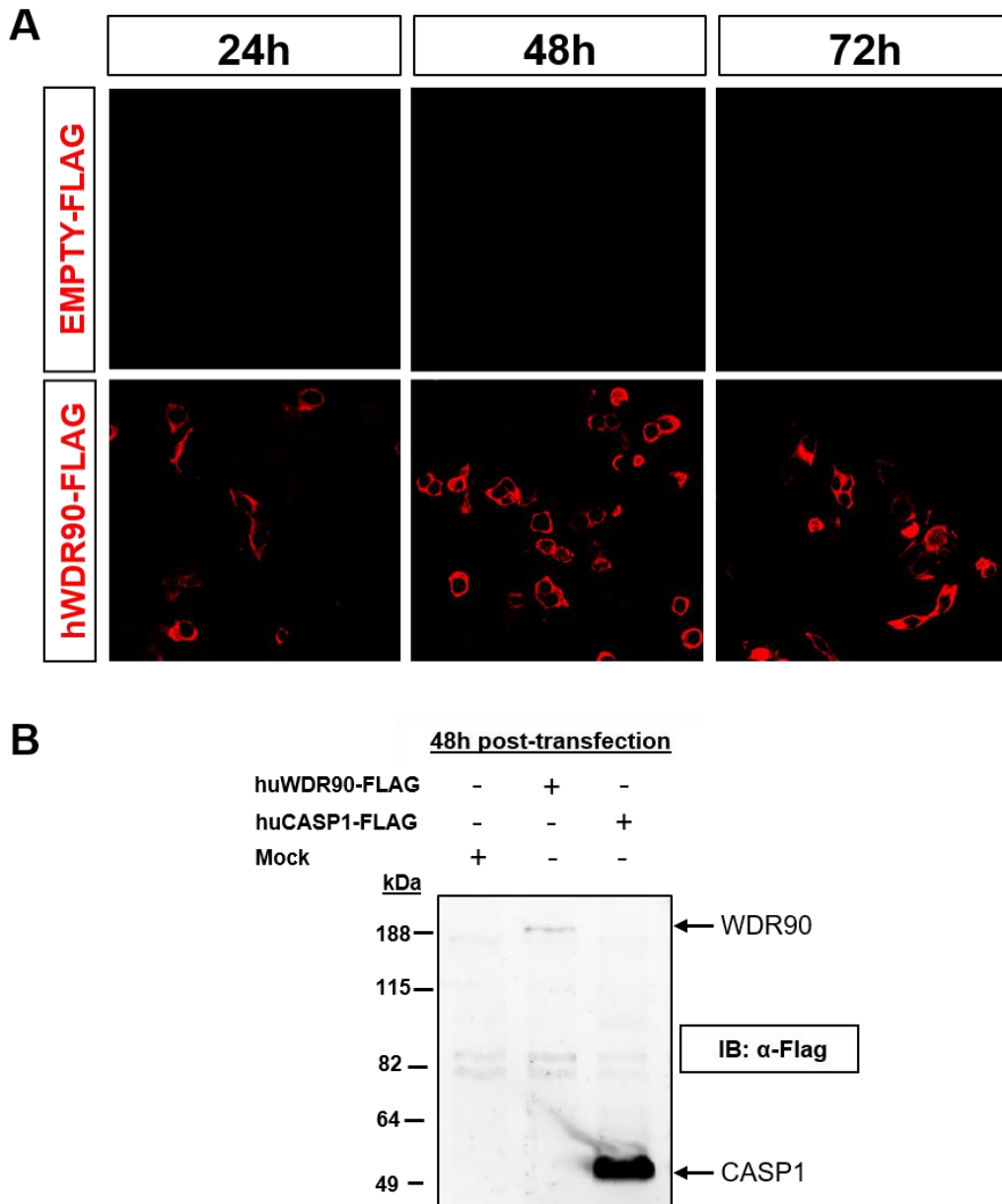


**Figure 31. Optimization of WDR90 expression conditions.** HEK293T cells were transfected with huWDR90-FLAG (A,B) and huCASP1-FLAG (B) as a positive control. Cells were fixed at 24,48 and 72h post-transfection and imaged using a laser confocal microscope (A), or lysed with a 1% SDS-containing buffer 48h post-transfection and then probed with an anti-FLAG-HRP antibody.

WDR90 protein has a large molecular weight with a repetitive number of WD40 domains. In order to optimize and get the best condition to detect WDR90 by WB, we decided to try different lysis buffers to increase the solubility of the protein. However, we had to avoid strong detergents-containing buffers as our final aim was to perform an immunoprecipitation (IP) to verify its interaction with other inflammasome components. To do that we used NP40 and Triton X-100 as detergents in the lysis buffer (Figure 32A),

but under these lysis conditions we were unable to clearly detect WDR90 by WB. Finally, we determined that the solubilization improved when the sample was not prewarmed at 95°C (Figure 32B).

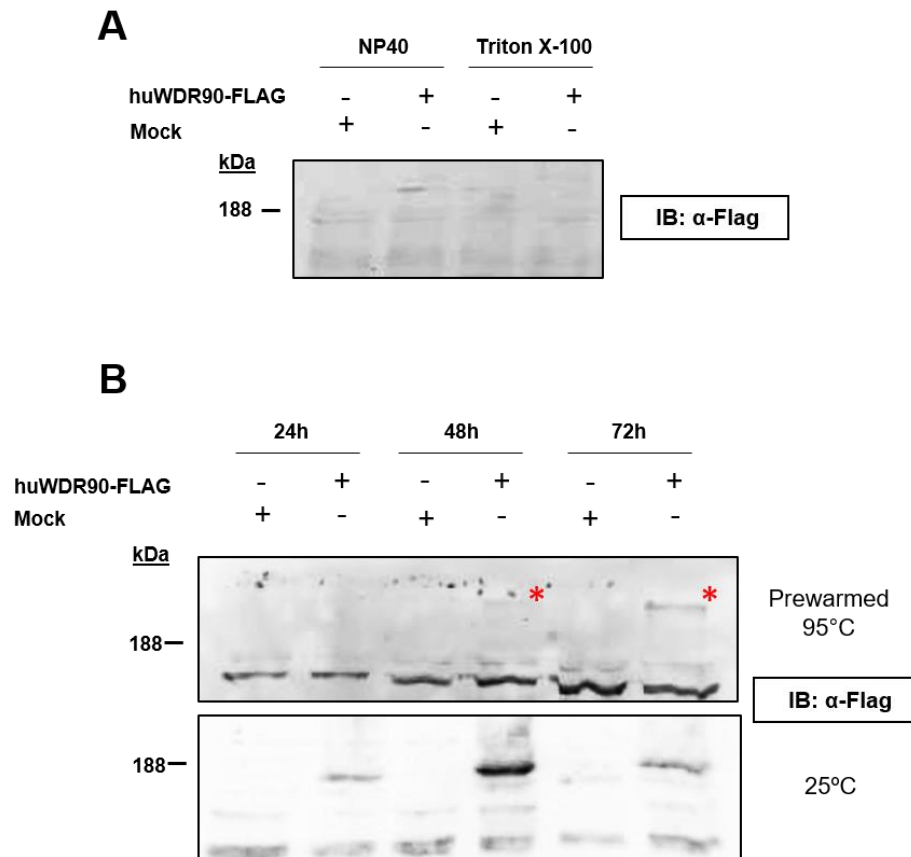


**Figure 32. Optimization of WB conditions for WDR90.** HEK293T cells were transfected with huWDR90-FLAG (A,B) and lysed 48h (A,B) or 24, 48 and 72 h (C) post-transfection with NP40- (A,B) or Triton X-100-containing (A) buffers. Samples were prewarmed at 95 °C (A, B) or at room temperature (B) during 5 min. \* WDR90 insoluble aggregates.

Once we had determined the optimal conditions to detect WDR90 by WB, we aimed to determine if WDR90 was able to interact with inflammasome receptors. The main mammalian receptor described to be activated after ST infection is NLRC4, although NLRP3 also acts in its recognition (Qu et al., 2016a) and it is the widest studied. Our hypothesis was that if WDR90 interacts with an NLR, it would be at least with one related to ST detection. To confirm if WDR90 was interacting with the canonical inflammasome receptor for ST, NLRC4 (Reyes Ruiz et al., 2017), we co-transfected huWDR90-FLAG with a human NLRC4-MYC and checked the proteins distribution by IF (Figure 33A). WDR90 was able to form small aggregates through the cytosol when a high

expression was achieved. In the same manner, NLRC4 appear in the cytoplasm but did not form aggregates when it is overexpressed, as previously reported (Man, Hopkins, et al., 2014). In contrast, co-transfection of both proteins resulted in their colocalization in the WDR90 aggregates (Figure 33A), suggesting that WDR90 could interact NLRC4.

In order to verify this result, we performed an IP of lysates from HEK293T co-transfected with huWDR90-FLAG and huNLRC4-Myc. As it was hard to detect WDR90 by WB, high amount of salts wash used during the washing procedure to avoid non-specific interactions. Efficient immunoprecipitation of WDR90 was observed when it was transfected alone (Figure 33B). However, after co-transfection, WB detection and IP of WDR90 was reduced. Unfortunately, under these circumstances we were not able to detect NLRC4 immunoprecipitated together with WDR90, being not able to confirm direct interaction between these proteins. The decrease of the detection of WDR90 in WB subsequent to NLRC4 co-transfection led us to wonder if aggregates formed between these proteins resulted in an insoluble complex that impaired the detection. Thereby, with the purpose of corroborating the interaction between WDR90 and NLRC4, we plan to develop a proximity ligation assay (PLA) (Gomez, Shankman, Nguyen, & Owens, 2013).

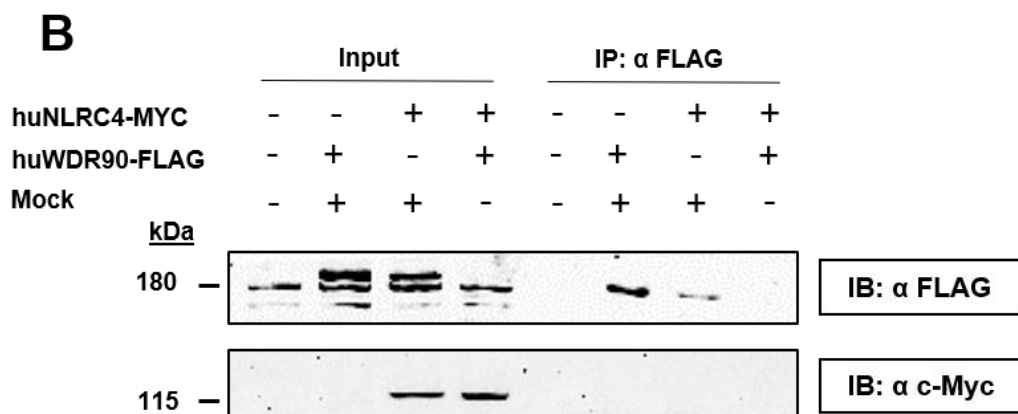
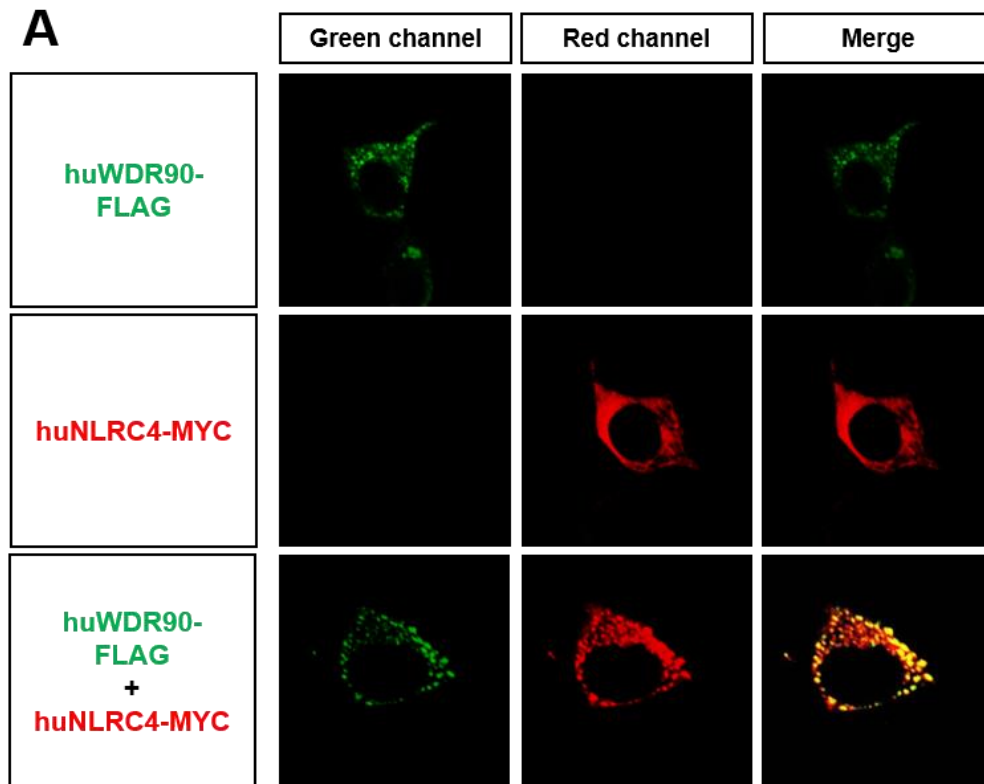


**Figure 33. NLRC4 cellular redistribution in the presence of WDR90.** HEK293T cells were transfected with human WDR90-FLAG and/or NLRC4-MYC, fixed at 48 h post-transfection, immunostained and imaged using a laser confocal microscope (A) or lysed, immunoprecipitated with anti-FLAG M2 Affinity Gel, and probed with antibodies to MYC and FLAG (B).

These led us to wonder if WDR90 specifically altered the cellular distribution of NLRC4 or other inflammasome receptors too. First, we developed the same co-transfection with the human NLRP3 receptor, as it also takes part in the inflammasome macromolecular complex in mouse macrophages infected with ST (Man, Hopkins, et al., 2014; Qu et al., 2016b). However, in contrast to NLRC4, NLRP3 did not change its distribution in the presence of WDR90 (Figure 34A). Similar results were obtained with AIM2 receptor which also presented its typical cytoplasmic distribution (Huang et al., 2017) without exhibiting any changes under the presence of WDR90 (Figure 34B). Nevertheless, the difficulties associated to the detection of WDR90 by WB and IP impaired to use these approaches to further confirm these results.

In conclusion, all these results show for the first time a role for WDR90 in inflammasome assembly and activation probably through the interactions with NLRC4. However, to confirm the importance of WDR90 in inflammasome, we decided to develop knockout (KO) and knockin (KI) models of this protein in human and mouse macrophages as well as nanobodies.

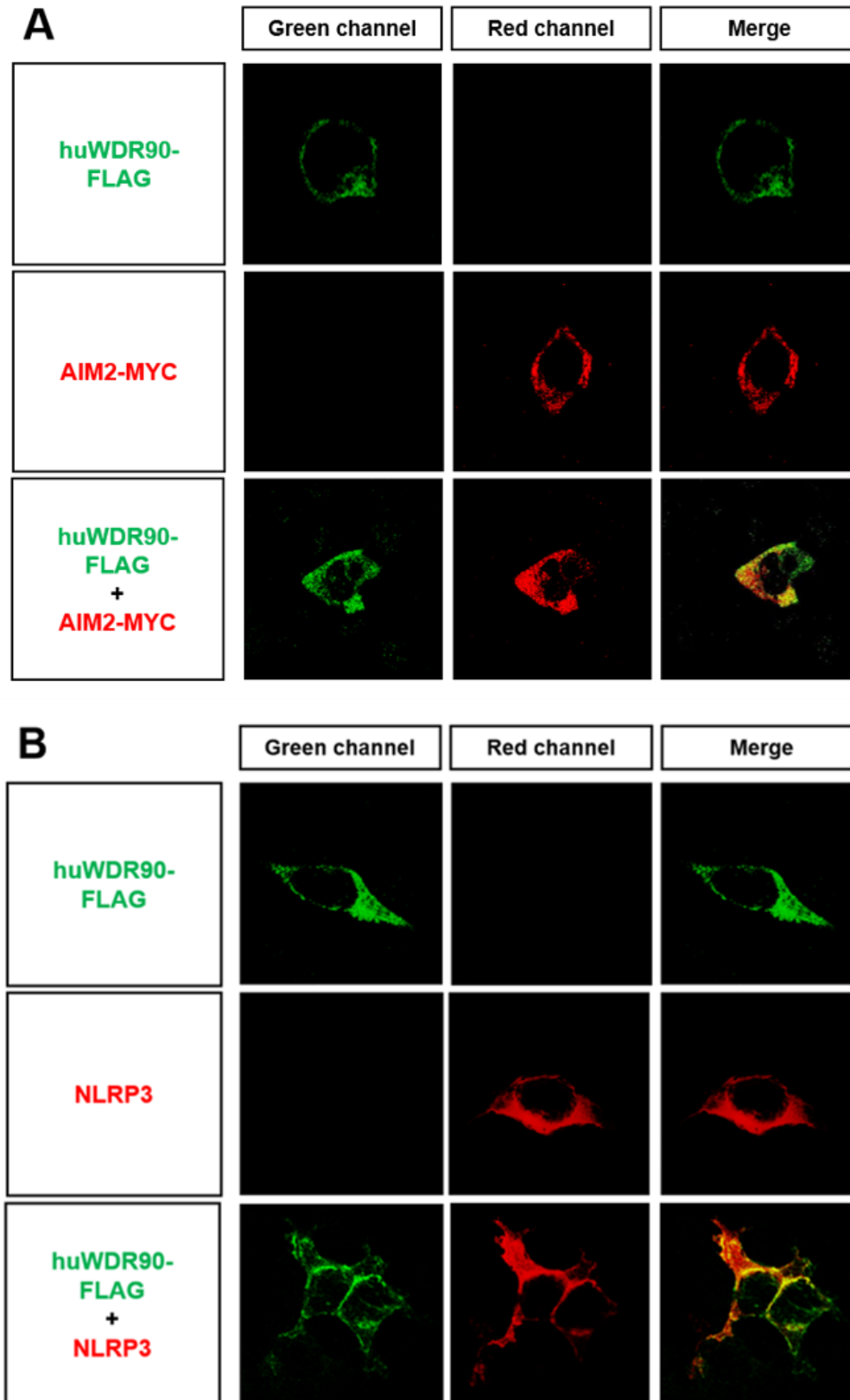


**Figure 34. WDR90 does not alter NLRP3 and AIM2 cellular distribution.** HEK293T cells were transfected with human WDR90-FLAG (A, B) together with NLRP3 (A) or AIM2-MYC (B), fixed at 48 h post-transfection, immunostained with antibodies to Flag, NLRP3 and Myc, and imaged using a laser confocal microscope.



### 3. New tools to study the inflammasome

#### 3.1. Generation of WDR90 KO mouse macrophages

In order to study if the role of WDR90 in zebrafish is conserved in mammalian cells, we decided to generate a KO of *Wdr90* in immortalized mouse bone marrow-derived macrophages (iBMDMs) expressing ASC-Cherry (a gift from Dr. P. Broz). To do that, we designed different sgRNA (see Table 2) that were cloned into inducible FgH1tUTG-GFP and non-inducible LentiCRISPRv2 vectors. Sequencing of the vectors showed correct insertion of the guides (Figure 35), so we proceeded to transduce the cells by viral particles using 3rd generation system. The inducible system was used taking into account the lethality of *Wdr90*-deficient zebrafish larvae.

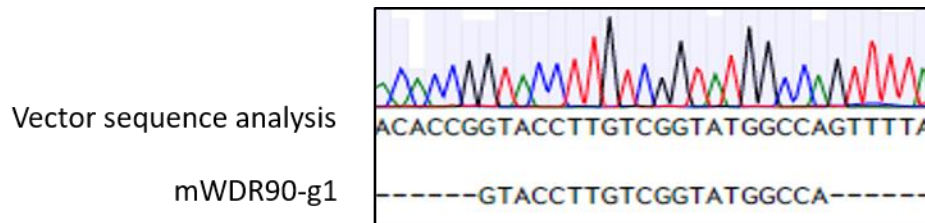


**Figure 35. Correct integration of mWdr90 sgRNAs into the lentiviral vector.** Alignment of the sgRNAs with the sequenced cloned lentiviral vector show a positive integration of the guides into the vector.

We tried to screen the clones using a commercially available antibody. However, it was found that his antibody only detected overexpressed WDR90 but not endogenous WDR90 in HeLa cells (Figure 364A and B), which is the cell line with the highest RNA expression of *WDR90* according to The Protein Atlas database (Figure 37). Although the expression of Cas9 was confirmed by WB iBMDM (Figure 364C), endogenous WDR90 was not detected in WT or KO clones (Figure 364D). The absence of commercial antibodies to validate the mutation of KO forced us to develop different strategies: screening by PCR (in progress) and generation of KI (see below).

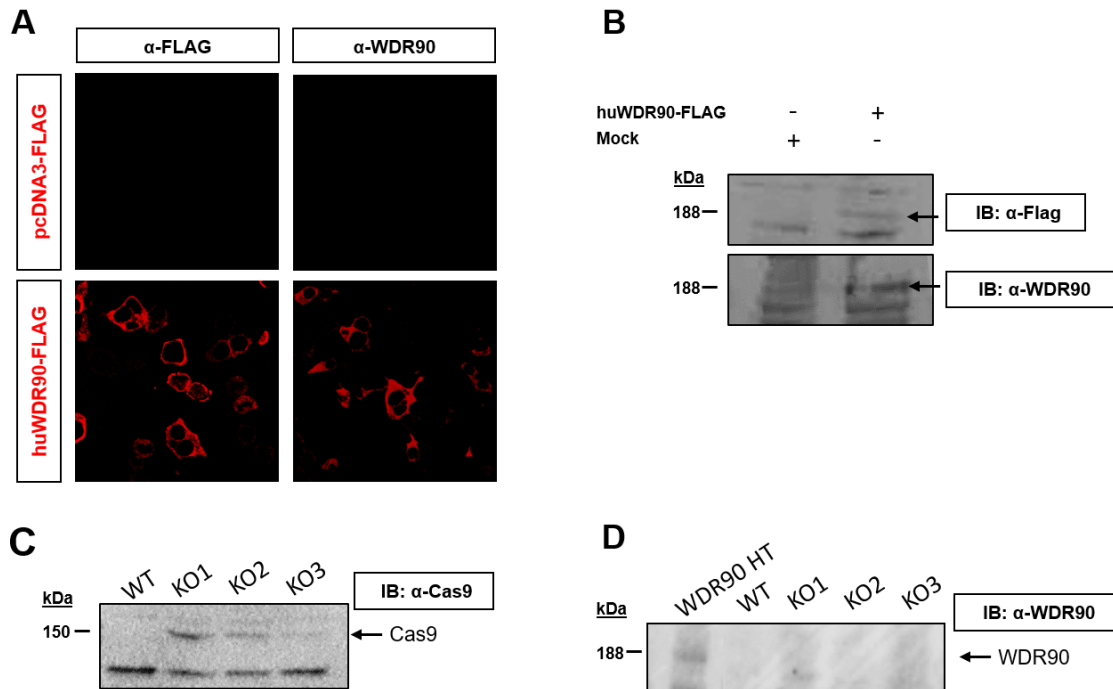


**Figure 36. Commercial antibodies fails to detect endogenous WDR90.** HeLa cells (A-B,D) were transfected with huWDR90-FLAG or pcDNA3-FLAG, fixed at 48 h post-transfection, immunostained with antibodies to FLAG or WDR90, and imaged using a laser confocal microscope (A) or lysed, and probed with antibodies to FLAG and WDR90 (B,D). iBMDMs were transduced with the indicated lentiviral plasmids, selected, lysed and probed with antibodies to Cas9 (C) and WDR90 (D). A transfected huWDR90 was used as positive control (D) of different KO lines.

## 2.6. Generation of WDR90 KI human cells

Due to the difficulties to detect WDR90 protein, including low transfection efficiency, lack of antibodies to detect the endogenous protein and poor resolution in WB, we decided to generate a KI lines. As mentioned above, The Protein Atlas database predicted HeLa cells to be the cell line with the highest RNA expression of *WDR90* (Figure 37). This cell line contains inflammasome components and is easy to be transfected, being a good cell line to develop the KI. We also tried to make the *Knock-in* in HEK293T but it was not possible to find a positive cell (data not shown).

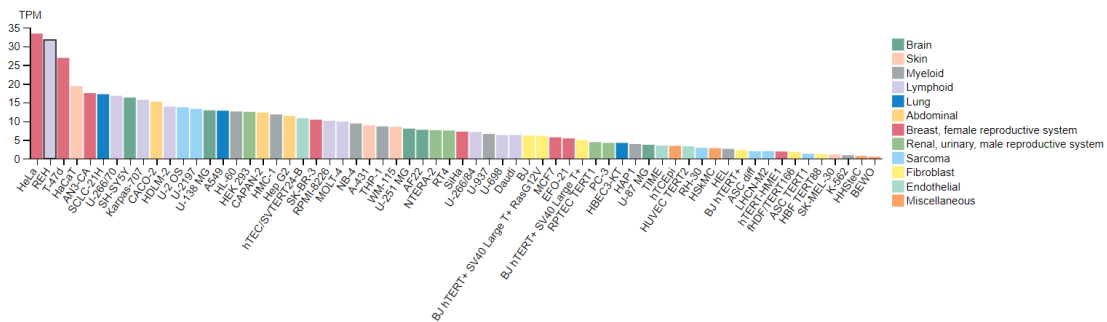


**Figure 37. Predicted *wdr90* expression levels in different cell types according to The Protein Atlas database.**

We designed two different sgRNAs in order to add a FLAG tag in the C-terminal of the *WDR90* gene (Table 2 Material & Methods). Moreover, to allow easy selection by FACS the donor vector was designed with a C-terminal P2A between the FLAG tag and YFP. Furthermore, the sequence coding for the last exon was modified to encode the same amino acids but with a different sequence in a way that Cas9 would only cut the endogenous sequence but not the vector. Then, HeLa cells expressing inducible Cas9 were transfected with one guide and the donor vector. After selection with puromycin, the cells were sorted for GFP positive (Figure 38). Although a few GFP<sup>+</sup> cells were found, we did not expect high efficiency due to the low efficiency of the system and the low expression of *WDR90* under normal conditions.

Despite the low number of positive cells (0,001%), we decided to sort them and check the right insertion by WB but we were not able to detect WDR90-FLAG.

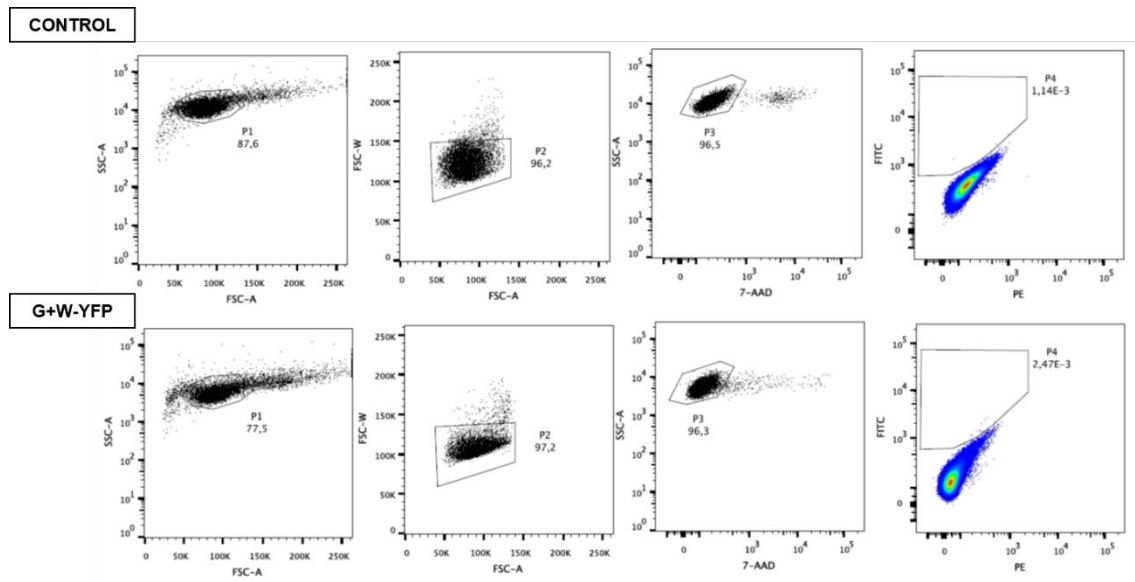


**Figure 38.** FACS analysis of WDR90-FLAG KI HeLa cells. HeLa were transfected only with the sgRNA (Control) and together with the donor vector (G+W-YFP), selected with puromycin and sorted for YFP.

## 2.7. Production of antibodies to human WDR90 and zebrafish Asc

One of the impediments to develop this study was the lack of commercially available antibodies. The commercial antibody for human WDR90 was not able to detect endogenous WDR90 in WB or in IF. In addition, using zebrafish as a model to study the inflammasome also has some limitations, for example, we were also limited by the lack of good antibodies against zebrafish inflammasome proteins. For these reasons, one of the aims of this thesis was to develop the tools needed to study deeply this complex. Alpacas are an excellent organism to generate antibodies, as they not only develop normal antibodies, but also nanobodies. We decided to generate both antibodies, one to recognize human WDR90 and the other to recognize zebrafish Asc. To do that, we had first to develop the recombinant protein, purify it and immunize the alpacas. The recombinant protein for zebrafish Asc was produced by our collaborator Prof. Álvaro Sánchez Ferrer. For human WDR90, a fragment encoding several WD40 domains of the protein was cloned into the pET30a vector and then transformed into *E. coli* BL21 (DE3). The recombinant protein was obtained after induction of its expression with IPTG using conventional conditions, i.e. 4h/24h, 0.1 mM IPTG and 37°C but a poor induction was obtained (Figure 39).

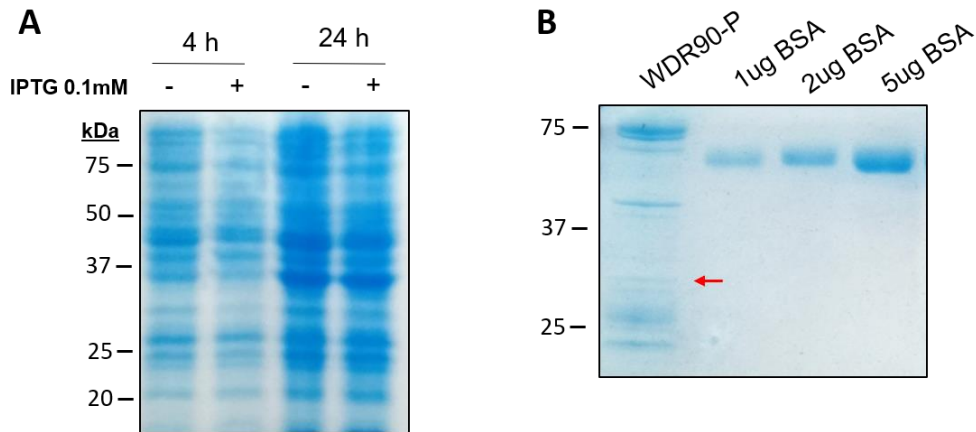


**Figure 39. Optimization of recombinant human WDR90 purification.** The induction of WDR90 was undetectable in a Coomassie staining before and after the IPTG stimulation at 37°C during 4 h and 24 h (A) and the better concentration reached of the purified protein (WDR90-P) was lower than 1ug (B). red arrow ( $\leftarrow$ ) indicates WDR90-P.

Ten different conditions were tried and the best induction and recovery was reached after inducing with 0.001 mM for 40 h at 16°C. We purified the recombinant WDR90 protein (WDR90-P) tagged with His using an affinity column and concentrated the obtained elution with ultrafiltration centrifugal concentrators (E1-E2) (Figure 40). The verification of the purification was checked by WB giving us a correct size using an anti-His antibody. Moreover, high exposure times showed high molecular weight polypeptides that could also correspond to WDR90-P oligomers, probably representing aggregates or post-transductional modified proteins (Figure 40).

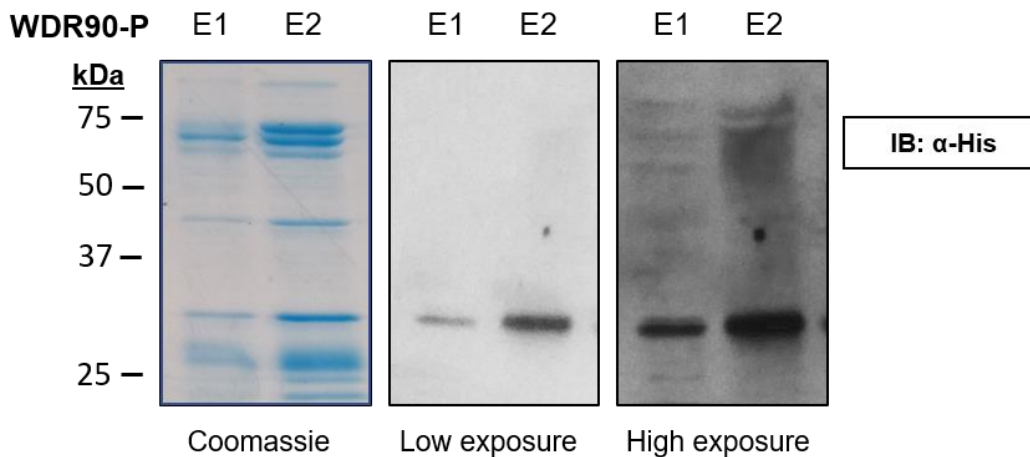


**Figure 40. Purified recombinant WDR90 protein (WDR90-P).** Coomassie blue staining (left panel) and WB with anti-His (middle and right panels) of the purified WDR90 present in two different elutions (E1 and E2). High exposure time reveals some WDR90-P aggregates.

Once the human WDR90 and zebrafish Asc antigens were ready, we proceeded to immunize the alpacas. One month before the immunization, blood was collected from the alpacas to have a control for the immunoreactivity against the target proteins. After the 4<sup>th</sup> immunization, 120mL of blood were collected from each alpaca and the serum collected before and after the immunization was analyzed by dot blot (Figure 41) and WB (Figure 42). The dot blot revealed that the pre-immune serum (Pre-I) did not recognize the recombinant proteins, while the post-immune serum (Post-I) did up to a dilution of 1:5000.

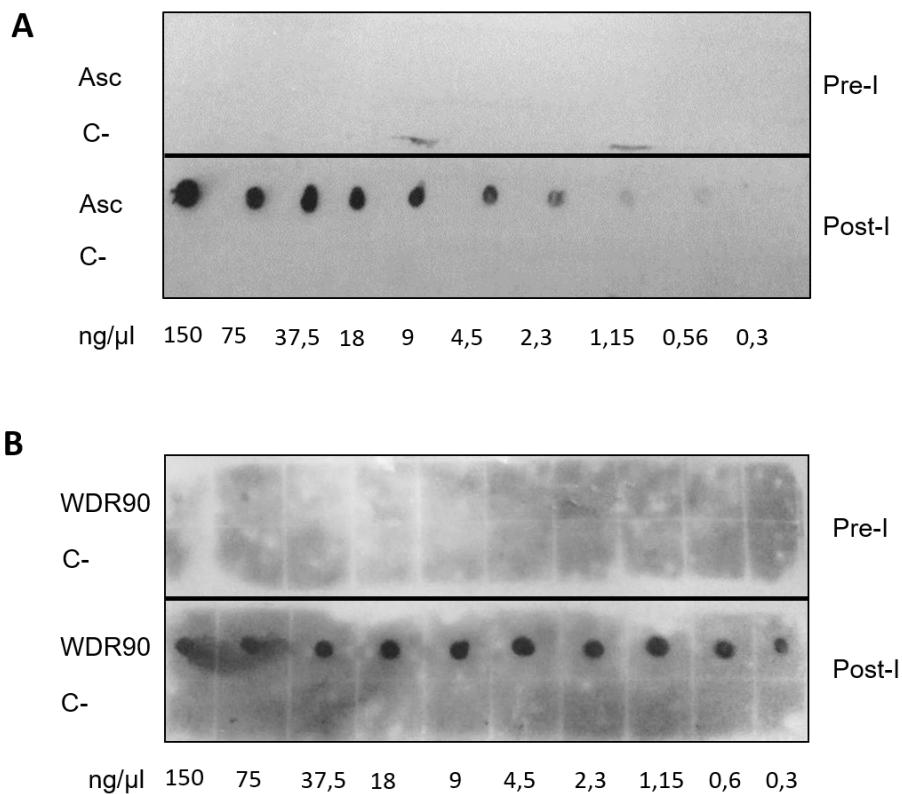


**Figure 41. Positive immunoreactivity of the alpaca serum to zebrafish Asc and human WDR90.** Immunoreactivity of the alpaca's serum against zebrafish Asc (A) and human WDR90 (B) was analysed before (Pre-immunization serum; Pre-I), and after (Post-immunization serum; Post-I) the 4<sup>th</sup> immunization by dot blot at 3 different concentrations of serum (1/500, 1/1000 and 1/5000). The best concentrations probed, 1/5000 (A) and 1/1000 (B), are shown.

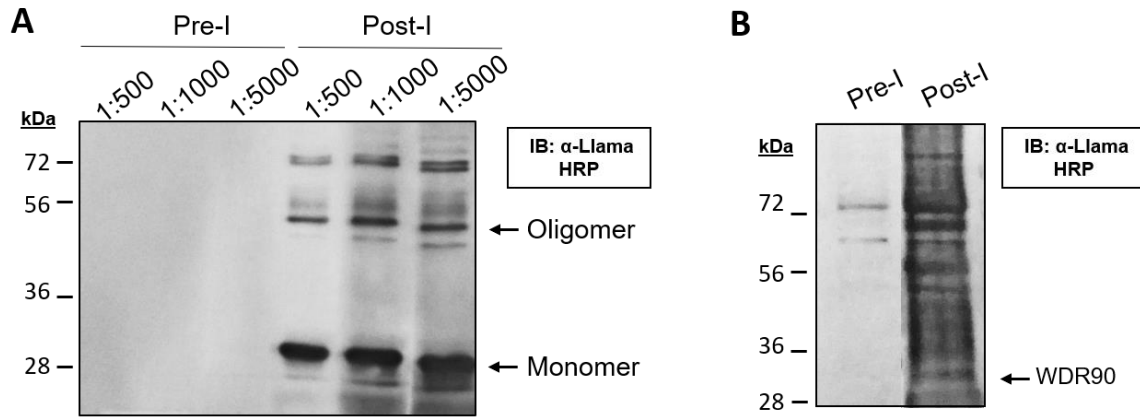


**Figure 42.** WB detection of zebrafish Asc and human WDR90 by the alpaca serum. Purified recombinant zebrafish Asc (A) and human WDR90 (B) were probed with Pre-I and Post-I sera at 1:500, 1:1000 (A) and 1:5000 (A,B) dilutions. Anti-llama HRP-conjugated (1:5000) was used as secondary antibody.

These results were confirmed using WB where the anti-Asc serum was able to detect the recombinant proteins. However, the results for WDR90 were not very promising, probably to the low purity of the protein. To reduce the unspecific recognition of bacterial proteins from the process of purification, we preincubated the alpaca serum with a lysate of the bacteria. The clean serum (Post-I/PB) was used as a primary antibody but it still needed to be improved (Figure 43), as we were unable to see a perceptibly reduction of the unspecific staining.

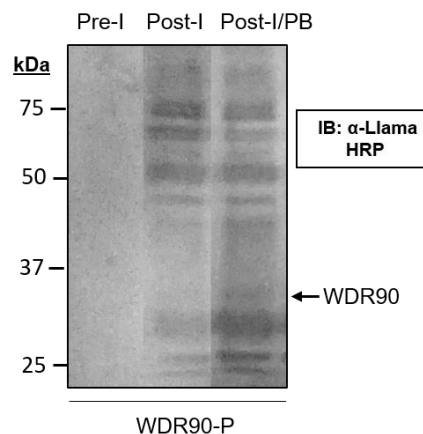


**Figure 43.** WDR90-P probed with alpaca serum pre-cleared with bacterial lysate. The unspecific recognition of the protein was reduced by preincubating the alpaca's serum with a BL21 lysate for 2h. Pre-I; Pre-immunization serum, Post-I; post-immunization serum, Post-I/PB; post-immunization serum post-bacterial lysate incubation. Anti-llama HRP-conjugated (1:5000) was used as secondary antibody.

We next wanted to check if the immune response generated in the alpacas developed nanobodies against the target proteins. If so, that would give us the chance to develop bacterial display to produce in a future specific nanobodies, without the need of reimmunize the alpaca. As it was described in 1993 by Hamers-Casterman et al., it is possible to separate the IgG1, which has affinity for the G protein, from the IgG2 and IgG3 of the alpacas, which have affinity for the A protein. We developed this technique to know if the antibodies generated in the alpaca had a different affinity for the antigen inoculated. However, although we managed to separate the different IgG contained in the serum (Figure 44), we could not find a clear specificity of the IgG1s or IgG2/3s for the recombinant proteins (data not shown).

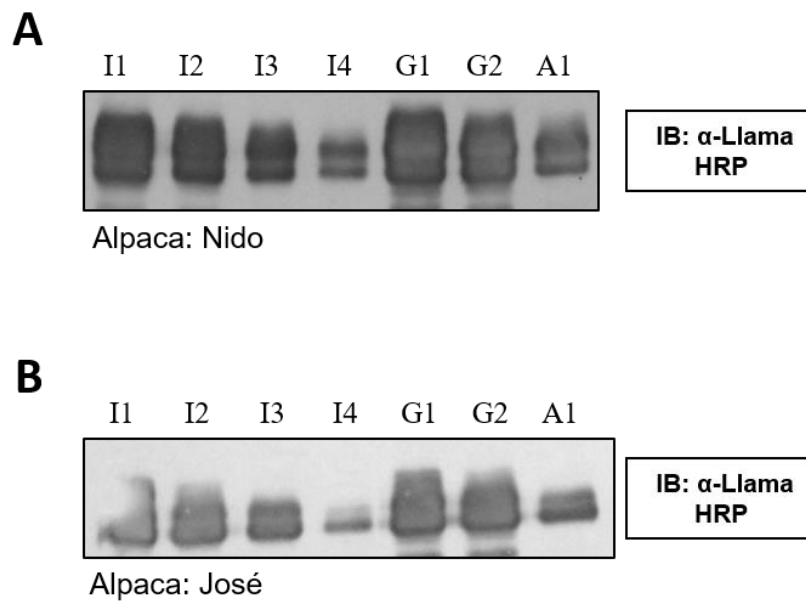


**Figure 44. Nanobody purification from alpacas serum.** The initial serum (I1) of two alpacas that were immunized with zebrafish Asc (Nido) (A) and WDR90-P (José) (B) was incubated twice with protein G (I2-I3) and once with protein A (I4) for 30 min each incubation to separate alpaca IgG1 (G1-G2) from IgG2/3 (A1). Anti-llama HRP-conjugated (1:5000) was used as secondary antibody.

Finally, we purified the antibodies by binding the recombinant proteins to NHS sepharose beads, although a lot of recombinant protein is required for this procedure. The purified antibodies were probed first with the recombinant proteins (Figure 45), resulting in a strong recognition of Asc but not detection of WDR90.

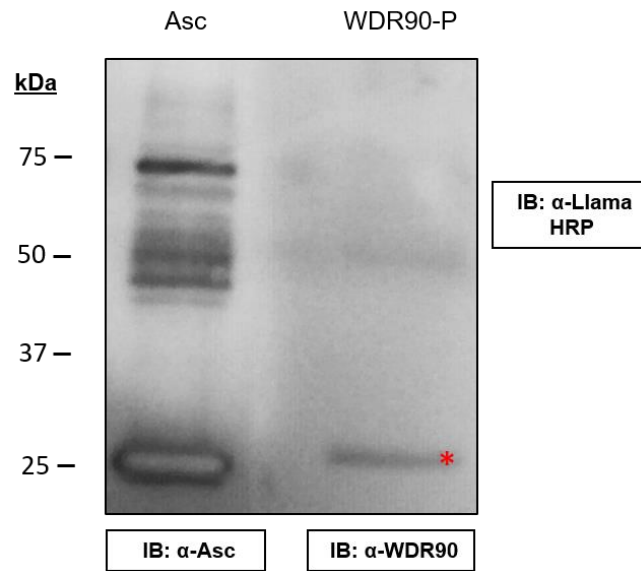


**Figure 45. Purified antibody recognition of zebrafish Asc and human WDR90.** Recombinant zebrafish Asc and human WDR90 were probed with monospecific anti-Asc and anti-WDR90. Anti-llama HRP-conjugated (1:5000) was used as secondary antibody. The asterisk denotes a nonspecific polypeptide.

To further confirm the usefulness of the Asc antibody, we showed that it was able to detect transfected zebrafish Asc-GFP in HEK923T cells (Figure 46).



**Figure 46. Asc antibody validation.** HEK293T were transfected with zebrafish Asc-GFP and an empty plasmid (A-B) and probed with the purified anti-Asc antibody (A) or anti-GFP (B) 1:3000.



# **DISCUSSION**



Although many recent studies have demonstrated the crucial role of the inflammasome as a molecular platform involved in the sensing of intracellular pathogens, little is known concerning phylogenetic aspects of its composition, activation and function. Analysis of genome databases has revealed (i) the enormous diversification of NLR in ray-finned fish (class Actinopterygii) (Laing et al., 2008); (ii) the existence of a single ortholog of the main inflammasome adaptor ASC in all non-mammalian species examined; (iii) that true orthologs of caspase-1, i.e., harboring N-terminal CARD and C-terminal caspase (P20/P10) domains, are restricted to the superorders Protacanthopterygii (trout and salmon) and Acanthopterygii (seabream, seabass, and medaka) of ray-finned fish (Angosto et al., 2012; López-Castejón et al., 2008), while most primitive Ostariophysi (catfishes and zebrafish) have a functional homolog of mammalian caspase-1, called Caspa in zebrafish, which harbors N-terminal PYD and C-terminal P20/P10 domains (Junya Masumoto et al., 2003; Tyrkalska et al., 2016; Vincent et al., 2016); (iv) the absence of a caspase-1 cleavage site in non-mammalian vertebrate IL-1 $\beta$  sequences (Bird et al., 2002); and (v) the absence of IL-18 in some ray-finned fish species, such as the zebrafish (Angosto et al., 2012). Although the functional relevance of this extended array of NLR genes in zebrafish still needs to be investigated, recent functional studies have shown that the mechanisms of activation of the inflammasome are not fully conserved in ray-finned fish and that IL-1 $\beta$  is not processed *in vivo* by caspase-1 in this animal group (Angosto et al., 2012; Compan et al., 2012; López-Castejón, Young, Meseguer, Surprenant, & Mulero, 2007; Tyrkalska et al., 2016). However, these studies also demonstrated that the inflammasome is activated *in vivo* in zebrafish macrophages and neutrophils upon bacterial and viral infection, which leads to differential outcomes: pyroptosis of macrophages (Varela et al., 2014; Vincent et al., 2016) or PLA2-dependent biosynthesis of eicosanoids in neutrophils (Tyrkalska et al., 2016). Together, these results support the idea that the use of the inflammasome as a molecular platform for the induction of pyroptotic cells death and the regulation of eicosanoid biosynthesis predates the split of fish and tetrapods more than 450 million years ago, while its use for processing pro-inflammatory IL-1 $\beta$  and IL-18 was later acquired in the tetrapod lineage.

## Discussion

To make this story more intriguing, we have identified a novel inflammasome component, Caiap, which is evolutionarily conserved from cartilaginous fish to marsupials, but unexpectedly absent in placental mammals. One of the most interesting observations of this study is the unprecedented combination of domains found in Caiap: an N-terminal CARD domain and several C-terminal ANK repeats. These domains are the regions of Caiap showing the highest degree of conservation at the primary structure level. In addition, 3D structure analysis predicts, with very high confidence, a strikingly similar tertiary structure of Caiap across all vertebrates, suggesting a conserved mechanism to regulate inflammasome activation. Caiap is expressed at very low levels in zebrafish, but its expression is modestly induced by infection in immune cells recruited to the infection and wounding sites. Although the expression profile of Caiap requires further investigation, the induction of *caiap* in sorted macrophages from infected animals, together with the WISH data and the increased resistance of larvae forced to express Caiap in macrophages, suggests that Caiap expression is restricted to a specific population of macrophages (Nguyen-Chi et al., 2015).

Genetic experiments demonstrate that Caiap acts downstream flagellin and mediates its antibacterial activity through Asc and Caspa, as we have recently found for Gbp4 which, in contrast, is expressed in neutrophils (Tyrkalska et al., 2016). Another important difference between Caiap and Gbp4 is that forced ubiquitous expression of Gbp4 results in increased larval resistance to the infection (Tyrkalska et al., 2016), while Caiap overexpression barely increases infection resistance. This difference may be related to the different mechanism of action of each protein, since Gbp4 directly binds Asc through homotypic CARD/CARD interactions (Tyrkalska et al., 2016), while Caiap does not directly interact with Asc but with enzymatically active Caspa (P20/ P10) through its ANK repeats (Figure 47).

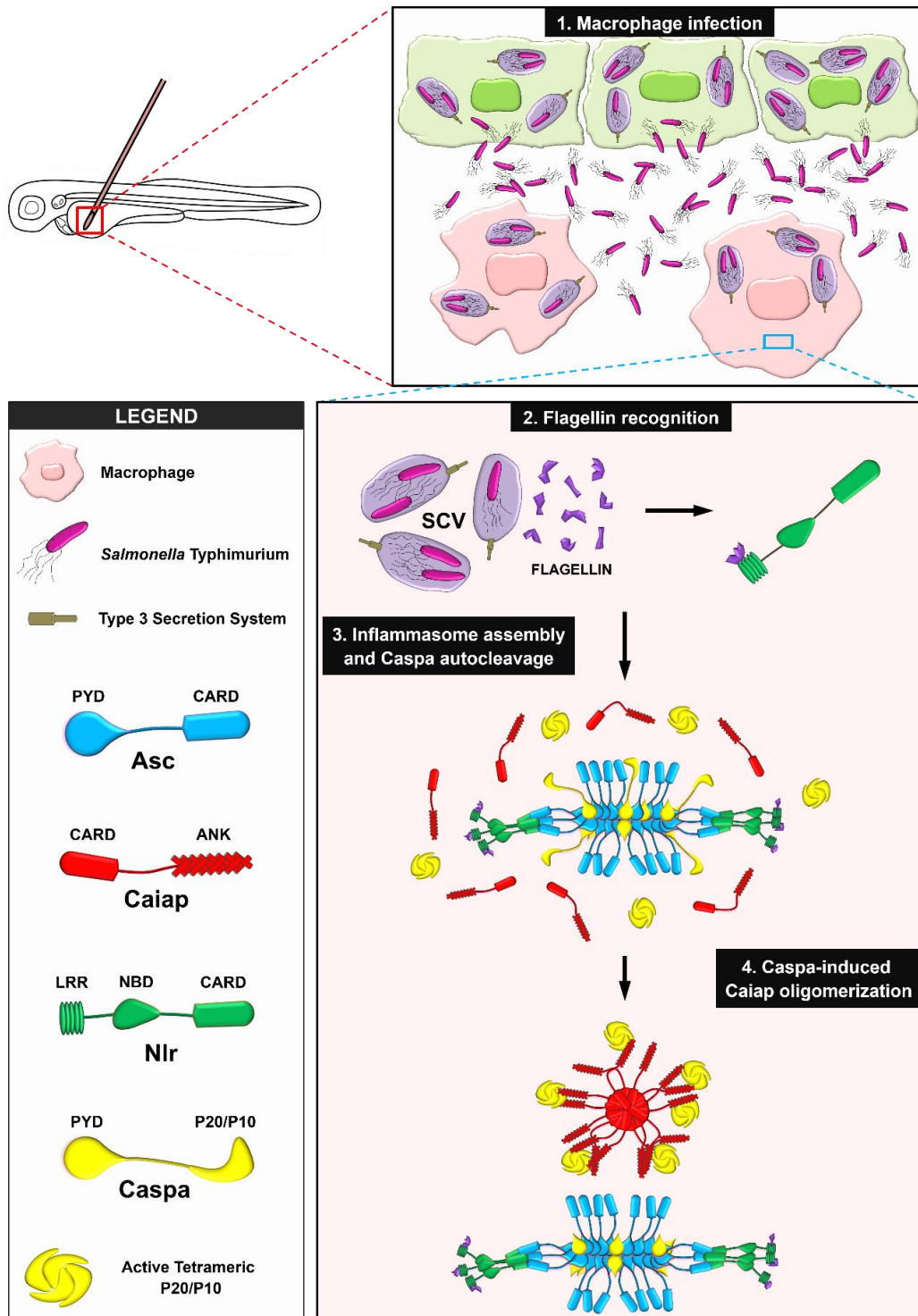


**Figure 47. Proposed model illustrating the stabilization of catalytic active Caspa tetramers by Caiap.** 1. Macrophages are recruited to the infection site where they are infected by *S. Typhimurium* (ST), which is contained within the Salmonella-contained vesicle (SCV). 2. Flagellin is inadvertently injected into the cytosol through the type 3 secretion system of ST where it is recognized by a Nlr. 3. The inflammasome is assembled via formation of Asc specks. 4. Active Caspa interacts with Caiap via its ANK domains and induces its self-oligomerization through CARD/CARD allowing Caspa stabilization in high molecular weight complexes upon its prodomain release.

Strikingly, the CARD domain of Caiap allows its self-oligomerization, what seems to be essential *in vivo* to mediate the inflammasome-dependent resistance to ST. To the best of our knowledge, this is the first description of an inflammasome adaptor protein that directly interacts with the active effector caspase further promoting its activation probably by stabilizing caspase-1 in functionally stable, high molecular weight complexes after its autoproteolytic cleavage and prodomain removal (Shamaa, Mitra, Gavrilin, & Wewers, 2015). Caiap, therefore, is reminiscent of the inflammasome inhibitors INCA and ICEBERG that directly interact with caspase-1 but, in this case, via CARD domains (Humke, Shriver, Starovasnik, Fairbrother, & Dixit, 2000; Lamkanfi et al., 2004; A. Lu et al., 2016), the former being able to cap and terminate the caspase-1 filament (A. Lu et al., 2016). Although the novel mechanism reported here also operates in other vertebrate species with orthologs of mammalian caspase-1 needs further investigation, the highly conserved primary and tertiary structure of Caiap across vertebrate species and the ability of zebrafish Caiap to interact with active Caspa through its ANK domains strongly support an evolutionarily conserved mechanism of action of Caiap.

The absence of Caiap in placental mammals suggests that Caiap was lost in this animal group after its split from marsupials. It is tempting to speculate, therefore, that other proteins replaced Caiap in placental mammals to carry out a similar function in the stabilization of the inflammasome. Strikingly, a recent interactome analysis of ASC complexes in human monocytic THP-1 cells has identified a protein called ArfGAP with GTPase domain, ankyrin repeat, and PH domain 3 (AGAP3)(L.-J. Wang et al., 2012), which curiously harbors both GTPase and ANK domains. It is tempting to speculate, therefore, that Caiap and other ANK domain-containing proteins are involved in the stabilization of caspase-1 in functionally stable, high molecular weight complexes (Shamaa et al., 2015).

On the contrary, WDR90 appears to be evolutionarily conserved from fish to placental mammals. Although WDR90 does not contain CARD domain, as Gbp4 and Caiap, WDR90 owns WD40 domain as a major structural domain. The presence of WD40 is common to many important proteins in higher vertebrates, where it mediates protein-protein interactions (PPI). The relevance of the WD40 domains is highlighted by the fact that about 1% of the human genes encode a protein that belongs to the WDR family

(Stirnimann, Petsalaki, Russell, & Müller, 2010). Despite the implication of WDR proteins in many vital processes, to date no WD40 domain has been found with intrinsic enzymatic activity (Stirnimann et al., 2010; C. Xu & Min, 2011). Nevertheless, the significance of these proteins is supported by a large number of studies which demonstrate the participation of this family in large molecular complexes. All of these data from isolated studies have been recently set up together in a study which reinforces the systematic implication of the WDR family in human complexes assembly (Zou, An, Wu, & Ye, 2018).

Strikingly, a recent genome-wide computational analysis of WD40 protein family in human identifies 21 different WDR protein classes based on their domain architectures. This analysis also includes a phylogenetic analysis that defines different evolutionary points in the emerging WD40 proteins, where WDR90 appears in the latest evolutionary group that corresponds to the 54 of 223 WD40 genes originated after the separation of vertebrates from invertebrates (Zou et al., 2016). Moreover, the authors describe the latest evolutionary WDR proteins to play more specific functions and more specific and narrow interactions, which is consistent with the specific interaction between WDR90 with NLRC4 and not with other inflammasome receptors that we report in this thesis.

Nevertheless, although WDR90 expression appears to be ubiquitous in almost every tissue, the detection of WDR90 into different cell types is still an issue. Bioinformatic analysis from the WDSP database (Y. Wang et al., 2015) suggest that this protein may be produced at very low levels due to a premature stop codon in the mRNA, leading to nonsense-mediated mRNA decay. Nonetheless, we have described that the mRNA levels of *wdr90* increase after Gbp4 overexpression or ST infection *in vivo*. Strikingly, Gbp4 is not the only inflammasome component that regulates the expression of other proteins, among them, caspase-1 activation is responsible of itself secretion as well as for the secretion of proIL-1 $\alpha$  and fibroblast growth factor (FGF)-2, even though these last two proteins are not substrates of the inflammasome (Keller, Rüegg, Werner, & Beer, 2008). Modification on gene expression levels occurs all along the different tissues and cells of the organisms to fight against infections and threats to maintain homeostasis, where the inflammatory response stands a principal function. For

instance, some GBPs have been reported to be increased in various mice tissues after *Leishmania major* infection (Sohrabi et al., 2018). Increased levels of *wdr90* after infection hint a function of this gene in physiological defence responses, which is supported by the higher survival and caspase-1 activity of zebrafish larvae to ST infection after its forced expression. The dependent expression of *wdr90* on Gbp4 and its GTPase activity, and not from other inflammasome components (Asc or caspase-1), denotes that Wdr90 plays a specific role related to Gbp4 GTPase activity, which as in humans, is essential for inflammasome activation and ST clearance (Finethy et al., 2017; Shenoy et al., 2012; Tyrkalska et al., 2016).

Remarkably, here we identify WDR90 as a new inflammasome component conserved in vertebrates that affects the cell distribution of NLRC4, probably by its interaction. These results sustain the importance of WD40 domains in large complexes assembly where receptors as NLRC4 need the interaction with WD40 by its LRR domains to allow an active conformational stage in order to form the inflammasome complex with Asc and activate caspase-1 and promote IL-1 $\beta$  release (W. Liu et al., 2017). Moreover, we suggests that WDR90 interacts with the NLR which is consistent with the results obtained from genetic experiments in zebrafish, where Wdr90 facilitates ST clearance upstream of the inflammasome components Gbp4, Asc and caspase-1. These results, together with the weak induction of caspase-1 activity by forced expression of *wdr90* in Gbp4-deficient conditions, suggest two different roles of these two components in inflammasome activity: WDR90 is probably essential to allow the NLRC4 conformational change needed for its activation, while the GTPase activity of GBPs, Gbp4 in zebrafish and GBP5 in mammals, is required to an active cleavage of caspase-1 probably through NLRP3 or its zebrafish ortholog (Figure 48) (Shenoy et al., 2012; Tyrkalska et al., 2016). This proposed model is supported by previous studies demonstrating a colocalization of NLRC4 and NLRP3 receptors in the same inflammasome complex after ST infection in macrophages (Qu et al., 2016b) and the requirement of the human homolog of Gbp4, GBP5, to allow NLRP3-inflammasome activation but not of NLRC4 (Finethy et al., 2017; B.-H. Kim et al., 2016; Shenoy et al., 2012; Tyrkalska et al., 2016).

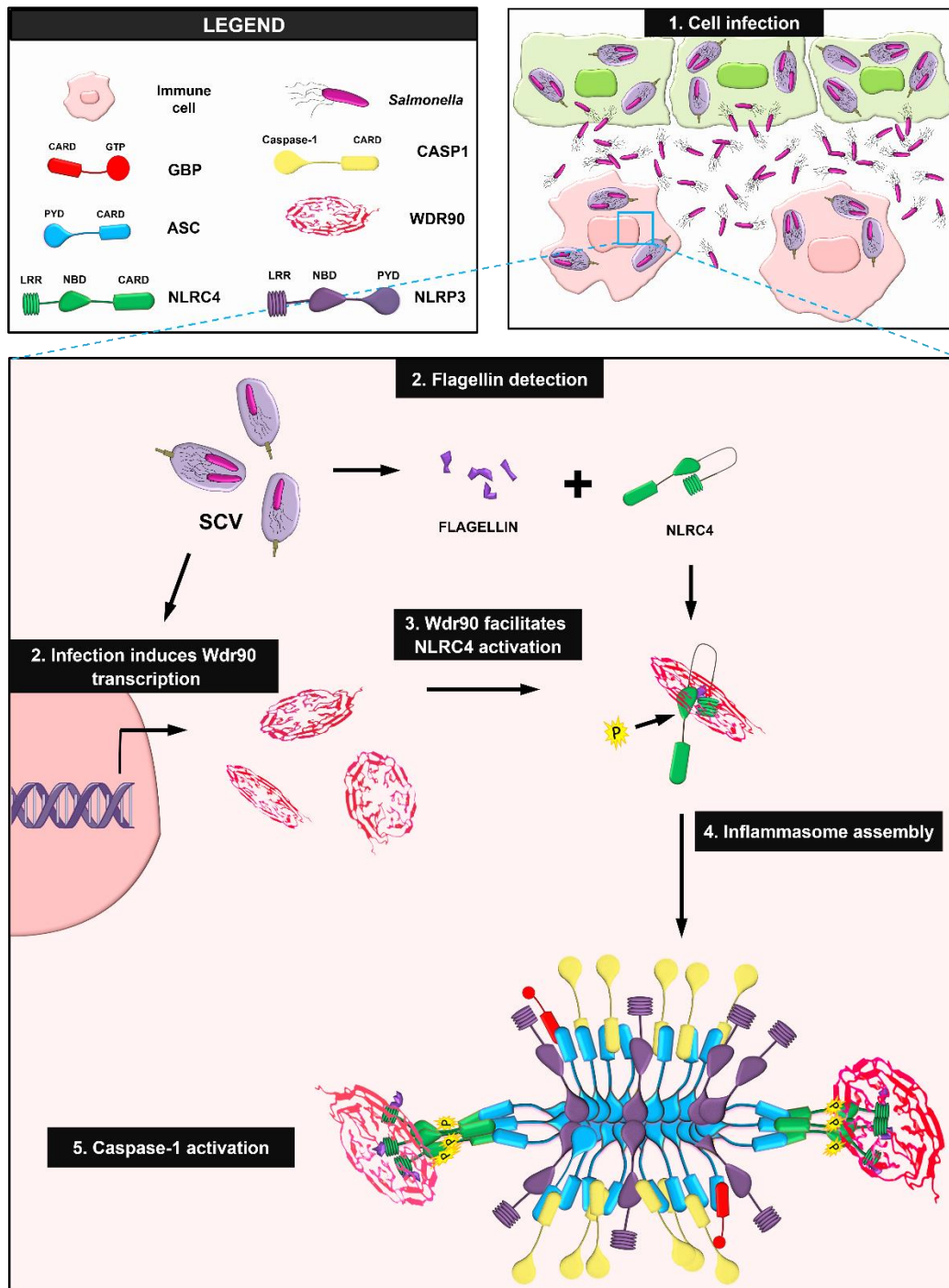


**Figure 48. Proposed model for the role of WDR90 in inflammasome.** 1. Immune cells are recruited to the infection site where they are infected by *S. Typhimurium* (ST), which is contained within the Salmonella-contained vesicle (SCV). 2. The presence of the bacteria induces WDR90 transcription. 2. Flagellin is injected into the cytosol through the type 3 secretion system of ST where it is recognized by a NLRC4. 3. WDR90 facilitates NLRC4 phosphorylation through conformational changes. 4. Active NLRC4 leads to inflammasome assembly which helps caspase-1 activation and the resolution of the infection.

Finally, we developed new tools that help to provide a deep insight into inflammasome by further defining the role of Wdr90 and other inflammasome

## Discussion

components. Among these tools we use CRISPR/Cas9 system to generate *Wdr90 knock out* mice macrophages and *Wdr90-flag knock in* HeLa cells. In addition, we have generated antibodies in alpacas to obtain antibodies against zebrafish Asc, which are not commercially available, and against human WDR90. Camelids possess unique functional heavy chain antibodies, which can be produced and modified *in vitro* as a single domain antibody (nanobody) with full antigen binding ability (Bever et al., 2016). Apart from their advantage of an easy production by bacterial or phage display without the necessity of reimmunization (L. He et al., 2017; M. Li, Fan, Liu, Hu, & Huang, 2015), nanobodies have been described to recognize epitopes that conventional antibodies are not able to reach (Hansen, Laursen, Andersen, & Andersen, 2017; X. Liu, Wang, Chu, Xu, & Wang, 2018; Peyrassol et al., 2016; Rajan et al., 2015). Although we were successful in the generation of a good antibody to detect zebrafish Asc, we failed so far to get good results with WDR90, due to the difficulties to produce the recombinant protein and to detect it by western blot. Together, all these tools would allow us to complete in the next future the characterization the role of WDR90 in inflammasome activation and assembly, as well as those of other inflammasome components.

In summary, we report here the identification of two novel and different inflammasome proteins: (i) Caiap, a novel, evolutionarily conserved inflammasome component with a unique domain organization, which interacts with active effector caspase and is required *in vivo* for the inflammasome-dependent resistance to bacterial infection and (ii) WDR90, a previous uncharacterized WDR protein highly conserved in vertebrates which changes the NLRC4 inflammasome receptor distribution and facilitates inflammasome activation and bacterial infection clearance. In addition, we have developed different tools to further study the inflammasome using both mammals *in vitro* and zebrafish *in vivo* models that in combination will provide a deeper knowledge about the role of this molecular platform in immunity. This study supports the relevance of (i) a broad evolutionary analysis of innate immunity mechanisms to understand the complexity of human immunity, (ii) the implication of ANK and WD40 domains in innate immune complexes assembly, and (iii) alpacas as an optimal organism to develop specific antibodies to difficult targets.

# **CONCLUSIONS**



**The results obtained in this work lead to the next conclusions:**

1. Caiap is evolutionarily conserved from cartilaginous fish to marsupials but is absent in placental mammals, suggesting that Caiap was lost in lung fish and placental mammals during evolution
2. Caiap harbors a unique domain organization with N-terminal CARD domain and several C-terminal ANK domains.
3. Caiap is required in zebrafish for the inflammasome-dependent resistance to *S. Typhimurium* infection.
4. Caiap acts downstream flagellin and interacts with catalytic active Caspa, the functional homolog of mammalian caspase-1, through its ANK domain, while its CARD domain promotes its self-oligomerization.
5. *wdr90* gene expression is induced by active Gbp4 and bacterial infection in zebrafish.
6. Wdr90 increases caspase-1 activity in zebrafish and their resistance to *S. Typhimurium* infection. Wdr90 acts upstream Gbp4 and Asc to regulate caspase-1 activity and *S. Typhimurium* resistance.
7. WDR90 ectopically expressed in HEK293 cells promotes NLRC4 redistribution, but it did not affect NLRP3 or AIM2 localization.
8. Alpacas antibodies were generated against zebrafish Asc and human WDR90. These antibodies will help to shed light into the inflammasome assembly and biological functions.



# **REFERENCES**



- Abbas, A. K., Lichtman, A. H., P. S. (2015). Cytokines. In *Cellular and Molecular Immunology* (Elsevier/S, pp. 493–496). Philadelphia.
- Agostini, L., Martinon, F., Burns, K., McDermott, M. F., Hawkins, P. N., & Tschopp, J. (2004). NALP3 forms an IL-1beta-processing inflammasome with increased activity in Muckle-Wells autoinflammatory disorder. *Immunity*, *20*(3), 319–325. Retrieved from <http://www.ncbi.nlm.nih.gov/pubmed/15030775>
- Ahn, H., Kang, S. G., Yoon, S., Ko, H.-J., Kim, P.-H., Hong, E.-J., ... Lee, G.-S. (2017). Methylene blue inhibits NLRP3, NLRC4, AIM2, and non-canonical inflammasome activation. *Scientific Reports*, *7*(1), 12409. <https://doi.org/10.1038/s41598-017-12635-6>
- Angosto, D., López-Castejón, G., López-Muñoz, A., Sepulcre, M. P., Arizcun, M., Meseguer, J., & Mulero, V. (2012). Evolution of inflammasome functions in vertebrates: Inflammasome and caspase-1 trigger fish macrophage cell death but are dispensable for the processing of IL-1 $\beta$ . *Innate Immunity*, *18*(6), 815–824. <https://doi.org/10.1177/1753425912441956>
- Angosto, D., & Mulero, V. (2014). The zebrafish as a model to study the inflammasome. *Inflammasome*, *1*(1). <https://doi.org/10.2478/infl-2014-0002>
- Atluri, V. S. R., Pilakka-Kanthikeel, S., Garcia, G., Jayant, R. D., Sagar, V., Samikkannu, T., ... Nair, M. (2016). Effect of Cocaine on HIV Infection and Inflammasome Gene Expression Profile in HIV Infected Macrophages. *Scientific Reports*, *6*(1), 27864. <https://doi.org/10.1038/srep27864>
- Bauernfeind, F., & Hornung, V. (2013). Of inflammasomes and pathogens--sensing of microbes by the inflammasome. *EMBO Molecular Medicine*, *5*(6), 814–826. <https://doi.org/10.1002/emmm.201201771>
- Bergsbaken, T., Fink, S. L., & Cookson, B. T. (2009). Pyroptosis: host cell death and inflammation. *Nature Reviews. Microbiology*, *7*(2), 99–109. <https://doi.org/10.1038/nrmicro2070>
- Bettelli, E., Carrier, Y., Gao, W., Korn, T., Strom, T. B., Oukka, M., ... Kuchroo, V. K. (2006).

## References

- Reciprocal developmental pathways for the generation of pathogenic effector TH17 and regulatory T cells. *Nature*, 441(7090), 235–238. <https://doi.org/10.1038/nature04753>
- Bever, C. S., Dong, J.-X., Vasylieva, N., Barnych, B., Cui, Y., Xu, Z.-L., ... Gee, S. J. (2016). VHH antibodies: emerging reagents for the analysis of environmental chemicals. *Analytical and Bioanalytical Chemistry*, 408(22), 5985–6002. <https://doi.org/10.1007/s00216-016-9585-x>
- Bezbradica, J. S., & Schroder, K. (2017). Zebrafish earns its stripes for in vivo ASC speck dynamics. *The Journal of Cell Biology*, 216(9), 2615–2618. <https://doi.org/10.1083/jcb.201708002>
- Bird, S., Zou, J., Wang, T., Munday, B., Cunningham, C., & Secombes, C. J. (2002). Evolution of interleukin-1beta. *Cytokine & Growth Factor Reviews*, 13(6), 483–502. Retrieved from <http://www.ncbi.nlm.nih.gov/pubmed/12401481>
- Boehm, T., Hess, I., & Swann, J. B. (2012). Evolution of lymphoid tissues. *Trends in Immunology*, 33(6), 315–321. <https://doi.org/10.1016/j.it.2012.02.005>
- Boshra, H., Li, J., & Sunyer, J. O. (2006). Recent advances on the complement system of teleost fish. *Fish & Shellfish Immunology*, 20(2), 239–262. <https://doi.org/10.1016/j.fsi.2005.04.004>
- Boucher, D., Chen, K. W., & Schroder, K. (2016). Burn the house, save the day: pyroptosis in pathogen restriction. *Inflammasome*, 2(1), 1–6. <https://doi.org/10.1515/infl-2015-0001>
- Boucher, D., Monteleone, M., Coll, R. C., Chen, K. W., Ross, C. M., Teo, J. L., ... Schroder, K. (2018). Caspase-1 self-cleavage is an intrinsic mechanism to terminate inflammasome activity. *The Journal of Experimental Medicine*, 215(3), 827–840. <https://doi.org/10.1084/jem.20172222>
- Branchu, P., Bawn, M., & Kingsley, R. A. (2018). Genome variation and molecular epidemiology of *Salmonella* Typhimurium pathovariants. *Infection and Immunity*, IAI.00079-18. <https://doi.org/10.1128/IAI.00079-18>

- Breeden, L., & Nasmyth, K. (1987). Similarity between cell-cycle genes of budding yeast and fission yeast and the Notch gene of *Drosophila*. *Nature*, *329*(6140), 651–654. <https://doi.org/10.1038/329651a0>
- Brennan, M. A., & Cookson, B. T. (2000). Salmonella induces macrophage death by caspase-1-dependent necrosis. *Molecular Microbiology*, *38*(1), 31–40. Retrieved from <http://www.ncbi.nlm.nih.gov/pubmed/11029688>
- Brinkworth, J. F., & Thorn, M. (2013). Vertebrate Immune System Evolution and Comparative Primate Immunity. In *Primates, Pathogens, and Evolution* (pp. 17–64). New York, NY: Springer New York. [https://doi.org/10.1007/978-1-4614-7181-3\\_2](https://doi.org/10.1007/978-1-4614-7181-3_2)
- Broz, P., & Monack, D. M. (2013). pathogens. *Nature Publishing Group*, *13*(8), 551–565. <https://doi.org/10.1038/nri3479>
- Broz, P., von Moltke, J., Jones, J. W., Vance, R. E., & Monack, D. M. (2010). Differential Requirement for Caspase-1 Autoproteolysis in Pathogen-Induced Cell Death and Cytokine Processing. *Cell Host & Microbe*, *8*(6), 471–483. <https://doi.org/10.1016/j.chom.2010.11.007>
- Bryant, C. E., Symmons, M., & Gay, N. J. (2015). Toll-like receptor signalling through macromolecular protein complexes. *Molecular Immunology*, *63*(2), 162–165. <https://doi.org/10.1016/J.MOLIMM.2014.06.033>
- Cao, X. (2016). Self-regulation and cross-regulation of pattern-recognition receptor signalling in health and disease. *Nature Publishing Group*, *16*(1), 35–50. <https://doi.org/10.1038/nri.2015.8>
- Case, C. L. (2011). Regulating caspase-1 during infection: roles of NLRs, AIM2, and ASC. *The Yale Journal of Biology and Medicine*, *84*(4), 333–343. Retrieved from <http://www.ncbi.nlm.nih.gov/pubmed/22180671>
- Case, C. L., & Roy, C. R. (2011). Asc modulates the function of NLRC4 in response to infection of macrophages by *Legionella pneumophila*. *mBio*, *2*(4), e00117-11. <https://doi.org/10.1128/mBio.00117-11>
- Cebra, C., Anderson, D. E. (Veterinarian), Tibary, A. (Ahmed), Van Saun, R. J., & Johnson,

## References

- L. W. (n.d.). *Llama and alpaca care : medicine, surgery, reproduction, nutrition, and herd health*.
- Chai, J., & Shi, Y. (2014). Apoptosome and inflammasome: conserved machineries for caspase activation. *National Science Review*, 1(1), 101–118. <https://doi.org/10.1093/nsr/nwt025>
- Chen, H.-M., Wang, Y., Su, L.-H., & Chiu, C.-H. (2013). Nontyphoid Salmonella Infection: Microbiology, Clinical Features, and Antimicrobial Therapy. *Pediatrics & Neonatology*, 54(3), 147–152. <https://doi.org/10.1016/j.pedneo.2013.01.010>
- Chen, K. W., Groß, C. J., Sotomayor, F. V., Stacey, K. J., Tschopp, J., Sweet, M. J., & Schroder, K. (2014). The Neutrophil NLRC4 Inflammasome Selectively Promotes IL-1 $\beta$  Maturation without Pyroptosis during Acute Salmonella Challenge. *Cell Reports*, 8(2), 570–582. <https://doi.org/10.1016/j.celrep.2014.06.028>
- Compan, V., Baroja-Mazo, A., López-Castejón, G., Gomez, A. I., Martínez, C. M., Angosto, D., ... Pelegrín, P. (2012). Cell Volume Regulation Modulates NLRP3 Inflammasome Activation. *Immunity*, 37(3), 487–500. <https://doi.org/10.1016/j.immuni.2012.06.013>
- Cornelis, G. R., & Van Gijsegem, F. (2000). Assembly and Function of Type III Secretory Systems. *Annual Review of Microbiology*, 54(1), 735–774. <https://doi.org/10.1146/annurev.micro.54.1.735>
- de Oliveira, S., Lopez-Muñoz, A., Martínez-Navarro, F. J., Galindo-Villegas, J., Mulero, V., & Calado, Â. (2015). Cxcl8-I1 and Cxcl8-I2 are required in the zebrafish defense against Salmonella Typhimurium. *Developmental & Comparative Immunology*, 49(1), 44–48. <https://doi.org/10.1016/j.dci.2014.11.004>
- de Oliveira, S., Reyes-Aldasoro, C. C., Candel, S., Renshaw, S. A., Mulero, V., & Calado, A. (2013). Cxcl8 (IL-8) Mediates Neutrophil Recruitment and Behavior in the Zebrafish Inflammatory Response. *The Journal of Immunology*, 190(8), 4349–4359. <https://doi.org/10.4049/jimmunol.1203266>
- de Vasconcelos, N. M., Van Opdenbosch, N., Van Gorp, H., Parthoens, E., & Lamkanfi, M. (2018). Single-cell analysis of pyroptosis dynamics reveals conserved GSDMD-

- mediated subcellular events that precede plasma membrane rupture. *Cell Death & Differentiation*. <https://doi.org/10.1038/s41418-018-0106-7>
- Di, A., Xiong, S., Ye, Z., Malireddi, R. K. S., Kometani, S., Zhong, M., ... Malik, A. B. (2018). The TWIK2 Potassium Efflux Channel in Macrophages Mediates NLRP3 Inflammasome-Induced Inflammation. *Immunity*. <https://doi.org/10.1016/j.immuni.2018.04.032>
- Dick, M. S., Sborgi, L., Rühl, S., Hiller, S., & Broz, P. (2016). ASC filament formation serves as a signal amplification mechanism for inflammasomes. *Nature Communications*, 7(May). <https://doi.org/10.1038/ncomms11929>
- Diebolder, C. A., Halff, E. F., Koster, A. J., Huizinga, E. G., & Koning, R. I. (2015). Cryoelectron Tomography of the NAIP5/NLRC4 Inflammasome: Implications for NLR Activation. *Structure*, 23(12), 2349–2357. <https://doi.org/10.1016/j.str.2015.10.001>
- dos Santos, N. M. ., Romano, N., de Sousa, M., Ellis, A. E., & Rombout, J. H. W. . (2000). Ontogeny of B and T cells in sea bass (*Dicentrarchus labrax*, L.). *Fish & Shellfish Immunology*, 10(7), 583–596. <https://doi.org/10.1006/fsim.2000.0273>
- Dueber, J. E., Yeh, B. J., Chak, K., & Lim, W. A. (2003). Reprogramming Control of an Allosteric Signaling Switch Through Modular Recombination. *Science*, 301(5641), 1904–1908. <https://doi.org/10.1126/science.1085945>
- Duncan, J. A., & Canna, S. W. (2018). The NLRC4 Inflammasome. *Immunological Reviews*, 281(1), 115–123. <https://doi.org/10.1111/imr.12607>
- Edgeworth, J. D., Spencer, J., Phalipon, A., Griffin, G. E., & Sansonetti, P. J. (2002). Cytotoxicity and interleukin-1 $\beta$  processing following *Shigella flexneri* infection of human monocyte-derived dendritic cells. *European Journal of Immunology*, 32(5), 1464. [https://doi.org/10.1002/1521-4141\(200205\)32:5<1464::AID-IMMU1464>3.0.CO;2-G](https://doi.org/10.1002/1521-4141(200205)32:5<1464::AID-IMMU1464>3.0.CO;2-G)
- Ellett, F., Pase, L., Hayman, J. W., Andrianopoulos, A., & Lieschke, G. J. (2011). mpeg1 promoter transgenes direct macrophage-lineage expression in zebrafish. *Blood*, 117(4), e49-56. <https://doi.org/10.1182/blood-2010-10-314120>

## References

- Finethy, R., Luoma, S., Orench-Rivera, N., Feeley, E. M., Haldar, A. K., Yamamoto, M., ... Coers, J. (2017). Inflammasome Activation by Bacterial Outer Membrane Vesicles Requires Guanylate Binding Proteins. *mBio*, 8(5), e01188-17. <https://doi.org/10.1128/mBio.01188-17>
- Fink, S. L., Bergsbaken, T., & Cookson, B. T. (2008). Anthrax lethal toxin and Salmonella elicit the common cell death pathway of caspase-1-dependent pyroptosis via distinct mechanisms. *Proceedings of the National Academy of Sciences*, 105(11), 4312–4317. <https://doi.org/10.1073/pnas.0707370105>
- Fink, S. L., & Cookson, B. T. (2005). Apoptosis, Pyroptosis, and Necrosis: Mechanistic Description of Dead and Dying Eukaryotic Cells. *Infection and Immunity*, 73(4), 1907–1916. <https://doi.org/10.1128/IAI.73.4.1907-1916.2005>
- Fink, S. L., & Cookson, B. T. (2006). Caspase-1-dependent pore formation during pyroptosis leads to osmotic lysis of infected host macrophages. *Cellular Microbiology*, 8(11), 1812–1825. <https://doi.org/10.1111/j.1462-5822.2006.00751.x>
- Franchi, L., Kamada, N., Nakamura, Y., Burberry, A., Kuffa, P., Suzuki, S., ... Núñez, G. (2012). NLR4-driven production of IL-1 $\beta$  discriminates between pathogenic and commensal bacteria and promotes host intestinal defense. *Nature Immunology*, 13(5), 449–456. <https://doi.org/10.1038/ni.2263>
- Frew, B. C., Joag, V. R., & Mogridge, J. (2012). Proteolytic Processing of Nlrp1b Is Required for Inflammasome Activity. *PLoS Pathogens*, 8(4), e1002659. <https://doi.org/10.1371/journal.ppat.1002659>
- Gao, W., Xiong, Y., Li, Q., & Yang, H. (2017a). Inhibition of Toll-Like Receptor Signaling as a Promising Therapy for Inflammatory Diseases : A Journey from Molecular to Nano Therapeutics, 8(July). <https://doi.org/10.3389/fphys.2017.00508>
- Gao, W., Xiong, Y., Li, Q., & Yang, H. (2017b). Inhibition of Toll-Like Receptor Signaling as a Promising Therapy for Inflammatory Diseases: A Journey from Molecular to Nano Therapeutics. *Frontiers in Physiology*, 8, 508. <https://doi.org/10.3389/fphys.2017.00508>

- Gomez, D., Shankman, L. S., Nguyen, A. T., & Owens, G. K. (2013). Detection of histone modifications at specific gene loci in single cells in histological sections. *Nature Methods*, *10*(2), 171–177. <https://doi.org/10.1038/nmeth.2332>
- Gray, C., Loynes, C., Whyte, M., Crossman, D., Renshaw, S., & Chico, T. (2011). Simultaneous intravital imaging of macrophage and neutrophil behaviour during inflammation using a novel transgenic zebrafish. *Thrombosis and Haemostasis*, *105*(5), 811–819. <https://doi.org/10.1160/TH10-08-0525>
- Guey, B., Bodnar, M., Manié, S. N., Tardivel, A., & Petrilli, V. (2014). Caspase-1 autoproteolysis is differentially required for NLRP1b and NLRP3 inflammasome function. *Proceedings of the National Academy of Sciences*, *111*(48), 17254–17259. <https://doi.org/10.1073/pnas.1415756111>
- Guo, H., Callaway, J. B., & Ting, J. P.-Y. (2015). Inflammasomes: mechanism of action, role in disease and therapeutics. *Nature Medicine*, *21*(7), 677–687. <https://doi.org/10.1038/nm.3893>
- Guo, Z. S., Liu, Z., & Bartlett, D. L. (2014). Oncolytic Immunotherapy: Dying the Right Way is a Key to Eliciting Potent Antitumor Immunity. *Frontiers in Oncology*, *4*, 74. <https://doi.org/10.3389/fonc.2014.00074>
- Hafner-Bratkovič, I. (2017). The NLRC4 inflammasome: The pieces of the puzzle are falling into place. *Inflammasome*, *3*(1), 10–23. <https://doi.org/10.1515/infl-2017-0002>
- Hamel, V., Steib, E., Hamelin, R., Armand, F., Borgers, S., Flückiger, I., ... Gönczy, P. (2017). Identification of Chlamydomonas Central Core Centriolar Proteins Reveals a Role for Human WDR90 in Ciliogenesis. *Current Biology*, *27*(16), 2486–2498.e6. <https://doi.org/10.1016/j.cub.2017.07.011>
- Hansen, S. B., Laursen, N. S., Andersen, G. R., & Andersen, K. R. (2017). Introducing site-specific cysteines into nanobodies for mercury labelling allows *de novo* phasing of their crystal structures. *Acta Crystallographica Section D Structural Biology*, *73*(10), 804–813. <https://doi.org/10.1107/S2059798317013171>
- Hashimoto, C., Hudson, K. L., & Anderson, K. V. (1988). The Toll gene of drosophila,

## References

- required for dorsal-ventral embryonic polarity, appears to encode a transmembrane protein. *Cell*, 52(2), 269–279. [https://doi.org/https://doi.org/10.1016/0092-8674\(88\)90516-8](https://doi.org/https://doi.org/10.1016/0092-8674(88)90516-8)
- He, L., Li, J., Ren, S., Sun, S., Guo, Y., Qiu, H., ... Zhou, Y. (2017). [Construction and identification of nanobody phage display library targeting Middle East respiratory syndrome coronavirus]. *Xi Bao Yu Fen Zi Mian Yi Xue Za Zhi = Chinese Journal of Cellular and Molecular Immunology*, 33(12), 1662–1668. Retrieved from <http://www.ncbi.nlm.nih.gov/pubmed/29382428>
- He, W., Wan, H., Hu, L., Chen, P., Wang, X., Huang, Z., ... Han, J. (2015). Gasdermin D is an executor of pyroptosis and required for interleukin-1 $\beta$  secretion. *Cell Research*, 25(12), 1285–1298. <https://doi.org/10.1038/cr.2015.139>
- Hodgkins, A., Farne, A., Perera, S., Grego, T., Parry-Smith, D. J., Skarnes, W. C., & Iyer, V. (2015). WGE: a CRISPR database for genome engineering: Fig. 1. *Bioinformatics*, 31(18), 3078–3080. <https://doi.org/10.1093/bioinformatics/btv308>
- Howe, K., Schiffer, P. H., Zielinski, J., Wiehe, T., Laird, G. K., Marioni, J. C., ... Leptin, M. (2016). Structure and evolutionary history of a large family of NLR proteins in the zebrafish. *Open Biology*, 6(4), 160009. <https://doi.org/10.1098/rsob.160009>
- Howlader, D. R., Sinha, R., Nag, D., Majumder, N., Mukherjee, P., Bhaumik, U., ... Koley, H. (2016). Zebrafish as a novel model for non-typhoidal Salmonella pathogenesis, transmission and vaccine efficacy. *Vaccine*, 34(42), 5099–5106. <https://doi.org/10.1016/J.VACCINE.2016.08.077>
- Hu, Z., Yan, C., Liu, P., Huang, Z., Ma, R., Zhang, C., ... Chai, J. (2013). Crystal Structure of NLRC4 Reveals Its Autoinhibition Mechanism. *Science*, 341(6142), 172–175. <https://doi.org/10.1126/science.1236381>
- Hu, Z., Zhou, Q., Zhang, C., Fan, S., Cheng, W., Zhao, Y., ... Chai, J. (2015). Structural and biochemical basis for induced self-propagation of NLRC4. *Science (New York, N.Y.)*, 350(6259), 399–404. <https://doi.org/10.1126/science.aac5489>
- Huang, Y., Ma, D., Huang, H., Lu, Y., Liao, Y., Liu, L., ... Fang, F. (2017). Interaction between HCMV pUL83 and human AIM2 disrupts the activation of the AIM2 inflammasome.

- Virology Journal*, 14(1), 34. <https://doi.org/10.1186/s12985-016-0673-5>
- Humke, E. W., Shriver, S. K., Starovasnik, M. A., Fairbrother, W. J., & Dixit, V. M. (2000). ICEBERG: a novel inhibitor of interleukin-1beta generation. *Cell*, 103(1), 99–111. Retrieved from <http://www.ncbi.nlm.nih.gov/pubmed/11051551>
- Hwang, W. Y., Fu, Y., Reyon, D., Maeder, M. L., Tsai, S. Q., Sander, J. D., ... Joung, J. K. (2013). Efficient genome editing in zebrafish using a CRISPR-Cas system. *Nature Biotechnology*, 31(3), 227–229. <https://doi.org/10.1038/nbt.2501>
- Iwama, G. K. (George K. ., & Nakanishi, T. (1996). *The fish immune system : organism, pathogen, and environment*. Academic Press.
- Jin, T., Perry, A., Jiang, J., Smith, P., Curry, J. A., Unterholzner, L., ... Xiao, T. S. (2012). Structures of the HIN Domain:DNA Complexes Reveal Ligand Binding and Activation Mechanisms of the AIM2 Inflammasome and IFI16 Receptor. *Immunity*, 36(4), 561–571. <https://doi.org/10.1016/j.immuni.2012.02.014>
- Jo, E.-K., Kim, J. K., Shin, D.-M., & Sasakawa, C. (2016). Molecular mechanisms regulating NLRP3 inflammasome activation. *Cellular & Molecular Immunology*, 13(2), 148–159. <https://doi.org/10.1038/cmi.2015.95>
- Kambara, H., Liu, F., Zhang, X., Liu, P., Bajrami, B., Teng, Y., ... Luo, H. R. (2018). Gasdermin D Exerts Anti-inflammatory Effects by Promoting Neutrophil Death. *Cell Reports*, 22(11), 2924–2936. <https://doi.org/10.1016/j.celrep.2018.02.067>
- Karki, R., Lee, E., Place, D., Samir, P., Mavuluri, J., Sharma, B. R., ... Kanneganti, T.-D. (2018). IRF8 Regulates Transcription of Naips for NLRC4 Inflammasome Activation. *Cell*, 173(4), 920–933.e13. <https://doi.org/10.1016/j.cell.2018.02.055>
- Kayagaki, N., Stowe, I. B., Lee, B. L., O'Rourke, K., Anderson, K., Warming, S., ... Dixit, V. M. (2015). Caspase-11 cleaves gasdermin D for non-canonical inflammasome signalling. *Nature*, 526(7575), 666–671. <https://doi.org/10.1038/nature15541>
- Keller, M., Rüegg, A., Werner, S., & Beer, H.-D. (2008). Active Caspase-1 Is a Regulator of Unconventional Protein Secretion. *Cell*, 132(5), 818–831. <https://doi.org/10.1016/j.cell.2007.12.040>

## References

- Kim, B.-H., Chee, J. D., Bradfield, C. J., Park, E.-S., Kumar, P., & MacMicking, J. D. (2016). Interferon-induced guanylate-binding proteins in inflammasome activation and host defense. *Nature Immunology*, *17*(5), 481–489. <https://doi.org/10.1038/ni.3440>
- Kim, Y. K., Shin, J., & Nahm, M. H. (2016a). NOD-Like Receptors in Infection, Immunity, and Diseases, *57*(1), 5–14.
- Kim, Y. K., Shin, J. S., & Nahm, M. H. (2016b). NOD-Like Receptors in Infection, Immunity, and Diseases. *Yonsei Medical Journal*, *57*(1), 5–14. <https://doi.org/10.3349/ymj.2016.57.1.5>
- Knodler, L. A., Crowley, S. M., Sham, H. P., Yang, H., Wrande, M., Ma, C., ... Vallance, B. A. (2014). Noncanonical Inflammasome Activation of Caspase-4/Caspase-11 Mediates Epithelial Defenses against Enteric Bacterial Pathogens. *Cell Host & Microbe*, *16*(2), 249–256. <https://doi.org/10.1016/j.chom.2014.07.002>
- Kofoed, E. M., & Vance, R. E. (2011). Innate immune recognition of bacterial ligands by NALPs determines inflammasome specificity. *Nature*, *477*(7366), 592–595. <https://doi.org/10.1038/nature10394>
- Kuri, P., Schieber, N. L., Thumberger, T., Wittbrodt, J., Schwab, Y., & Leptin, M. (2017). Dynamics of in vivo ASC speck formation. *The Journal of Cell Biology*, *216*(9), 2891–2909. <https://doi.org/10.1083/jcb.201703103>
- Laing, K. J., Purcell, M. K., Winton, J. R., & Hansen, J. D. (2008). A genomic view of the NOD-like receptor family in teleost fish: identification of a novel NLR subfamily in zebrafish. *BMC Evolutionary Biology*, *8*(1), 42. <https://doi.org/10.1186/1471-2148-8-42>
- Lamkanfi, M., Denecker, G., Kalai, M., D'hondt, K., Meeus, A., Declercq, W., ... Vandenabeele, P. (2004). INCA, a novel human caspase recruitment domain protein that inhibits interleukin-1beta generation. *The Journal of Biological Chemistry*, *279*(50), 51729–51738. <https://doi.org/10.1074/jbc.M407891200>
- Lamkanfi, M., & Dixit, V. M. (2014). Mechanisms and Functions of Inflammasomes. *Cell*, *157*(5), 1013–1022. <https://doi.org/10.1016/J.CELL.2014.04.007>

- Lamkanfi, M., Walle, L. Vande, & Kanneganti, T.-D. (2011). Deregulated inflammasome signaling in disease. *Immunological Reviews*, 243(1), 163–173. <https://doi.org/10.1111/j.1600-065X.2011.01042.x>
- Latz, E., Xiao, T. S., & Stutz, A. (2013). Activation and regulation of the inflammasomes. *Nature Reviews Immunology*, 13(6), 397–411. <https://doi.org/10.1038/nri3452>
- Lee, B. L., Mirrashidi, K. M., Stowe, I. B., Kummerfeld, S. K., Watanabe, C., Haley, B., ... Kayagaki, N. (2018). ASC- And caspase-8-dependent apoptotic pathway diverges from the NLRC4 inflammasome in macrophages. *Scientific Reports*, 8(1), 1–12. <https://doi.org/10.1038/s41598-018-21998-3>
- Letunic, I., Doerks, T., & Bork, P. (2009). SMART 6: recent updates and new developments. *Nucleic Acids Research*, 37(Database), D229–D232. <https://doi.org/10.1093/nar/gkn808>
- Levinsohn, J. L., Newman, Z. L., Hellmich, K. A., Fattah, R., Getz, M. A., Liu, S., ... Moayeri, M. (2012). Anthrax lethal factor cleavage of Nlrp1 is required for activation of the inflammasome. *PLoS Pathogens*, 8(3), e1002638. <https://doi.org/10.1371/journal.ppat.1002638>
- Li, M., Fan, X., Liu, J., Hu, Y., & Huang, H. (2015). Selection by phage display of nanobodies directed against hypoxia inducible factor-1 $\alpha$  (HIF-1 $\alpha$ ). *Biotechnology and Applied Biochemistry*, 62(6), 738–745. <https://doi.org/10.1002/bab.1340>
- Li, Y., Li, Y., Cao, X., Jin, X., & Jin, T. (2017). Pattern recognition receptors in zebrafish provide functional and evolutionary insight into innate immune signaling pathways. *Cellular and Molecular Immunology*, 14(1), 80–89. <https://doi.org/10.1038/cmi.2016.50>
- Lightfield, K. L., Persson, J., Trinidad, N. J., Brubaker, S. W., Kofoed, E. M., Sauer, J.-D., ... Vance, R. E. (2011). Differential Requirements for NAIP5 in Activation of the NLRC4 Inflammasome. *Infection and Immunity*, 79(4), 1606–1614. <https://doi.org/10.1128/IAI.01187-10>
- Liu, J., Zhou, Y., Qi, X., Chen, J., Chen, W., Qiu, G., ... Wu, N. (2017). CRISPR/Cas9 in zebrafish: an efficient combination for human genetic diseases modeling. *Human*

## References

- Genetics*, 136(1), 1–12. <https://doi.org/10.1007/s00439-016-1739-6>
- Liu, W., Liu, X., Li, Y., Zhao, J., Liu, Z., Hu, Z., ... Kang, Z. (2017). LRRK2 promotes the activation of NLRC4 inflammasome during *Salmonella Typhimurium* infection. *The Journal of Experimental Medicine*, jem.20170014. <https://doi.org/10.1084/jem.20170014>
- Liu, X., Wang, D., Chu, J., Xu, Y., & Wang, W. (2018). Sandwich pair nanobodies, a potential tool for electrochemical immunosensing serum prostate-specific antigen with preferable specificity. *Journal of Pharmaceutical and Biomedical Analysis*, 158, 361–369. <https://doi.org/10.1016/j.jpba.2018.06.021>
- Liu, Z., Wang, C., Rathkey, J. K., Yang, J., Dubyak, G. R., Abbott, D. W., & Xiao, T. S. (2018). Structures of the Gasdermin D C-Terminal Domains Reveal Mechanisms of Autoinhibition. *Structure*, 26(5), 778–784.e3. <https://doi.org/10.1016/j.str.2018.03.002>
- López-Castejón, G., Sepulcre, M. P., Mulero, I., Pelegrín, P., Meseguer, J., & Mulero, V. (2008). Molecular and functional characterization of gilthead seabream *Sparus aurata* caspase-1: the first identification of an inflammatory caspase in fish. *Molecular Immunology*, 45(1), 49–57. <https://doi.org/10.1016/j.molimm.2007.05.015>
- López-Castejón, G., Young, M. T., Meseguer, J., Surprenant, A., & Mulero, V. (2007). Characterization of ATP-gated P2X7 receptors in fish provides new insights into the mechanism of release of the leaderless cytokine interleukin-1 $\beta$ . *Molecular Immunology*, 44(6), 1286–1299. <https://doi.org/10.1016/j.molimm.2006.05.015>
- Lu, A., Li, Y., Schmidt, F. I., Yin, Q., Chen, S., Fu, T.-M., ... Wu, H. (2016). Molecular basis of caspase-1 polymerization and its inhibition by a new capping mechanism. *Nature Structural & Molecular Biology*, 23(5), 416–425. <https://doi.org/10.1038/nsmb.3199>
- Lu, A., Magupalli, V. G., Ruan, J., Yin, Q., Atianand, M. K., Vos, M. R., ... Egelman, E. H. (2014). Unified polymerization mechanism for the assembly of ASC-dependent inflammasomes. *Cell*, 156(6), 1193–1206.

- <https://doi.org/10.1016/j.cell.2014.02.008>
- Lu, W., Karuppagounder, S. S., Springer, D. A., Allen, M. D., Zheng, L., Chao, B., ... Sciences, M. (2015). HHS Public Access, 350(6259), 404–409. <https://doi.org/10.1038/ncomms5930>.Genetic
- Lux, S. E., John, K. M., & Bennett, V. (1990). Analysis of cDNA for human erythrocyte ankyrin indicates a repeated structure with homology to tissue-differentiation and cell-cycle control proteins. *Nature*, 344(6261), 36–42. <https://doi.org/10.1038/344036a0>
- Man, S. M., Ekpenyong, A., Turlomousis, P., Achouri, S., Cammarota, E., Hughes, K., ... Bryant, C. E. (2014). Actin polymerization as a key innate immune effector mechanism to control <em>Salmonella</em> infection. *Proceedings of the National Academy of Sciences*, 111(49), 17588 LP-17593. Retrieved from <http://www.pnas.org/content/111/49/17588.abstract>
- Man, S. M., Hopkins, L. J., Nugent, E., Cox, S., Glück, I. M., Turlomousis, P., ... Bryant, C. E. (2014). Inflammasome activation causes dual recruitment of NLRC4 and NLRP3 to the same macromolecular complex. *Proceedings of the National Academy of Sciences of the United States of America*, 111(20), 7403–7408. <https://doi.org/10.1073/pnas.1402911111>
- Man, S. M., & Kanneganti, T.-D. (2015). Regulation of inflammasome activation. *Immunological Reviews*, 265(1), 6–21. <https://doi.org/10.1111/imr.12296>
- Man, S. M., Karki, R., & Kanneganti, T.-D. (2016). AIM2 inflammasome in infection, cancer, and autoimmunity: Role in DNA sensing, inflammation, and innate immunity. *European Journal of Immunology*, 46(2), 269–280. <https://doi.org/10.1002/eji.201545839>
- Mariathasan, S., Newton, K., Monack, D. M., Vucic, D., French, D. M., Lee, W. P., ... Dixit, V. M. (2004). Differential activation of the inflammasome by caspase-1 adaptors ASC and Ipaf. *Nature*, 430(6996), 213–218. <https://doi.org/10.1038/nature02664>
- Martinon, F., Burns, K., & Tschopp, J. (2002). The inflammasome: a molecular platform triggering activation of inflammatory caspases and processing of proIL-beta.

## References

- Molecular Cell*, 10(2), 417–426. Retrieved from <http://www.ncbi.nlm.nih.gov/pubmed/12191486>
- Martinon, F., Mayor, A., & Tschopp, J. (2009). The Inflammasomes: Guardians of the Body. *Annual Review of Immunology*, 27(1), 229–265. <https://doi.org/10.1146/annurev.immunol.021908.132715>
- Mascarenhas, D. P. A., Cerqueira, D. M., Pereira, M. S. F., Castanheira, F. V. S., Fernandes, T. D., Manin, G. Z., ... Zamboni, D. S. (2017). Inhibition of caspase-1 or gasdermin-D enable caspase-8 activation in the Naip5/NLRC4/ASC inflammasome. *PLoS Pathogens*, 13(8), 1–28. <https://doi.org/10.1371/journal.ppat.1006502>
- Masumoto, J., Taniguchi, S., Ayukawa, K., Sarvotham, H., Kishino, T., Niikawa, N., ... Sagara, J. (1999). ASC, a novel 22-kDa protein, aggregates during apoptosis of human promyelocytic leukemia HL-60 cells. *The Journal of Biological Chemistry*, 274(48), 33835–33838. <https://doi.org/10.1074/JBC.274.48.33835>
- Masumoto, J., Zhou, W., Chen, F. F., Su, F., Kuwada, J. Y., Hidaka, E., ... Inohara, N. (2003). Caspy, a zebrafish caspase, activated by ASC oligomerization is required for pharyngeal arch development. *The Journal of Biological Chemistry*, 278(6), 4268–4276. <https://doi.org/10.1074/jbc.M203944200>
- Matusiak, M., Van Opdenbosch, N., Vande Walle, L., Sirard, J.-C., Kanneganti, T.-D., & Lamkanfi, M. (2015). Flagellin-induced NLRC4 phosphorylation primes the inflammasome for activation by NAIP5. *Proceedings of the National Academy of Sciences*, 112(5), 1541–1546. <https://doi.org/10.1073/pnas.1417945112>
- McGuffin, L. J., Atkins, J. D., Salehe, B. R., Shuid, A. N., & Roche, D. B. (2015). IntFOLD: an integrated server for modelling protein structures and functions from amino acid sequences: Figure 1. *Nucleic Acids Research*, 43(W1), W169–W173. <https://doi.org/10.1093/nar/gkv236>
- McGuffin, L. J., Buenavista, M. T., & Roche, D. B. (2013). The ModFOLD4 server for the quality assessment of 3D protein models. *Nucleic Acids Research*, 41(W1), W368–W372. <https://doi.org/10.1093/nar/gkt294>
- Miao, E. A., Alpuche-Aranda, C. M., Dors, M., Clark, A. E., Bader, M. W., Miller, S. I., &

- Aderem, A. (2006). Cytoplasmic flagellin activates caspase-1 and secretion of interleukin 1 $\beta$  via Ipaf. *Nature Immunology*, 7(6), 569–575. <https://doi.org/10.1038/ni1344>
- Miao, E. A., Mao, D. P., Yudkovsky, N., Bonneau, R., Lorang, C. G., Warren, S. E., ... Aderem, A. (2010). Innate immune detection of the type III secretion apparatus through the NLRC4 inflammasome. *Proceedings of the National Academy of Sciences*, 107(7), 3076–3080. <https://doi.org/10.1073/pnas.0913087107>
- Monack, D. M., Raupach, B., Hromockyj, A. E., & Falkow, S. (1996). Salmonella typhimurium invasion induces apoptosis in infected macrophages. *Proceedings of the National Academy of Sciences of the United States of America*, 93(18), 9833–9838. Retrieved from <http://www.ncbi.nlm.nih.gov/pubmed/8790417>
- Morrone, S. R., Matyszewski, M., Yu, X., Delannoy, M., Egelman, E. H., & Sohn, J. (2015). Assembly-driven activation of the AIM2 foreign-dsDNA sensor provides a polymerization template for downstream ASC. *Nature Communications*, 6(1), 7827. <https://doi.org/10.1038/ncomms8827>
- Mosavi, L. K., Cammett, T. J., Desrosiers, D. C., & Peng, Z.-Y. (2004). The ankyrin repeat as molecular architecture for protein recognition. *Protein Science : A Publication of the Protein Society*, 13(6), 1435–1448. <https://doi.org/10.1110/ps.03554604>
- Neely, H. R., & Flajnik, M. F. (2016). Emergence and Evolution of Secondary Lymphoid Organs. *Annual Review of Cell and Developmental Biology*, 32(1), 693–711. <https://doi.org/10.1146/annurev-cellbio-111315-125306>
- Neer, E. J., Schmidt, C. J., Nambudripad, R., & Smith, T. F. (1994). The ancient regulatory-protein family of WD-repeat proteins. *Nature*, 371(6495), 297–300. <https://doi.org/10.1038/371297a0>
- Newton, K., & Dixit, V. M. (2012). Signaling in innate immunity and inflammation. *Cold Spring Harbor Perspectives in Biology*, 4(3). <https://doi.org/10.1101/cshperspect.a006049>
- Nguyen-Chi, M., Laplace-Builhe, B., Travnickova, J., Luz-Crawford, P., Tejedor, G., Phan, Q. T., ... Djouad, F. (2015). Identification of polarized macrophage subsets in

## References

- zebrafish. *eLife*, 4, e07288. <https://doi.org/10.7554/eLife.07288>
- Parra, D., Korytář, T., Takizawa, F., & Sunyer, J. O. (2016). B cells and their role in the teleost gut. *Developmental and Comparative Immunology*, 64, 150–166. <https://doi.org/10.1016/j.dci.2016.03.013>
- Peyrassol, X., Laeremans, T., Gouwy, M., Lahura, V., Debulpaep, M., Van Damme, J., ... Langer, I. (2016). Development by Genetic Immunization of Monovalent Antibodies (Nanobodies) Behaving as Antagonists of the Human ChemR23 Receptor. *The Journal of Immunology*, 196(6), 2893–2901. <https://doi.org/10.4049/jimmunol.1500888>
- Prehoda, K. E., Scott, J. A., Mullins, R. D., & Lim, W. A. (2000). Integration of multiple signals through cooperative regulation of the N-WASP-Arp2/3 complex. *Science (New York, N.Y.)*, 290(5492), 801–806. Retrieved from <http://www.ncbi.nlm.nih.gov/pubmed/11052943>
- Qian, C., Liu, J., & Cao, X. (2014). Innate signaling in the inflammatory immune disorders. *Cytokine and Growth Factor Reviews*, 25(6), 731–738. <https://doi.org/10.1016/j.cytogfr.2014.06.003>
- Qu, Y., Misaghi, S., Izrael-Tomasevic, A., Newton, K., Gilmour, L. L., Lamkanfi, M., ... Dixit, V. M. (2012). Phosphorylation of NLRC4 is critical for inflammasome activation. *Nature*, 490(7421), 539–542. <https://doi.org/10.1038/nature11429>
- Qu, Y., Misaghi, S., Newton, K., Maltzman, A., Izrael-Tomasevic, A., Arnott, D., & Dixit, V. M. (2016a). NLRP3 recruitment by NLRC4 during *Salmonella* infection. *The Journal of Experimental Medicine*, 213(6), 877–885. <https://doi.org/10.1084/jem.20132234>
- Qu, Y., Misaghi, S., Newton, K., Maltzman, A., Izrael-Tomasevic, A., Arnott, D., & Dixit, V. M. (2016b). NLRP3 recruitment by NLRC4 during *Salmonella* infection. *The Journal of Experimental Medicine*, 213(6), 877–885. <https://doi.org/10.1084/jem.20132234>
- Rajan, M., Mortusewicz, O., Rothbauer, U., Hastert, F. D., Schmidthals, K., Rapp, A., ... Cardoso, M. C. (2015). Generation of an alpaca-derived nanobody recognizing  $\gamma$ -

- H2AX. *FEBS Open Bio*, 5(1), 779–788. <https://doi.org/10.1016/j.fob.2015.09.005>
- Ramos-Junior, E. S., & Morandini, A. C. (2017). Gasdermin: A new player to the inflammasome game. *Biomedical Journal*, 40(6), 313–316. <https://doi.org/10.1016/j.bj.2017.10.002>
- Reis, M. I. R., do Vale, A., Pereira, P. J. B., Azevedo, J. E., & Dos Santos, N. M. S. (2012). Caspase-1 and IL-1 $\beta$  processing in a teleost fish. *PloS One*, 7(11), e50450. <https://doi.org/10.1371/journal.pone.0050450>
- Renshaw, S. A., Loynes, C. A., Trushell, D. M. I., Elworthy, S., Ingham, P. W., & Whyte, M. K. B. (2006). A transgenic zebrafish model of neutrophilic inflammation. *Blood*, 108(13), 3976–3978. <https://doi.org/10.1182/blood-2006-05-024075>
- Reyes Ruiz, V. M., Ramirez, J., Naseer, N., Palacio, N. M., Siddarthan, I. J., Yan, B. M., ... Shin, S. (2017). Broad detection of bacterial type III secretion system and flagellin proteins by the human NAIP/NLRC4 inflammasome. *Proceedings of the National Academy of Sciences*, 114(50), 13242–13247. <https://doi.org/10.1073/pnas.1710433114>
- Saleh, M., Mathison, J. C., Wolinski, M. K., Bensinger, S. J., Fitzgerald, P., Droin, N., ... Nicholson, D. W. (2006). Enhanced bacterial clearance and sepsis resistance in caspase-12-deficient mice. *Nature*, 440(7087), 1064–1068. <https://doi.org/10.1038/nature04656>
- Saurabh, S., & Sahoo, P. K. (2008). Lysozyme: an important defence molecule of fish innate immune system. *Aquaculture Research*, 39(3), 223–239. <https://doi.org/10.1111/j.1365-2109.2007.01883.x>
- Saxena, M., & Yeretssian, G. (2014). NOD-Like Receptors: Master Regulators of Inflammation and Cancer. *Frontiers in Immunology*, 5, 327. <https://doi.org/10.3389/fimmu.2014.00327>
- Schapira, M., Tyers, M., Torrent, M., & Arrowsmith, C. H. (2017a). WD40 repeat domain proteins: a novel target class? *Nature Reviews Drug Discovery*, 16(11), 773–786. <https://doi.org/10.1038/nrd.2017.179>

## References

- Schapira, M., Tyers, M., Torrent, M., & Arrowsmith, C. H. (2017b). WD40 repeat domain proteins: a novel target class? *Nature Reviews Drug Discovery*, *16*(11), 773–786. <https://doi.org/10.1038/nrd.2017.179>
- Schroder, K., & Tschopp, J. (2010). The Inflammasomes. *Cell*, *140*(6), 821–832. <https://doi.org/10.1016/j.cell.2010.01.040>
- Sellin, M. E., Müller, A. A., Felmy, B., Dolowschiak, T., Diard, M., Tardivel, A., ... Hardt, W.-D. (2014). Epithelium-Intrinsic NAIP/NLRC4 Inflammasome Drives Infected Enterocyte Expulsion to Restrict Salmonella Replication in the Intestinal Mucosa. *Cell Host & Microbe*, *16*(2), 237–248. <https://doi.org/10.1016/J.CHOM.2014.07.001>
- Shamaa, O. R., Mitra, S., Gavrilin, M. A., & Wewers, M. D. (2015). Monocyte Caspase-1 Is Released in a Stable, Active High Molecular Weight Complex Distinct from the Unstable Cell Lysate-Activated Caspase-1. *PLOS ONE*, *10*(11), e0142203. <https://doi.org/10.1371/journal.pone.0142203>
- Sharma, D., & Kanneganti, T. D. (2016). The cell biology of inflammasomes: Mechanisms of inflammasome activation and regulation. *Journal of Cell Biology*, *213*(6), 617–629. <https://doi.org/10.1083/jcb.201602089>
- Shea, J. E., Beuzon, C. R., Gleeson, C., Mundy, R., & Holden, D. W. (1999). Influence of the Salmonella typhimurium pathogenicity island 2 type III secretion system on bacterial growth in the mouse. *Infection and Immunity*, *67*(1), 213–219. Retrieved from <http://www.ncbi.nlm.nih.gov/pubmed/9864218>
- Shenoy, A. R., Wellington, D. A., Kumar, P., Kassa, H., Booth, C. J., Cresswell, P., & MacMicking, J. D. (2012). GBP5 Promotes NLRP3 Inflammasome Assembly and Immunity in Mammals. *Science*, *336*(6080), 481–485. <https://doi.org/10.1126/science.1217141>
- Shi, J., Zhao, Y., Wang, K., Shi, X., Wang, Y., Huang, H., ... Shao, F. (2015). Cleavage of GSDMD by inflammatory caspases determines pyroptotic cell death. *Nature*, *526*(7575), 660–665. <https://doi.org/10.1038/nature15514>
- Sohrabi, Y., Volkova, V., Kobets, T., Havelková, H., Krayem, I., Slapničková, M., ...

- Lipoldová, M. (2018). Genetic Regulation of Guanylate-Binding Proteins 2b and 5 during Leishmaniasis in Mice. *Frontiers in Immunology*, 9, 130. <https://doi.org/10.3389/fimmu.2018.00130>
- Sotomayor, C., Wang, Q., Arnott, A., Howard, P., Hope, K., Lan, R., & Sintchenko, V. (2018). Novel *Salmonella enterica* Serovar Typhimurium Genotype Levels as Herald of Seasonal Salmonellosis Epidemics. *Emerging Infectious Diseases*, 24(6), 1079–1082. <https://doi.org/10.3201/eid2406.171096>
- Stirnimann, C. U., Petsalaki, E., Russell, R. B., & Müller, C. W. (2010). WD40 proteins propel cellular networks. *Trends in Biochemical Sciences*, 35(10), 565–574. <https://doi.org/10.1016/j.tibs.2010.04.003>
- Thisse, C., Thisse, B., Schilling, T. F., & Postlethwait, J. H. (1993). Structure of the zebrafish snail1 gene and its expression in wild-type, spadetail and no tail mutant embryos. *Development (Cambridge, England)*, 119(4), 1203–1215. Retrieved from <http://www.ncbi.nlm.nih.gov/pubmed/8306883>
- Torraca, V., & Mostowy, S. (2018). Zebrafish Infection: From Pathogenesis to Cell Biology. *Trends in Cell Biology*, 28(2), 143–156. <https://doi.org/10.1016/j.tcb.2017.10.002>
- Tschopp, J., Martinon, F., & Burns, K. (2003). NALPs: a novel protein family involved in inflammation. *Nature Reviews Molecular Cell Biology*, 4(2), 95–104. <https://doi.org/10.1038/nrm1019>
- Tyrkalska, S. D., Candel, S., Angosto, D., Gómez-Abellán, V., Martín-Sánchez, F., García-Moreno, D., ... Mulero, V. (2016). Neutrophils mediate *Salmonella* Typhimurium clearance through the GBP4 inflammasome-dependent production of prostaglandins. *Nature Communications*, 7(May). <https://doi.org/10.1038/ncomms12077>
- Uribe, C., Folch, H., Enriquez, R., & Moran, G. (2011). Innate and adaptive immunity in teleost fish: a review. *Veterinarni Medicina*, 56(10), 486–503. Retrieved from <http://vri.cz/docs/vetmed/56-10-486.pdf>
- Vance, R. E. (2015). The NAIP/NLRC4 inflammasomes. *Current Opinion in Immunology*,

## References

- 32, 84–89. <https://doi.org/10.1016/j.coi.2015.01.010>
- Varela, M., Romero, A., Dios, S., van der Vaart, M., Figueras, A., Meijer, A. H., & Novoa, B. (2014). Cellular visualization of macrophage pyroptosis and interleukin-1 $\beta$  release in a viral hemorrhagic infection in zebrafish larvae. *Journal of Virology*, *88*(20), 12026–12040. <https://doi.org/10.1128/JVI.02056-14>
- Vincent, W. J. B., Freisinger, C. M., Lam, P., Huttenlocher, A., & Sauer, J.-D. (2016). Macrophages mediate flagellin induced inflammasome activation and host defense in zebrafish. *Cellular Microbiology*, *18*(4), 591–604. <https://doi.org/10.1111/cmi.12536>
- Vojtech, L. N., Scharping, N., Woodson, J. C., & Hansen, J. D. (2012). Roles of inflammatory caspases during processing of zebrafish interleukin-1 $\beta$  in *Francisella noatunensis* infection. *Infection and Immunity*, *80*(8), 2878–2885. <https://doi.org/10.1128/IAI.00543-12>
- von Moltke, J., Trinidad, N. J., Moayeri, M., Kintzer, A. F., Wang, S. B., van Rooijen, N., ... Vance, R. E. (2012). Rapid induction of inflammatory lipid mediators by the inflammasome in vivo. *Nature*, *490*(7418), 107–111. <https://doi.org/10.1038/nature11351>
- Wang, L.-J., Hsu, C.-W., Chen, C.-C., Liang, Y., Chen, L.-C., Ojcius, D. M., ... Chang, Y.-S. (2012). Interactome-wide analysis identifies end-binding protein 1 as a crucial component for the speck-like particle formation of activated absence in melanoma 2 (AIM2) inflammasomes. *Molecular & Cellular Proteomics : MCP*, *11*(11), 1230–1244. <https://doi.org/10.1074/mcp.M112.020594>
- Wang, Y., Hu, X.-J., Zou, X.-D., Wu, X.-H., Ye, Z.-Q., & Wu, Y.-D. (2015). WDSPdb: a database for WD40-repeat proteins. *Nucleic Acids Research*, *43*(Database issue), D339–44. <https://doi.org/10.1093/nar/gku1023>
- Xu, C., & Min, J. (2011). Structure and function of WD40 domain proteins. *Protein & Cell*, *2*(3), 202–214. <https://doi.org/10.1007/s13238-011-1018-1>
- Xu, Z., Takizawa, F., Parra, D., Gómez, D., von Gersdorff Jørgensen, L., LaPatra, S. E., & Sunyer, J. O. (2016). Mucosal immunoglobulins at respiratory surfaces mark an

- ancient association that predates the emergence of tetrapods. *Nature Communications*, 7, 10728. <https://doi.org/10.1038/ncomms10728>
- Zakrzewska, A., Cui, C., Stockhammer, O. W., Benard, E. L., Spaink, H. P., & Meijer, A. H. (2010). Macrophage-specific gene functions in Spi1-directed innate immunity. *Blood*, 116(3), e1–e11. <https://doi.org/10.1182/blood-2010-01-262873>
- Zhang, Y.-A., Salinas, I., Li, J., Parra, D., Bjork, S., Xu, Z., ... Sunyer, J. O. (2010). IgT, a primitive immunoglobulin class specialized in mucosal immunity. *Nature Immunology*, 11(9), 827–835. <https://doi.org/10.1038/ni.1913>
- Zhao, Y., Yang, J., Shi, J., Gong, Y.-N., Lu, Q., Xu, H., ... Shao, F. (2011). The NLRC4 inflammasome receptors for bacterial flagellin and type III secretion apparatus. *Nature*, 477(7366), 596–600. <https://doi.org/10.1038/nature10510>
- Zou, X.-D., An, K., Wu, Y.-D., & Ye, Z.-Q. (2018). PPI network analyses of human WD40 protein family systematically reveal their tendency to assemble complexes and facilitate the complex predictions. *BMC Systems Biology*, 12(S4), 41. <https://doi.org/10.1186/s12918-018-0567-9>
- Zou, X.-D., Hu, X.-J., Ma, J., Li, T., Ye, Z.-Q., & Wu, Y.-D. (2016). Genome-wide Analysis of WD40 Protein Family in Human. *Scientific Reports*, 6, 39262. <https://doi.org/10.1038/srep39262>
- Zychlinsky, A., Prevost, M. C., & Sansonetti, P. J. (1992). *Shigella flexneri* induces apoptosis in infected macrophages. *Nature*, 358(6382), 167–169. <https://doi.org/10.1038/358167a0>



**RESUMEN EN  
CASTELLANO**



## **Caracterización de Caiap y Wdr90 como nuevos componentes del inflamasoma implicados en la resistencia a *Salmonella enterica* serovar Typhimurium**

El sistema inmunitario es el conjunto de estructuras y procesos biológicos que protegen a un organismo de padecer enfermedades, siendo esencial para el mantenimiento de un estado de equilibrio fisiológico. La respuesta inmunitaria puede dividirse a su vez en respuesta inmunitaria innata o inespecífica y respuesta inmunitaria adaptativa. La respuesta inmunitaria innata es la primera en actuar, siendo la primera barrera de defensa frente a patógenos. Ésta incluye barreras físicas como la piel y diferentes tipos celulares entre los que se encuentran neutrófilos, macrófagos, células dendríticas, monocitos, células epiteliales y un amplio rango de moléculas solubles. Esta respuesta es la más conservada evolutivamente en todos los organismos. Por otro lado, la respuesta inmunitaria adaptativa es más específica y duradera, aumentando su efectividad tras un primer contacto con el antígeno. Está compuesta por el sistema complemento, linfocitos y anticuerpos (Abbas, A. K., Lichtman, A. H., 2015). El sistema adaptativo aparece sólo en vertebrados, siendo los peces teleósteos los primeros en poseer un sistema inmunitario complejo y bien estructurado (Uribe et al., 2011).

La detección de los patógenos por la respuesta inmunitaria innata ocurre a través de los receptores de reconocimiento de patrones (PRRs) localizados tanto intra- como extracelularmente, y que son capaces de reconocer los patrones moleculares asociados a patógenos (PAMPs). Existen dos familias principales de PRRs, los receptores tipo toll (TLRs), cuya activación induce citoquinas proinflamatorias como IL-1 e IL-18 pero no activación directa de caspasas, y los tipo NOD (NLRs), cuya activación provoca su oligomerización en complejos moleculares activadores de caspasas proinflamatorias (Broz & Monack, 2013).

Los complejos macromoleculares iniciados a partir de la activación de los NLRs son denominados inflamasomas (Martinon et al., 2002). Se componen principalmente de un receptor de la familia NLR, una proteína adaptadora (generalmente ASC) y una caspasa efectora (comúnmente caspasa-1). Estos complejos son un componente esencial de la respuesta innata pues su correcta activación es crítica para la eliminación de patógenos o células dañadas. Una vez activado el inflamasoma dará lugar al procesamiento de citoquinas proinflamatorias (IL-1 $\beta$ ) y a la muerte celular programada

denominada piroptosis a través de Gasdermina-D (GSDMD) (Shi et al., 2015). A su vez, el mal funcionamiento del inflamasoma es la causa principal de enfermedades autoinmunes y síndromes metabólicos, por lo que es importante conocer su funcionamiento en contextos tanto fisiológicos como patológicos.

Los NLRs presentan tres dominios estructurales: uno central de unión a nucleótidos y oligomerización (NACHT) que es comúnmente flanqueado por repeticiones C-terminales ricos en leucina (LRR), que detectan diferentes ligandos, y por dominios N-terminales de reclutamiento de la caspasa (CARD) o dominios Pyrin (PYD). Esta diversidad de dominios efectores permite que los NLRs puedan interactuar con una amplia variedad de moléculas y que, por tanto, puedan activar múltiples vías de señalización. Por ello están involucrados en diversas funciones de las que destacan la activación de inflamasoma, transducción de señales, activación de la transcripción y autofagia (Y. K. Kim et al., 2016b). Para este trabajo nos interesa conocer aquellos que actúan en el ensamblaje del inflamasoma entre los que destacan NLRP3, NLRC4 y AIM2.

Generalmente los receptores se encuentran localizados en el citoplasma en forma inactiva, y necesitan de un cambio conformacional para poder activarse y comenzar la oligomerización del inflamasoma. NLRP3 se activa por numerosos estímulos procedentes de patógenos o señales de daño celular mientras que NLRC4 y AIM2 son receptores un poco más específicos que reconocen bacterias Gram negativas con sistema tipo 2 o 3 de secreción y ADN de doble cadena respectivamente (H. Guo et al., 2015; Matusiak et al., 2015; Morrone et al., 2015).

En colaboración con los NLRs actúa la molécula adaptadora ASC, compuesta por un dominio PYD N-terminal y un dominio CARD C-terminal. La interacción entre los principales componentes del inflamasoma ocurre a través de interacciones homotípicas PYD-PYD o CARD-CARD. El dominio PYD de ASC es necesario para formar filamentos mientras que el dominio CARD es esencial para interacciones cruzadas que dan lugar a la formación de la plataforma cerrada esencial para el procesamiento eficiente de IL-1 $\beta$ , pero que no es necesaria para la piroptosis (Dick et al., 2016).

Finalmente, la activación de los NLRs en conjunto o no con ASC permitirá la formación de una plataforma necesaria para el autoprosesamiento de caspasa-1 a su

forma activa. Además, la actividad proteasa también es regulada por el inflamasoma, procesándose en dos subunidades, p10 y p20, que a su vez forman un heterotetrámero inestable acabando así con la respuesta (Boucher et al., 2018).

En los últimos años se ha demostrado que el pez cebra es un excelente modelo para la investigación. Presenta numerosas ventajas como su pequeño tamaño, alta resistencia a patógenos, alta tasa de fecundidad y número de individuos por puesta, tiempo de generación corto, transparencia de sus embriones con un desarrollo extrauterino, genoma secuenciado y alta similitud con el del humano. Este modelo también ha tomado una mayor importancia recientemente en los estudios relativos al inflamasoma, donde ortólogos para ASC o caspasa-1 (Caspas) ya han sido descritos (Bezbradica & Schroder, 2017; Tyrkalska et al., 2016). Sin embargo, presenta ciertas dificultades como la falta de ortólogos directos para los NLRs de mamíferos.

Para el estudio del sistema inmunitario en pez cebra se ha demostrado previamente su utilidad para un modelo de infección con *Salmonella enterica* serovar Typhimurium (ST) (Zakrzewska et al., 2010). La utilización de este modelo ha permitido además avances en la investigación sobre los inflasomas (Sofia de Oliveira et al., 2015; Kuri et al., 2017). Asimismo, el modelo de infección de pez cebra con ST ha permitido recientemente en nuestro laboratorio la identificación de la función de Gbp4, una GTPasa homóloga a GBP5 humana, involucrada en la activación del inflamasoma y la eliminación de la infección, siendo indispensable la actividad GTPasa para este proceso (Tyrkalska et al., 2016). De este modo se demostró que el proceso de eliminación bacteriana ocurre en dos etapas; primero, un reclutamiento de los neutrófilos al sitio de infección a través de una producción de CXCL8 y LTB4 independiente de inflamasoma, y segundo, la eliminación de ST a través de la producción de prostaglandina 2 dependiente de inflamasoma.

Para continuar con el estudio del inflamasoma utilizando el modelo de pez cebra-ST, en esta Tesis doctoral nos hemos centrado en la caracterización de dos proteínas, Caiap y WDR90, cuyos dominios estructurales están involucrados en la formación de plataformas multiproteicas. Por otra parte, estos estudios han sido complementados con el desarrollo de anticuerpos frente a los componentes del inflamasoma Asc (de pez cebra) y WDR90 (humano), y de líneas celulares *knock-out* y *knock-in* para WDR90.

**Caiap** (Proteína adaptadora del inflammasoma con dominios CARD-ANK) fue identificada a partir de una búsqueda bioinformática de proteínas con dominios CARD. El gen que codifica para *caiap* está formado por dos exones que dan lugar a un péptido de 744 aminoácidos con un dominio CARD N-terminal y 16 dominios ANK (de repeticiones de ankirina) C-terminales muy conservados filogenéticamente en vertebrados, a excepción de mamíferos placentarios. Los análisis filogenéticos sugieren que el origen de Caiap data de hace más de 450 millones de años, siendo anterior a la divergencia entre peces y tetrápodos, por lo que debe haber sido perdido en mamíferos placentarios y peces pulmonados a lo largo de la evolución.

La secuencia de aminoácidos de Caiap en pez cebra respecto a otros organismos tiene desde un 47 a un 66% de similitud. Además, las regiones mejor conservadas de la proteína se corresponden con el dominio CARD y el dominio ANK y la predicción de la estructura terciaria de la molécula muestra una misma distribución en todas las especies analizadas. Además, se analizó el perfil de expresión de *caiap* en larvas infectadas de pez cebra, observándose un ligero aumento de la expresión 24h tras la infección, que además se corresponde con una detección positiva por WISH de Caiap en el sitio de infección. Con el fin de conocer en qué células estaba actuando Caiap se realizó un análisis de RT-qPCR de macrófagos y neutrófilos sorteados. Los resultados demostraron el aumento de *caiap* en macrófagos, pero no en neutrófilos tras la infección.

Por otro lado, para profundizar en la caracterización de Caiap como parte del inflammasoma de pez cebra, se llevó a cabo su inactivación genética por medio de morfolidos y CRISPR/Cas9. Los peces deficientes en Caiap resultaron más susceptibles a la infección por ST y su actividad caspasa-1 se vio reducida. Este efecto negativo no pudo ser rescatado por la forma mutante de Caiap que carece del dominio CARD denominada Caiap $\Delta$ CARD. Además, aunque la sobreexpresión ubicua de Caiap no confirió ninguna ventaja a los peces frente a la infección, su sobreexpresión específica en macrófagos sí lo hizo, de manera que la susceptibilidad ante la infección se vio reducida.

Asimismo, dada la presencia de dominio CARD en Caiap, se quiso comprobar si su función podía suplir el papel de Asc en la activación de caspasa-1. Sin embargo, los peces deficientes en Asc exhibieron alta susceptibilidad a ST y una gran reducción de la actividad caspasa-1, que no pudo ser evitada al sobreexpresar Caiap. Del mismo modo,

la importancia del papel de Asc era independiente de Caiap, ya que su inactivación no tiene ningún efecto cuando Asc es sobreexpresado. Por otro lado observamos que la sobreexpresión de Caspa, la proteína efectora del inflammasoma en pez cebra, era capaz de suprimir la susceptibilidad frente a ST tras la inactivación de Caiap, pero podía rescatar solo parcialmente la actividad caspasa-1.

Con el fin de discernir el papel de Caiap en este proceso, reconstituimos los complejos de Caiap-Asc, Caiap $\Delta$ CARD-Asc y Caiap o Caiap $\Delta$ CARD junto con Caspa activa e inactiva en HEK293T. Sorprendentemente pudimos observar mediante inmunofluorescencia que a pesar de la presencia de dominios CARD, Caiap no interaccionaba directamente con Asc aunque ambas formas (silvestre y mutante) formaban un anillo alrededor de ésta proteína. Por otro lado, Caiap y Caiap $\Delta$ CARD se concentraban en un speck bajo la presencia de Caspa activa, pero no frente a la inactiva. Estos resultados fueron corroborados mediante experimentos de inmunoprecipitación, donde demostramos que Asc no interacciona directamente con Caiap, mientras que la forma catalíticamente activa de Caspa lo hace a través del dominio ANK. Además, comprobamos que el dominio CARD de Caiap es necesario para su auto-oligomerización, que parece esencial *in vivo* para mediar la resistencia a ST dependiente de inflammasoma.

Por otro lado, **Wdr90** está compuesto fundamentalmente por dominios WD40 que forman estructuras en barril de hojas beta ideales para mediar interacciones proteicas (Schapira, Tyers, Torrent, & Arrowsmith, 2017b). A diferencia de Caiap, también se encuentra conservado en mamíferos placentarios, lo que aumenta su interés dentro de la investigación del inflammasoma y las enfermedades asociadas. Esta proteína de alto peso molecular fue identificada a partir de un análisis de RNA-Seq realizado en nuestro laboratorio en larvas infectadas de pez cebra bajo la sobreexpresión de la GTPasa antes mencionada, Gbp4. El análisis de RNA-Seq mostraba una estrecha relación en la expresión génica de *wdr90* en presencia de Gbp4, y fue confirmado por RT-qPCR mostrando a su vez que la actividad GTPasa de Gbp4 era responsable del incremento en los niveles de *wdr90*. Además, pudimos comprobar que la expresión de *wdr90* en pez cebra es independiente de Asc o la actividad caspasa-1 mediante la inactivación génica o farmacológica de los mismos respectivamente, mientras que la infección por ST también era responsable de una mayor expresión de *wdr90* en pez cebra.

Asimismo, se realizaron estudios funcionales *in vivo* similares a los llevados a cabo con Caiap, a diferencia de que no pudimos inactivar Wdr90 ya que su eliminación génica en embriones de pez cebra era letal. Por ello, todos los análisis de supervivencia y actividad caspasa-1 se llevaron a cabo en condiciones de sobreexpresión de Wdr90. Primero pudimos comprobar que ésta aumentaba la resistencia de las larvas a la infección de ST y a su vez generaba un incremento en la actividad caspasa-1, en condiciones de infección y no infección. Más tarde quisimos comprobar su relación con otros componentes del inflamasoma. Para ello, se utilizaron morfolinós para bloquear la expresión de Asc, Gbp4, y el inhibidor farmacológico de caspasa-1. Los resultados de estos estudios muestran como Wdr90 actúa en la resistencia a ST y la actividad caspasa-1 ocurre aguas arriba de los componentes antes mencionados, pues la sobreexpresión de Wdr90 no era capaz de rescatar la mayor susceptibilidad de las larvas y reducción de la actividad caspasa-1 de larvas deficientes en Gbp4 y Asc.

Posteriormente, para comprobar si la función de Wdr90 en el inflamasoma estaba relacionada con un receptor NLR, se reconstruyó en HEK93T WDR90 humano junto con 3 de los receptores principales del inflamasoma, NLRC4, NLRP3 y AIM2, estando descritos los dos primeros como participantes del inflamasoma en respuesta a ST (Qu et al., 2016a). El análisis de estas proteínas por inmunofluorescencia, muestra un cambio en la distribución del receptor NLRC4, que no ocurre en NLRP3 y AIM2 en presencia de WDR90. Para corroborar si el cambio producido en NLRC4 era causa de una interacción directa entre WDR90 y este receptor realizamos una inmunoprecipitación de estas muestras. Sin embargo, la proteína WDR90 presenta un comportamiento inusual que dificulta su estudio utilizando técnicas de electrotransferencia, ya que se vuelve insoluble al ser precalentada para su penetración al gel. Por este motivo, los resultados de la inmunoprecipitación NLRC4 con WDR90, a pesar de ser negativos, no son totalmente concluyentes y se requiere el uso de otras técnicas como el análisis de ligado por proximidad (PLA) para corroborar si WDR90 genera un cambio en la distribución de NLRC4 de forma directa o indirecta.

Finalmente, con el fin de determinar en mayor profundidad la importancia de WDR90 en el inflamasoma nos propusimos desarrollar **nuevas herramientas** para su estudio. Entre estas herramientas se encuentran la generación de un *knock-out* en

macrófagos inmortalizados de ratón, el cual nos permitirá determinar la importancia de WDR90 frente a la infección y de un *knock-in* WDR90-FLAG que facilitará su detección endógena utilizando el sistema de CRISPR/Cas9. La validación de estas herramientas se vio obstaculizada por la falta de un anticuerpo comercial capaz de detectar WDR90 y una baja expresión de la proteína en condiciones estándar de la célula respectivamente. Para solventarlo, decidimos generar anticuerpos de WDR90 y Asc (el cual es necesario para facilitar los estudios de inflammasoma en pez cebra ya que no está disponible comercialmente) en alpacas. Las alpacas son camélidos capaces de producir los denominados nanoanticuerpos, que son capaces de reconocer epítomos más inaccesibles y a su vez se pueden producir de manera sistemática *in vitro* una vez han sido identificados (L. He et al., 2017; X. Liu et al., 2018). El anticuerpo producido contra Asc fue validado positivamente, sin embargo, no pudimos obtener el mismo resultado con WDR90. Para solucionar estos problemas hemos decidido realizar una librería de nanoanticuerpos, creada a partir del cDNA de linfocitos de alpaca inmunizada. De esta forma podremos seleccionar un nanoanticuerpo capaz de reconocer eficazmente WDR90 y obtener una fuente fácilmente accesible de anticuerpos, lo que facilitará el análisis de la función de WDR90 en inflammasoma y los estudios de inflammasoma en pez cebra.



